GAMMA RAY SPECTROSCOPIC STUDIES OF MEMBERS OF THE A=141 DECAY CHAIN

By

Richard Ross Todd

A THESIS

Submitted to
Michigan State University
in partial fulfillment of the requirements
for the degree of

DOCTOR OF PHILOSOPHY

Department of Physics

1971

ABSTRACT

GAMMA RAY SPECTROSCOPIC STUDIES OF MEMBERS OF THE A=141 DECAY CHAIN

By

Richard Ross Todd

The techniques of beta and gamma ray spectroscopy have been applied to a study of the decay schemes of $^{141m+g}Sm$ and ^{141}Pm. The goal of this study was to increase our understanding of nuclear structure and to obtain information about energy level systematics in these members of the A=141 decay chain below the N=82 closed shell.

Ge(Li) singles, Ge(Li)-Ge(Li) two parameter coincidence and Ge(Li)-NaI(Tℓ) (anti) coincidence spectrometers were used to identify and establish the sequence of gamma ray transitions. The decay schemes were determined and comparisons are made with previous studies as well as the results of recent reaction work.

Forty-seven transitions have been identified with the beta decay of ^{141m}Sm and 40 of these have been incorporated in a decay scheme involving 16 levels in the daughter ^{141}Pm. These levels are at 0, 196.6, 628.6, 804.5, 837.1, 974.0, 1108.1, 1167.2, 1313.2, 1414.8, 1834.0, 1983.1, 2063.5, 2091.6, 2119.0, and 2702.4 keV. The lifetime of the state at 628.6 keV in ^{141}Pm was measured to be 700±20 ns and the E3 transition from this level to the ground

state was found to exhibit an enhancement of 1.6 spu. The decay of ^{141g}Sm was observed to populate levels at 403.9, 438.4, 728.0, 1292.7, 1495.7, 2004.5, and 2037.7 keV in ^{141}Pm.

Of the 50 transitions observed in the decay of ^{141}Pm, 43 of these have been placed in a level scheme containing 23 levels. The levels identified are at 0, 193.8, 1223.3, 1345.8, 1564.8, 1596.8, 1820.4, 1897.1, 1968.0, 2066.4, 2073.7, 2109.6, 2145.2, 2246.6, 2265.3, 2303.4, 2354.4, 2388.4, 2430, 2506, 2620, 2805, and 2986 keV.

Limits on the possible spin assignments of the levels identified, have been made from calculated log ft values and observation of transitions to levels of known spins. A three-quasiparticle multiplet of high-spin, odd parity states was identified between 1.4 and 2.7 MeV in ^{141}Pm. The decay characteristics of the multiplet suggest the possibility of obtaining information about its structure from shell model calculations using a limited basis.

A survey has been made of the energy level systematics and properties of low-lying states in the N=80, 81, and 82 odd mass isotones. These observations have led to some predictions and suggestions for future experiments.

ACKNOWLEDGEMENTS

I wish to thank Dr. W.H. Kelly for suggesting this area of study. He has always found time, despite a busy schedule, to offer his personal assistance and encouragement in all aspects of this work. His guidance and patience during the writing of this thesis are deeply appreciated.

I also wish to thank Dr. Wm.C. McHarris for his considerable help and advice on many phases of these investigations.

Dr. H.G. Blosser and Mr. H. Hilbert have assisted with the operation of the Michigan State University sector-focused cyclotron. The variety of available beam energies and the high beam flux have facilitated the production of the isotopes studied in this investigation.

Drs. B.H. Wildenthal and F.M. Bernthal have contributed to various phases of this investigation through informal discussions. Their generous cooperation is gratefully acknowledged.

The ^{141}Sm research has involved a joint effort with Dr. R. Eppley. His significant assistance and advice are gratefully acknowledged. Dr. F.Y. Yap has shared in the ^{141}Pm research and his considerable aid in this project is appreciated.

Special thanks is due to Dr. R. Warner for his assistance with these experiments. He and Dr. Eppley have

provided me with many satisfying hours of informal discussion pertaining to research and things philosophical.

The members and former members of the research group here all contributed in various ways to the successful completion of this thesis work. Dr. D. Beery, Dr. R. Doebler, Dr. G. Giesler, Dr. R. Goles, K. Kosanke, J. Black, L. Samuelson, W. Chaffee, C. Morgan, R. Firestone, and Miss J. Guile have all helped in this work. Dr. D. Beery was of particular assistance in the early stages of these projects.

The help of Mr. R.N. Mercer and the staff of the cyclotron machine shop is appreciated.

This thesis has been very capably typed by Mrs. Sandi Bauer. Her assistance and effort in the completion of this project is appreciated. Mrs. Peri-Anne Warstler has assisted with some of the Tables and Figures.

Much of the financial assistance for this research has been provided by the National Science Foundation, the U.S. Atomic Energy Commission, and Michigan State University.

Finally I thank my wife Jeanne and Chuck and Elizabeth for their patient understanding and continued encouragement during this study.

TABLE OF CONTENTS

Chapter

LIST OF TABLES

LIST OF FIGURES

Chapter I

Introduction

A measure of our current understanding of nuclear structure is demonstrated by the ability of current nuclear models to explain observed properties of nuclei and to predict other properties previously unobserved. The origin and development of these models involves the observation of these same nuclear state properties. In this interplay of theory and experiment, both the quality and quantity of the available experimental data serve to test the existing models and aid in the development of new and improved ones.

Radioactive decay studies and nuclear reaction studies complement one another as basic tools of nuclear research. Their ability to determine significant nuclear state properties serves to test and advance our knowledge of nuclear structure. By means of beta and gamma ray spectroscopy, this investigation seeks to increase our current knowledge, and, where possible, to improve the existing information in the field of radioactive decay.

In the past few years there have been many radioactive decay studies of odd mass isotopes in the $50 \leq Z \leq 65$, $62 \leq N \leq 82$ region of the nuclidic chart (Ti 67)(NDS)(NSA). These studies attempt to characterize the states in the daughter as completely as possible by comparing their results with

those of reaction studies and theoretical calculations. Recently there have also been a number of nuclear reaction studies on odd mass nuclei in and near the N=82 closed shell. These involved particle transfer studies such as $(d,{}^3He)$, $({}^3He,d)$, (p,d), (d,p), (p,t), inelastic scattering experiments such as (α,α'), (d,d'), (p,p') and in-beam gamma experiments such as $(n,n'\gamma)$, $(\alpha,2n\gamma)$

This region is bounded by the magic numbers of Z=50 protons and N=82 neutrons. Nuclei with these magic numbers have tightly bound or relatively inert spherical cores of protons (Z=50) or neutrons (N=82). As one moves far from these spherical cores, it is expected the nuclei will acquire a permanently deformed shape. The transitional region between these extremes is characterized by a change in the nature of the levels, produced by the increasing admixture of various combinations of shell model orbitals and intermixed collective effects. As a result, there are a greater number of low-lying levels suggesting a softer nucleus. In the transitional region the line of stability runs approximately through the nuclei ${}^{121}_{51}Sb_{70}$, ${}^{127}_{53}I_{74}$, ${}^{133}_{55}Cs_{78}$, and ${}^{139}_{57}La_{82}$. These nuclei, along with the large number of stable nuclei in the Z=50 and N=82 closed shells, are conveniently located for systematically probing part of the transitional region by means of the $({}^3He,xn)$ and (p,xn) reactions.

The beta and gamma ray spectroscopy group at MSU is currently conducting a systematic study of the region between the Z=50 and N=82 closed shells. In the process of conducting such a study it is useful to begin with a knowledge of levels in the nuclei close to the line of stability. As more information becomes available regarding these levels, it will be convenient to move away from stability in successive steps toward the region of permanent deformation.

During the course of earlier investigations in this region, the study of ^{139m}Nd resulted in the identification of a three-quasiparticle multiplet of low-lying, high-spin states in ^{139}Pr (Bee 69b). The existence of such states is rare, and, because they can be characterized in rather simple shell model terms, they yield a significant amount of information about nuclear structure. As a result of the information to be gained, it seemed worthwhile to attempt to identify these three-quasiparticle levels in other nuclei in the vicinity of ^{139}Pr. It was suggested by McHarris et al. (McH 69) that the decays of ^{141m}Sm and ^{137m}Nd would populate similar multiplets in the daughters ^{141}Pm and ^{137}Pr. The ready accessibility of ^{141}Sm by means of the reaction ^{142}Nd(^{3}He,4n)^{141}Sm (Q=-27.3 MeV) suggested it as the next system to be studied.

A satisfactory study of ^{141m}Sm necessitates a knowledge of other members of the A=141 decay chain as they appear in the sequence $^{141m+g}_{Sm\rightarrow}{}^{141}_{Pm\rightarrow}{}^{141m+g}_{Nd\rightarrow}{}^{141}$Pr (stable). The

decays of ^{141m}Nd and ^{141g}Nd have been previously reported by Beery et al. (Bee 68). However, little was known about the 20.6m ^{141}Pm and 22.1m ^{141m}Sm activities other than their half-lives and the isomer ^{141g}Sm had not been identified at all prior to initiating this investigation. In light of the existing situation, a concurrent study of the decays of $^{141m+g}$Sm and ^{141}Pm was undertaken. The study of ^{141}Sm was initiated through a joint effort with R. Eppley. Some preliminary results concerning ^{141}Sm appear in (Epp 70a).

The decay of ^{141}Pm is of interest because the daughter ^{141}Nd is one neutron removed from the N=82 closed shell. As a result, the low-lying states are expected to be of a fairly pure single-particle nature, (i.e. neutron hole states). During the course of this investigation several studies have appeared directed at locating the neutron hole states in the N=81 nuclei by means of pickup reactions such as (p,d) and (d,t) on N=82 nuclei. As a consequence, it has been possible to compare the ^{141}Pm decay study with these data.

During the course of the ^{141m}Sm investigation, a delayed state was observed in ^{141}Pm at 628.6-keV. This state is suggested to decay via M2 and E3 transitions of 431.8- and 628.6-keV, respectively. Lifetime measurements indicate the E3 transition is enhanced. This observed enhancement, coupled with a study of systematic trends in the N=82 nuclei, suggests a series of interesting experiments to be performed on odd proton odd mass nuclides in the region.

At the present time there exists little in the way of theoretical calculations with which to compare the experimental results presented here. Muthukrishnan and Kromminga have performed a shell model calculation of the three-quasiparticle odd parity states in ^{139}Pr by using several phenomenological potentials and limiting the basis states to those suggested by McHarris et al. (McH 69) for the three-quasiparticle multiplet. The results obtained on the energies of the states were in rough agreement with experiment. However, the theoretical transition probabilities did not agree very well with experiment. Preliminary calculations of energies of states below 2 MeV in ^{141}Nd have been carried out very recently by Reehal using the pairing-plus-quadrupole Hamiltonian of Kisslinger and Sorensen (Ree 71), reasonable agreement was obtained. The recent shell model calculations of Wildenthal on the N=82 isotones appear very promising. It is hoped that in the near future these calculations might be extended to the N=81 and N=80 isotones. Moderately successful calculations might be performed using a rather limited basis such as the one proposed for the three quasiparticle multiplets in ^{141}Pm and ^{139}Pr.

Chapter II describes in a general way the techniques involved in decay scheme construction and contains a brief description of the experimental apparatus and techniques along with a discussion of the methods of data analysis.

Chapter III describes in some detail the steps involved in the systematic identification of the transitions associated with the radioactive decay of members of the A=141 chain below the N=82 closed shell.

Chapter IV describes the experimental results of this study. The decay of ^{141m}Sm involved the identification of 47 gamma rays and the placement of 16 levels in the daughter ^{141}Pm populated by this decay. A set of six odd-parity levels between 1.6 and 2.2 MeV were identified as members of a three-quasiparticle multiplet having the configuration

$$[(\pi d_{5/2})^3(\nu d_{3/2})^{-1}(\nu h_{11/2})^{-1}]_{J^-}.$$

The properties of these states are compared with the corresponding ones in ^{139}Pr. The half-life of the delayed $11/2^-$ state at 628.6-keV in ^{141}Pm was measured and the partial half-lives of the 628.6-keV E3 and 431.8-keV M2 transitions were determined. The decay scheme of ^{141g}Sm resulted in the placement of an additional 7 levels in the daughter ^{141}Pm and the identification of 12 transitions belonging to this decay.

The study of the decay of ^{141}Pm resulted in the placement of 23 levels in ^{141}Nd and the identification of 50 transitions associated with this decay. A comparison is made between the levels of ^{141}Nd populated via the beta decay of ^{141}Pm and levels identified in ^{141}Nd by means of the reaction

studies (p,d) and (d,t) on ^{142}Nd (Jol 71), (Cha 71), and (Fos 71). These results are compared with very preliminary theoretical calculations by Reehal (Ree 71) using the pairing-plus-quadrupole Hamiltonian of Kisslinger and Sorensen.

In Chapter V the systematic behavior of some nuclear properties in the N=82 region are discussed. The characteristics of the three-quasiparticle multiplet in ^{141}Pm are discussed and compared with similar states in other nuclei in and near the N=82 closed shell.

Chapter II

Experimental Methods and Apparatus

As one moves further away from the region of β-stability the identification of radioactive isotopes and the construction of their decay schemes becomes increasingly difficult. The difficulties arise principally because the half-lives become shorter and the reactions used to produce the various desired isotopes are not as clean. The limitations on studying a specific activity depend on several factors such as (1) the types of bombarding beams available, (2) the energies of these beams, (3) the specific nuclear reactions desired, (4) the stable isotopes available for targets, (5) the location of these isotopes with respect to the line of beta-stability, (6) the half-lives of the desired activity and the competing activities, and (7) the data acquisiton facilities available.

The isotopes considered in this study were produced by either (p,xn) or (^{3}He,xn) reactions ($x \leq 4$) on stable isotones in the N=82 closed-shell. The complex decay characteristics of these isotopes required the use of the latest highest quality electronic equipment such as high resolution Ge(Li) detectors (∿2.0-keV FWHM for the 1332.4-keV transition in ^{60}Co), FET preamplifiers, low noise amplifiers with Gaussian shaping, base-line restoration, dc-coupling, pile-up rejection and significant (anti-) coincidence circuitry

as well as the PDP-9 and XDS Sigma-7 computers and their available data acquisition programs.

Section 2.1 describes in a general way the pattern followed in the acquisition of the experimental data and the construction of parts of a nuclear decay scheme. Section 2.2 discusses the two types of gamma ray detectors used in this study and compares the factors influencing their resolution. A description of the various gamma ray spectrometers used in this investigation is also included. In Section 2.3 some of the methods used in the data analysis are broadly outlined. A detailed description of the logical identification of the members of the A=141 decay chain considered in this study is deferred to Chapter III. Peculiarities pertaining to a specific experiment are included in the discussion of the experimental results in Chapter IV.

2.1 Decay Scheme Construction

One of the primary objectives of this study has been the incorporation of the significant experimental results into a consistent description of the manner in which an isotope decays and a comparison of these results with theories and other data such as reaction studies. The important features of such a study involve proper identification of

the activity to be studied, determination of the half-life of the parent activity, precise measurement of the energies of the transitions, beta and gamma transition intensities, electron capture disintegration energies, calculation of log ft values for beta decay to each level in the daughter, and spin and parity assignments. There are a wide variety of experimental techniques available and each isotope has special characteristics requiring variations in the method of approach.

The placement of energy levels may be suggested initially by energy sums and gamma-ray intensity balances. Additional evidence for level placement comes from coincidence evidence such as 511-511-keV-gamma coincidences, anti-coincidence, prompt and delayed coincidence results, as well as other accessible parameters. As one moves further from stability, the energy available for decay increases generally resulting in an increase in the number of transitions to be placed. In addition to this difficulty, the half-life generally decreases, and, as it becomes shorter, it makes Ge(Li)-Ge(Li) 2-dimensional coincidence experiments more difficult. As a result such problems make the interpretation of the data more difficult.

After placing the energy levels, the determination of beta and gamma transition intensities follows. Then, providing the EC decay energies are known, the log ft values for decay to each state in the daughter can be calculated.

This involves a rather lengthy but generally routine sequence. A description of the procedure to be followed in doing these calculations appears in (Bee 69a) and (Epp 70a). Computer programs are available which calculate per cent feeding to each level, electron capture to positron ratios and log ft values. The program used in this study was DECAY SCHEME written by D. Beery for use on the Sigma-7 computer and modified by R. Epply for use on the PDP-9 computer (Epp 70a).

2.2. Gamma-Ray Spectrometers

In the following study we have used two different photon detectors: NaI(Tℓ) scintillation spectrometers and Ge(Li) solid state spectrometers. The processes involved in the detection of the energy deposited in the NaI(Tℓ) crystal and the Ge(Li) crystal are quite different. As a result the energy resolution of the two types of spectrometers differs markedly. As a means of comparison the energy resolution of a very good NaI(Tℓ) system is ∿60 keV full-width-half-maximum (FWHM) for the 1332-keV γ-rays of ^{60}Co. The energy resolution of a typical Ge(Li) system is 2.0- to 3.0-keV FWHM for these same ^{60}Co γ-rays. The reason for the difference in resolution can be understood from the following brief description of the processes involved.

Each spectrometer relies on the fact that incident radiation deposits some portion of its energy in the crystal. In the NaI(Tℓ) spectrometer the deposited energy appears as visible and ultraviolet light. This light is detected by a photomultiplier tube optically coupled to the NaI(Tℓ) crystal. This produces a voltage pulse proportional to the intensity of the incident light that is in turn proportional to the energy deposited in the crystal. In the Ge(Li) spectrometer the incident radiation creates hole-electron pairs that are collected by an electric field across the crystal. The result is a current pulse proportional to the energy deposited by the radiation; this is converted to a voltage pulse by the preamplifier for purposes of pulse shaping etc.

The basic reason for the disparity in the energy resolution of the two systems is essentially statistical. The signal resolution in NaI(Tℓ) results from the large statistical fluctuations in the relatively small number of resultant photoelectrons emitted by the photocathode per given amount of energy deposited in the scintillating crystal. Ge(Li) solid state detectors employ direct collection of the ionization produced by the radiation. In Ge(Li) a hole-electron pair is produced for every 3-eV of energy (on the average) absorbed from the radiation. Correspondingly in NaI(Tℓ) on the order of 300 eV are required for every photoelectron produced.

Hence in the NaI(Tℓ) system the relatively large statistical fluctuation is due to the small number of electrons ejected from the photocathode of the photomultiplier, whereas in the solid state detector the primary energy is distributed over a far greater number of carriers and the relative statistical fluctuation is considerably reduced.

2.2.1 Singles Experiments

In the present study, singles experiments refer specifically to pulse height spectra taken with the aid of a single Ge(Li) spectrometer. In point of fact the Ge(Li) spectrometer is an electronic system composed of the following components: a) A lithium-drifted germanium crystal enclosed in a cryostat and cooled in liquid nitrogen, temperature (77°K), b) a high voltage bias supply and a charge-sensitive preamplifier with an associated field-effect transistor (FET)—the FET may be either cooled to ∿120°K or operated at room temperature, c) a spectroscopy amplifier (for purposes of amplification and pulse shaping) with pole-zero cancellation, base-line restoration, and dc level adjustment, d) an analog-to-digital converter (ADC) and computer or multichannel analyzer (MCA), and e) a storage unit of some type with associated spectrum readout.

The performance characteristics of a particular Ge(Li) spectrometer are primarily determined by the Ge(Li) crystal

and the associated FET preamplifier. Such features as the volume of the Ge(Li) crystal, the manner in which the crystal is drifted (i.e. true-coaxial, trapezoidal or wrap-around, or planar), the capacitance of the crystal, and the operating bias all play interrelated parts in determining the final resolution of the system. The cooled FET will usually result in a lower noise system and as a result yields somewhat better resolution as compared to a room temperature FET preamplifier. The volume and shape of the crystal will play important parts in determining the efficiency and peak-to-Compton ratio for a particular detector. In general a larger volume crystal results in increased counting efficiency (related to the size) but this increase in volume usually results in a decrease in the resolution produced by an increase in crystal capacitance and poorer charge collection.

Other experimental features which are important in achieving satisfactory resolution are amplifier shaping constants, proper pole-zero cancellation, base-line restoration and correct dc-level adjustment. These can be determined rather quickly by using an oscilloscope and observing pulse-shapes and dc-levels at appropriate places in the system. The use of base-line restoration is strongly dependent on the counting rate and usually is best determined empirically.

The characteristics of several different Ge(Li) spectrometers used in the current gamma-ray studies are listed in Table I.

2.2.2. Coincidence Experiments

In the course of this study the character of the overwhelming majority of nuclear states observed suggested they had lifetimes <<100 nanoseconds (ns). Consequently it proved beneficial to use two or three singles spectrometers in various coincidence configurations to perform anticoincidence, prompt coincidence and delayed coincidence experiments. The standard procedure employed in a typical decay scheme study is to determine a) a singles spectrum, b) an anticoincidence spectrum, and c) coincidence spectra.

Table I

Eff.*	Shape	Peak-to Compton	Res. FWHM 1332-keV ^{60}Co	Manufacturer
0.4%	Trapezoidal	4.5:1	3.4 keV	MSU Cyclotron Lab
2.5%	Trapezoidal	12:1	2.2 keV	Nuclear Diodes
3.6%#	True Coaxial	18:1	2.0 keV	Ortec
4.5%	True Coaxial	24:1	1.9 keV	Ortec
10.4%	True Coaxial	36:1	2.2 keV	Nuclear Diodes

*With respect to the 1332 keV peak of ^{60}Co at 25 cm from a 7.6 x 7.6-cm NaI(Tl) detector.

#This detector was damaged by an electronic malfunction and replaced by the manufacturer with the 4.5% detector.

The techniques involved are routine and are discussed in greater detail in (Bee 69a) and (Epp 70a).

A "classical" pattern of experiments was used in the study of the ^{141}Pm decay described in Section 3.2, whereas the study of the Sm isotopes ^{141g}Sm and ^{141m}Sm required the use of a wider variety of methods to determine the decay schemes and their characteristics. The study of ^{141}Sm involved isotopes with similar enough half-lives, 11.3m in the case of ^{141g}Sm and 22.1m in the case of ^{141m}Sm, that the counting methods had to be modified. As an added feature, the decay of ^{141m}Sm involved the population of an $11/2^-$ isomeric level in ^{141}Pm which was observed to be a delayed state. The measurement of this half-life is discussed in Section 3.1.3.D.

By using two Ge(Li) detectors placed in 180° geometry we were able to perform several useful prompt-coincidence experiments as described below in Section 2.2.2.A. Other prompt and delayed coincidence experiments performed with Ge(Li) detectors inside a split-ring NaI(Tℓ) annulus are outlined in Section 2.2.2.B.

2.2.2.A. Multiparameter Ge(Li)-Ge(Li) Spectrometer

With the availability of larger volume and more efficient Ge(Li) detectors it has become practical to use them in obtaining 2 parameter coincidence information.

The goal of such an experiment is to simultaneously provide coincidence information for any and all peaks or regions of the spectrum in a single run.

Despite the relative inefficiency of Ge(Li) detectors, as opposed to NaI(Tℓ) detectors, there are decided advantages associated with their use in a multiparameter experiment. The most important features are the excellent energy resolution and the greater peak-to-Compton background ratio. As a result, satisfactory coincidence information can be obtained with fewer counts per channel using a Ge(Li)-Ge(Li) system than are normally required when using Ge(Li)-NaI(Tℓ). The electronics arrangement used in this lab is a relatively standard technique and is discussed in more detail in several theses and journals (Epp 70a). A diagram of the arrangement can be seen in Fig. 1.

With minor modifications, it is possible to obtain more information than described above. This information refers to a third parameter, namely the time between the two coincident events. It is with this in mind that I describe an alternate Ge(Li)-Ge(Li) coincidence spectrometer as seen in Fig. 2.

This is still a double coincidence experiment where we wish to record the linear signal from each of the detectors. The added feature in this configuration is the presence of a time to pulse height convertor (TPHC) in place of the fast coincidence unit. This provides us with

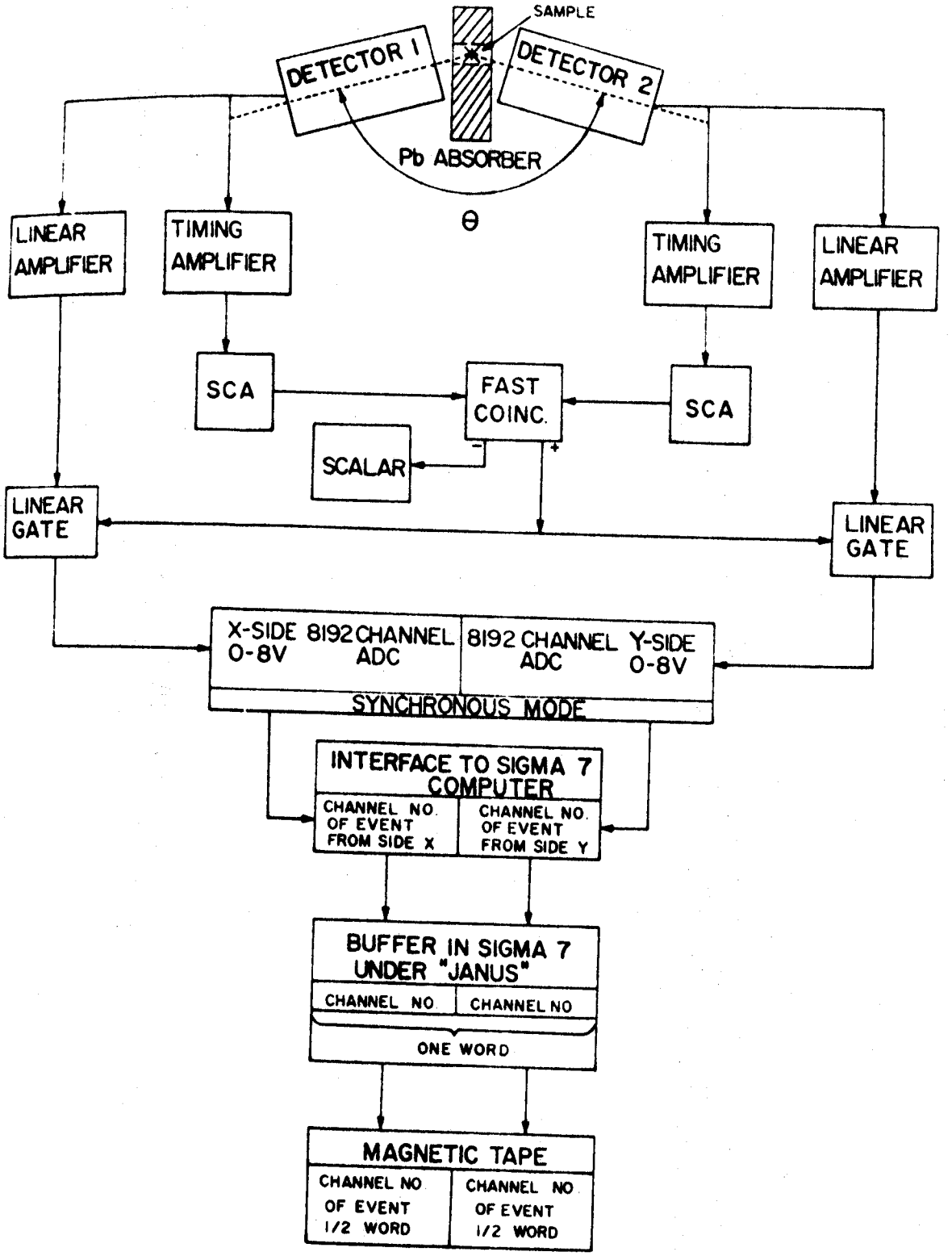

Figure 1. Block diagram of the apparatus used to collect two-dimensional "megachannel" γ-γ coincidence spectra, using the Sigma-7 computer.

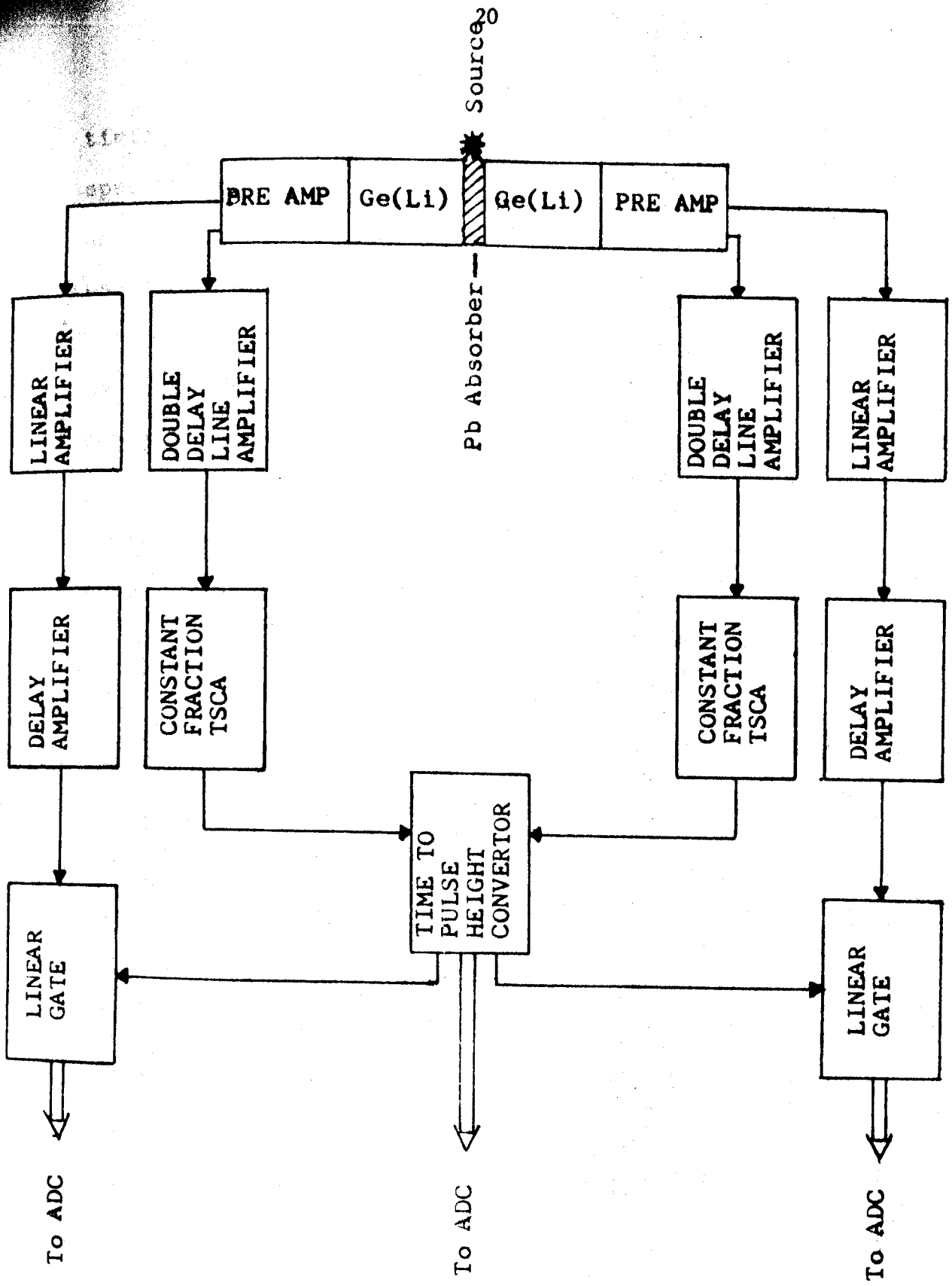

Figure 2. Schematic illustration of Ge(Li)-Ge(Li) multiparameter coincidence apparatus with time-to-pulse-height convertor (TPHC).

timing information pertaining to the resolving time of the spectrometer. In the future when it is possible to store and recover more than two parameters of information we can use the TPHC output as a third parameter.

In the configuration described above one of the Ge(Li) detectors must be chosen to start the TPHC and the other must provide the stop pulse. The logical choice to provide the stop pulse for the TPHC is the detector with the higher counting rate. Normally this would be the detector with the greater efficiency, however the source geometry influences the relative counting rate significantly and as a result this choice should be made after experimentally comparing the count rates in the two detectors.

2.2.2.B. Split Ring NaI(Tℓ) Annulus-Ge(Li) Spectrometer

Several useful coincidence experiments can be performed using the 8-inx8-in NaI(Tℓ) annulus and a Ge(Li) gamma-ray spectrometer. The configurations found useful in this study included an anticoincidence spectrometer and a pair spectrometer. In addition to these basic techniques, the annulus was also used in conjuction with a Ge(Li) spectrometer to obtain delayed coincidence spectra. These latter methods are discussed in Section 3.1.5.C. The electronic configurations for the anticoincidence and pair spectrometer experiments are shown in Fig. 3. These last two types of

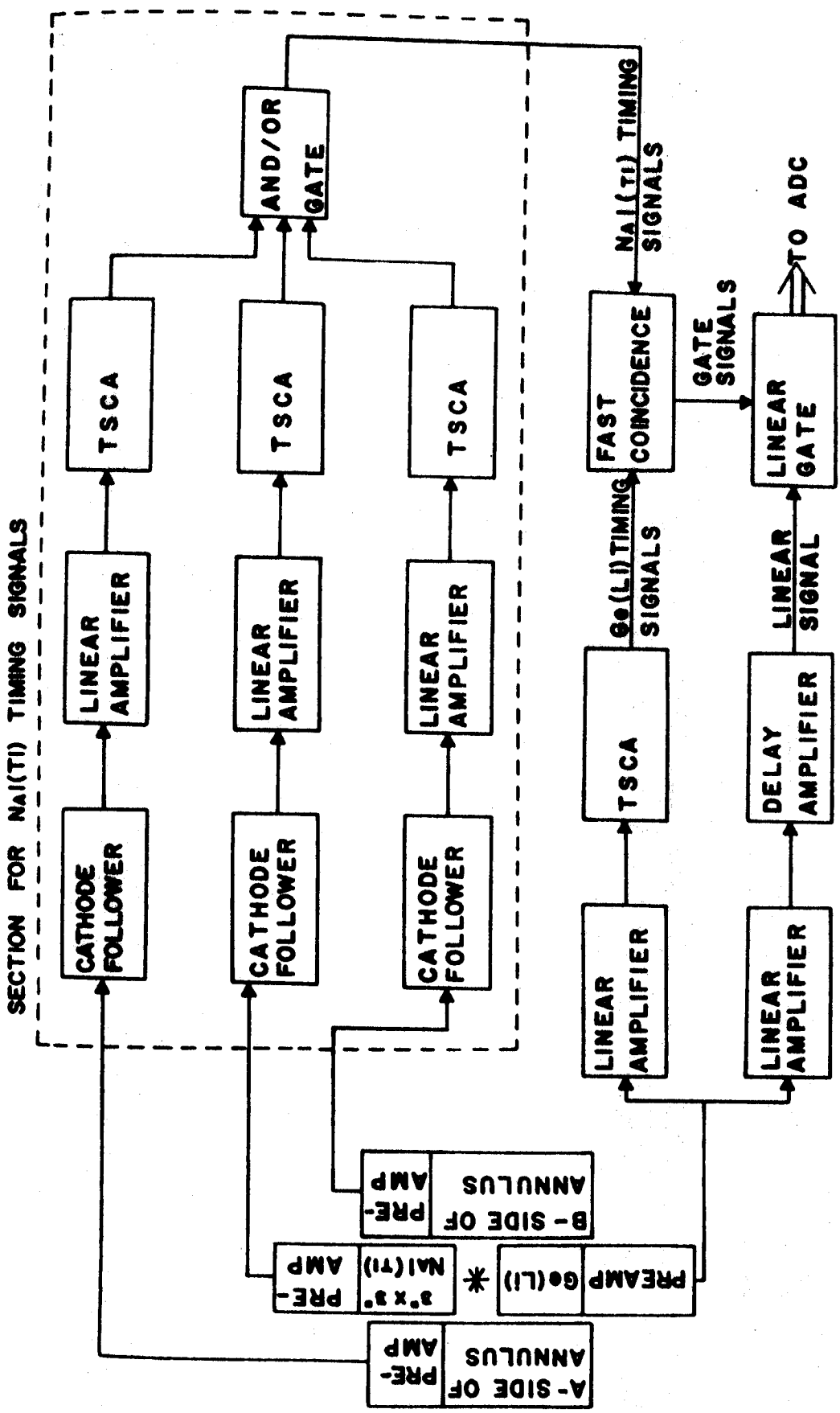

Figure 3. Schematic illustration of the anticoincidence apparatus. This same apparatus is used for the integral, anti-Compton, and triple coincidence experiments after the elimination of the 3×3-in. NaI(Tl) detector [Epp70a].

experiments are first discussed in (Aub 67) and additional discussions appear in (Bee 69a) and (Epp 70a).

2.3 Data Acquisition and Analysis

The lifetimes of the nuclides considered in this study are relatively short, ranging from ∿20m down to ∿1m. Because of this time limitation and the high resolution of our Ge(Li) detectors (2.0 to 2.5 keV) the spectrum size has varied from 1024 channels for some x-ray spectra to 8192 channels from some γ-ray spectra, with 4096 channels being the normal spectrum size. These spectra have been taken using several different data acquisition modes. The vast majority were taken using either the Sigma-7 or the PDP-9 computers with the particular choice being determined by the acquisition time and convenience. There are various data acquisition programs available to users of the Sigma-7 and some of the important programs used in this study were GEORGE (GEO), HYDRA (HYD), TOOTSIE (TOO), EVENT (EVE) and POLYPHEMUS (POL).[1] Choice of a particular program is governed by the requirements of the particular experiment.

The data analyses required for this study were performed using the Sigma-7 and PDP-9 and programs written or adapted for these computers. Brief descriptions of the programs used to determine gamma-ray energies and intensities, MOIRAE and SAMPO, are given below. A brief description of EVENT RECOVERY, the program used in the recovery of two-parameter information for magnetic tape, also follows in Section 2.3.1.C.

[1]Brief descriptions of these programs will be found in the Bibliography.

Discussions pertaining to peculiarities encountered in specific experiments are mentioned in Chapter IV.

2.3.1. Program MOIRAE

The areas and centroids of many of the photo peaks appearing in this study were analysed with the aid of the Sigma-7 computer and program MOIRAE. MOIRAE is a machine language program operated on-line with the Sigma-7 computer. It incorporates the major functions of the program MIKIMAUS, originally written by G. Berzins and outlined in Appendix D of (Ber 67).

The program provides a live display of the spectrum to be analyzed and provides the operator with the ability to execute instructions on the computer by means of sense switches arranged below the display oscilloscope. The spectrum may be expanded both horizontally and vertically and, if desired, the entire spectrum may be walked across the screen horizontally. In addition to the live spectrum display, the oscilloscope provides a movable channel marker, a display of the fitted background curve, the centroid position of the analysed peak, and the option of displaying the net spectrum resulting from the subtraction of all points below the fitted background. By means of the channel marker, the operator is allowed to select a set of points in the spectrum for determination of the background.

A polynomial curve of preselected order (up to degree 10) is fit to the data by means of an internal least squares fitting routine and displayed on the oscilloscope. If the curve is not satisfactory it may be rejected. If the curve is satisfactory the channel markers can then be released to define the limits of a particular peak. The computer then determines the center of gravity of the peak and its net area after subtracting the area below the background curve. This information (i.e. centroid, net peak area) is then output in the form of punched cards and/or via the line printer.

In order to determine the energies and relative intensities of the various gamma-ray peaks from such an analysis, it is necessary to use the data with an external program on the Sigma-7. The primary program for such an analysis is MOIRAE E(I). It determines the energies by performing a least squares quadratic fit to preselected peak centroids and interpolating for the others. Internal provisions allow for the calculation of the relative intensities of the peaks with an efficiency curve for the particular detector used in obtaining the spectrum.

There are some distinct disadvantages to the use of MOIRAE. Among them are the need for auxiliary programs and the inability of MOIRAE to strip out the individual peaks in an unresolved multiplet. This must either be performed by hand or by another program, such as SAMPO (a program which does many of the same operations as MOIRAE and is described in the following section).

2.3.2. Program SAMPO

This program was developed for the express purpose of performing automatic peak search and analysis of γ-ray spectra from semiconductor systems. It is described by Routti and Prussin (Rou 69) and, with modifications, has been adapted by C. Morgan for use on the Michigan State Sigma-7 computer. During the course of this study the program has been modified to allow the user to interact with the program via a storage oscilloscope. However, the majority of spectra in this study were analyzed without this feature.

The intent of the program is a development of a mathematical formalism for the representation of photopeaks and the continua in their vicinity. This formalism will then be applicable to the analysis of such spectra taken under a wide variety of experimental conditions. The program and its use on the Sigma-7 computer are described in greater detail in (Rou 69) and (Epp 70a) and in the MSU Nuclear Chemistry Annual Report for 1970. An abbreviated description follows.

The important features of the program are: a) the fitting of photopeaks to an analytical function (Gaussian-plus-exponential tails) in order to determine the precise centroid of each peak, b) a routine that searches the spectra and finds peaks, c) fitting and subtraction of background,

determination of energies and their statistical errors from an internally determined calibration curve, e) calculation of the net area of peaks, including the statistical error in the area, with conversion of these areas into relative intensities by means of an internally prepared calibration curve, and f) the stripping of multiplets using parameters determined from other well-resolved peaks.

The program determines peak fitting parameters from preselected, intense, well-isolated lines designated by the user. These peaks are fit with a Gaussian-plus-exponential shape function using a linear approximation for the background continua under the peak. Parameters for the other peaks in the spectrum are calculated by linearly interpolating between the selected fiducial lines.

Energies are determined by doing a piecewise linear fit between successive standard points selected by the user. If it is desired, higher order fits may be calculated but caution should be used in these cases to be sure the curve is smooth and does not oscillate. Relative intensities are calculated by means of an internal efficiency curve. This curve may be calculated for the program or determined by supplying external parameters.

Other features of the program include an option which instructs the program to automatically search for peaks in the spectrum. This option is useful in the initial inspection of the data, but is not to be relied on for the final analysis.

Proper use of the program involves considerable attention on the part of the user but the overall power of the program certainly warrants this.

2.3.3. Programs EVENT and EVENT RECOVERY

With the availability of large volume Ge(Li) detectors, the capability of doing high resolution Ge(Li)-Ge(Li) 2-dimensional coincidence experiments is easily realized. The immediate goal of such an experiment is to obtain coincidence information on any and all peaks or energy regions of a spectrum in a single run. A system capable of realizing this goal is diagrammed in Fig. 1.

Coincidence infomation is recorded using the task EVENT which runs under the JANUS monitor system of the Sigma-7 computer. Basically the program does the following. The addresses of the two coincidence events are each written in two halves of a word in one of two buffers. When the buffer is filled the 256 words are then stored sequentially on magnetic tape. Further details concerning this can be found in (Doe 69) and (Epp 70a).

The magnetic tape contains all the information concerning pairs of coincident events. All that remains is to retrieve the information from the tape. This is accomplished by selecting a peak or energy region of interest and searching the other half of the tape for events in coincidence with those of interest. These gated spectra are recovered

off-line on the Sigma-7 computer by means of the program EVENT RECOVERY (EV RE). This code allows the user to search the tape for a maximum of 10 gated regions per single pass through the tape. If desired, background subtraction may be affected for any and all of the gates included in a single pass. In the current study all the coincidence runs used a 4096x4096 array.

Chapter III

Identification of Members of the A=141 Decay Chain

The identification of a radioactive species to be studied relies on several interrelated techniques, such as a knowledge of the excitation function of the reaction used in the production of the isotope, identification of a known activity in the decay of the daughter, production of the isotope by other reactions (i.e. cross bombardments), a knowledge of the systematics of other nuclei in the region being studied, information obtained from charged particle reaction data, chemical separation, isotopic mass separation and identification of the x-rays associated with the decay.

What follows is a general description of the methods used in identifying the radioactive decays of members of the A=141 chain below the N=82 closed-shell. These include $^{141m+g}Nd$, ^{141}Pm, and $^{141m+g}Sm$. The sequence of decay is $^{141}Sm \rightarrow ^{141}Pm \rightarrow ^{141}Nd \rightarrow ^{141}Pr$ (stable), but the identification process starts with the stable isotope ^{141}Pr and proceeds away from stability in successive steps.

$^{141m+g}Nd$ constitutes the first link in the chain and has been studied by Beery (Bee 68). The following is a brief discussion of his results.

3.1. ^{141}Nd

^{141}Nd is produced by bombarding Pr_2O_3 (which is 99.97% pure) with 9-MeV protons to produce the reaction $^{141}Pr(p,n)^{141}Nd$. The energy at which this reaction occurs

is low enough that it is relatively free from the presence of unwanted competing reaction products. As an additional check on the identification, chemical separation was also used. The half-life of ^{141g}Nd was determined to be 2.5-hrs. and 10 transitions were identified with the decay. The energies of the more intense gamma-rays listed in order of increasing relative intensities in the gamma-ray singles spectrum are 1126.8-, 1292.8-, 145.4-, and 1298.7-keV.

The decay of ^{141m}Nd was found to involve a single transition of 756.7-keV from an $11/2^-$ isomeric level with a 60s half-life to the $3/2^+$ ground state. Additional information about the levels in ^{141}Pr comes from their observation in reaction studies such as (^{3}He,d), (d,^{3}He) (Wil 71) and (n,n'γ) (Dav 70).

3.2. ^{141}Pm

Making use of these ^{141}Nd results we can then proceed to identify the decay of ^{141}Pm. The principal means of producing ^{141}Pm was via the reaction ^{142}Nd(p,2n)^{141}Pm. Targets of Nd_2O_3 (enriched to $\geq$90% ^{142}Nd) were usually bombarded with 25-MeV protons from the Michigan State University cyclotron. An excitation curve was obtained using absorbers of different thickness to vary the incident beam energy from below threshold for the (p,2n) (Q=-14.2 MeV) reaction to well above the threshold for

the (p,3n) reaction (Q=-24.7 MeV). Results indicated the (p,2n) reaction to be relatively free from unwanted competing activity. Confirmation of the production of ^{141}Pm was established by observing transitions associated with the decay of the daughter ^{141}Nd. The ^{141}Nd transitions appeared in the spectra with the proper time dependence and in the correct relative intensity ratio. An additional check on the identification of ^{141}Pm was made by producing it via the ^{141}Pr(^{3}He,3n)^{141}Pm. These results comfirmed our identification of ^{141}Pm.

Several strong transitions associated with this decay were identified at 1223.3-, 886.3-, and 193.8-keV. Measurement of their intensities as a function of time corroborated previous results which had assigned a half-life of 22m to this isotope (Fis 52). Weaker transitions associated with the ^{141}Pm decay were identified by comparing their intensity to that of the 1223.3-keV line as a function of time.

Beginning 2m after each bombardment five successive 10 minute spectra were accumulated with the process repeated several times to improve statistics. Those gamma-rays which maintained a constant intensity relative to the 1223.3-keV line in the five successive spectra were identified with the decay of ^{141}Pm. Other transitions could be ruled out because their intensities varied erratically when compared to that of the 1223.3-keV transition.

Additional confirmation of the ^{141}Pm decay scheme resulted from the identification of several levels in ^{141}Nd populated in the charged particle reactions ^{142}Nd(p,d)^{141}Nd (Jol 71) (Cha 71) and ^{142}(d,t)^{141}Nd (Fos 71).

3.3. ^{141}Sm

Continuing up the A=141 chain we arrive at ^{141}Sm. From studies of systematics in the N=79 isotones it was expected that ^{141}Sm would possess two decay modes. A first mode associated with the decay of the ^{141}Sm ground state and the other mode would involve direct beta-decay from an $11/2^-$ isomeric level. This latter decay would be characterized by the population of three quasi-particle states in the daughter ^{141}Pm.

The primary method of production of ^{141}Sm was via the reaction ^{142}Nd(^{3}He,4n)^{141}Sm (Nd_2O_3 enriched to ≥90% ^{142}Nd) with a Q value of -27.3 MeV. This method proved to be relatively free from unwanted interfering activities. A careful study of the energy systematics of the reaction was performed by varying the incident beam energy from below the (^{3}He,4n) threshold to well beyond the (^{3}He,5n) threshold (Q=-36.2 MeV) in 1 MeV steps. It was observed that the maximum yield of ^{141}Sm occurred at 40 MeV, slightly beyond the (^{3}He,5n) threshold. These results were found to compare favorably with theoretical predictions made with the computer code CS8N. This is a Berkeley code used for the calculation

of heavy-ion cross sections. It has been modified for use on the Sigma-7 computer by Clare Morgan.

Assurance of the production of $^{141m+g}Sm$ came from the excitation function, the time dependence of the decay and finally from the growth and decay of the daughter activity ^{141}Pm. The strong transitions in the ^{141}Pm decay, such as the 886.3- and the 1223.3-keV lines, were readily identified in the proper intensity ratio. In addition, the x-ray spectra prominently displayed the Pm x-rays, which would arise from the beta-decay of a Sm isotope.

Results of the excitation function work indicated the presence of two distinct activities with half-lives of 11.3m and 22.1m. The longer lived 22.1m activity was identified as originating from the isomer ^{141m}Sm. This identification was made after determining that the 22.1m activity populated a delayed state in the daughter at 628.6-keV, which we concluded had a spin of $11/2^-$. The shorter lived activity was then identified with the decay of ^{141g}Sm. The similarity of the resultant ^{141g}Sm decay scheme with that of ^{139g}Nd is additional evidence which tends to support this identification.

In order to identify the transitions belonging to the decay of ^{141g}Sm and ^{141m}Sm, we took 6 successive 5 minute spectra, with the first such beginning 2 minutes after the end of the bombardment. The process was repeated

several times to enhance the statistics. Those transitions associated with the decay of ^{141g}Sm were identified as maintaining a constant intensity when normalized to the 403.9-keV transition ($\tau_{1/2}$=11.3m) in each of the six spectra. The transitions arising from the ^{141m}Sm decay were identified as exhibiting a constant intensity when compared to the 431.8-keV transition ($\tau_{1/2}$=22.1m) in each spectrum. On this basis we could then rule out transitions in the spectra which might arise from the decay of ^{140}Sm ($\tau_{1/2}$=6.0m) or ^{142}Sm ($\tau_{1/2}$=72m).

To further check the identification of the 11.3m activity as arising from the ^{141g}Sm decay we produced ^{141}Eu via the reaction ^{144}Sm(p,4n)^{141}Eu. We were then able to observe the presence of ^{141g}Sm peaks in the correct intensity ratio as they were fed by the decay ^{141}Eu $\underset{EC}{\beta^+}$ ^{141g}Sm. In addition to this we have been able to identify the vast majority of contaminant peaks.

Chapter IV

Experimental Results

4.1 Decay Schemes of ^{141m}Sm and ^{141g}Sm

Section 4.1.1. Introduction

These results of our study of the decay of $^{141m}_{62}Sm_{79}$ complement the similar work done on the decay of $^{139m}_{60}Nd_{79}$ by Beery, Kelly, and McHarris (Bee 69b). The decay of $11/2^-$ ^{139m}Nd selectively populates six high-spin states at relatively high energies in ^{139}Pr. These states were characterized as three-quasiparticle states having the configuration, $(\pi d_{5/2})(\nu d_{3/2})^{-1}(\nu h_{11/2})^{-1}$, and the preferred EC decay of ^{139m}Nd could be written as $(\pi d_{5/2})^2(\nu d_{3/2})^{-2}$ $(\nu h_{11/2})^{-1} \rightarrow (\pi d_{5/2})(\nu d_{3/2})^{-1}(\nu h_{11/2})^{-1}$.

The work on ^{139m}Nd decay led to the prediction by McHarris, Beery, and Kelly (McH 69) that other N=79 or N=77 nuclides might possess the requisite configurations for similar EC or β^+ decay into three-quasiparticle multiplets. In addition to the configuration, such a nuclide must also have sufficient decay energy to populate states above the pairing gap in its daughter, and it must be "hung up" with respect to other modes of decay—for example, if it is a metastable state the energy for the isomeric transition must be low enough to make that transition quite slow.

Working ones way out from β stability, he finds that ^{141m}Sm and ^{137m}Nd are the next likely candidates. For

ample, the addition of two protons to the ^{139m}Nd configuration duces the very similar configuration for ^{141m}Sm, $(\nu d_{5/2})^4(\nu d_{3/2})^{-2}(\nu h_{11/2})^{-1}$. The calculated Q_{EC} is more than MeV, allowing it to populate high-lying states in ^{141}Pm. nally, as in the other N=79 odd-mass isotones, the $h_{11/2}$→ $d_{3/2}$ (metastable → ground state) separation is small 171 keV) making the M4 isomeric transition very slow. The esults that we present in this study do indeed confirm these predictions—a multiplet of six, possibly seven, states lying between 1414.8 and 2702.4 keV in ^{141}Pm receives some 67% of the decay, and they appear to be three-quasiparticle states similar to those populated by ^{139m}Nd. Prior to the current investigation very little work had been done on ^{141}Sm, and, in fact, it is doubtful if it had been observed at all prior to 1967. In 1957 an activity reported (Pav 57) as ^{141}Sm was assigned a half-life of 17.5 to 22 days, in 1966 another report (Lad 66) concluded that ^{141}Sm must have a shorter half-life, probably less than three days. The first correct identification of ^{141m}Sm seems to have been made at about the same time by Bleyl, Münzel, and Pfinning (Ble 67) and by Arl't et al. (Arl 67). The results from these studies, primarily just half-life assignments are essentially in agreement with our results—we obtain a half-life of 22.1±0.3 min for ^{141m}Sm. In 1969 Hesse (Hes 69) published a more complete decay scheme and identified 32 γ rays as belonging

to the decay of this nuclide. However, his decay scheme was incomplete and there was some confusion in his not recognizing the presence of 11.3±0.3-min ^{141g}Sm. The latter species was first identified by Eppley and Todd (Epp 70a) and has a decay scheme paralleling that of ^{139g}Nd, (Section 4.1.4). Most recently, we presented (McH 70) a preliminary decay scheme of ^{141m}Sm in a talk at the Leysin Conference on Properties of Nuclei Far from the Region of Beta-Stability, and Arl't et al. (Arl 70b) presented an abstract at the same conference in which they recognized the three-quasiparticle nature of the three states in ^{141}Pm that receive the strongest population and in which they report a half-life of 9.5±0.5 min for ^{141g}Sm.

Section 4.1.2. Source Preparation and Identification of ^{141m}Sm and ^{141g}Sm

The principal means of producing ^{141g}Sm and ^{141m}Sm was via the reaction ^{142}Nd(^{3}He,4n)^{141}Sm (Q=-27.3 MeV). We have also produced ^{141}Sm indirectly by the ^{141}Sm(p,4n)^{141}Eu $\xrightarrow{EC}$ ^{141}Sm reaction (Q=-36.8 MeV). The second reaction was used primarily to enhance the production of ^{141g}Sm with the hope of being able to distinguish it better from ^{141m}Sm which is (too) abundantly produced in the first reaction.

The targets used in the ^{3}He bombardments consisted of 10-25 mg of separated $^{142}Nd_2O_3$ (>90% ^{142}Nd) obtained from

Ridge National Laboratory). These targets were bombarded with a 40-MeV ^{3}He beam from the MSU Sector-Focused Cyclotron. Beam currents were typically 0.1-1.0-μA, and bombardments were usually for periods of 1 to 5 minutes. For the proton bombardments, the targets consisted of ≈25 mg $^{144}Sm_2O_3$ (enriched to 95.1% ^{144}Sm, also from ORNL), the beam current was ≈0.5-μA at 45 MeV, for a period of 1-min. No chemical separation was attempted because of the short half-lives of ^{141g}Sm (11.3 min) and ^{141m}Sm (22.1 min).

In order to be certain of the identification of the two isotopes ^{141g}Sm and ^{141m}Sm, several methods of identification have been employed in this study. The principal reaction (^{3}He,4n) takes place rather far from the line of stability and at an energy of 40 MeV, and other reactions such as (^{3}He,αxn) might offer serious competition to the desired production mechanism making identification of the products a problem. For this reason a systematic study was made of the excitation function for the (^{3}He,4n) reaction from below threshold (Q=-27.3 MeV), to well beyond the threshold for the (^{3}He,5n) reaction (Q=-36.1 MeV). The study involved increasing the incident beam energy in 1 MeV steps from 27 MeV to 50 MeV. Several spectra were taken at each energy to aid in identification of the primary activity produced. These results demonstrated that the (^{3}He,4n) reaction was the dominant reaction between 34- and 40-MeV and competing

reactions were of little signifcance. We were able to identify several strong transitions which exhibited excitation curves consistent with the energy dependence of this reaction. The energies of these transitions were 196.6-, 403.8-, 431.8-, 438.4-, and 538.5-keV.

After the initial identification of these transitions as belonging to the decay of ^{141}Sm we measured the half-lives of their decay. The results of this half-life measurement indicated the 196.6-, 431.8-, and 538.5-keV transitions were associated with an activity whose half-life was 22.1±0.3m and the 403.8-keV and 438.4-keV were associated with an activity whose half-life was 11.3±0.3-min.

The longer lived 22.1-min activity was identified as belonging to ^{141m}Sm. This identification of the ^{141m}Sm activity was made by observing that the 538.5-keV transition fed a delayed $11/2^-$ isomeric level in ^{141}Pm (half-life of 700±20 ns). This would be the case if the state in ^{141m}Sm was a high spin state, i.e. an $11/2^-$ isomeric level. This result was anticipated from a previous knowledge of other odd mass N=79 isotones which possessed $11/2^-$ isomeric levels. The 403.9-keV transition ($\tau_{1/2}$=11.3-min) was then identified as belonging to the decay of ^{141g}Sm.

Further evidence that these five transitions are associated with the decay of a Sm isotope comes from x-ray-gamma 2-dimensional coincidence studies. This

experiment is identical to a Ge(Li)-Ge(Li) 2-dimensional experiment except one of the Ge(Li) detectors is replaced by a Si(Li) x-ray detector. Each of these 5 transitions was found to be in coincidence with the x-rays of Pm, confirming that their production arises from the beta decay of a Sm isotope.

4.1.3. Experimental Results

4.1.3.A. Half-Life Determinations of ^{141g}Sm and ^{141m}Sm

The half-lives of ^{141m}Sm and ^{141g}Sm were determined simultaneously with the aid of the MSU Cyclotron Laboratory Sigma-7 computer and a computer code called GEORGE (GEOR). This allowed the accumulation of 40 successive 4096-channel spectra, each of 2-min duration. A pulser peak (60 Hz) was included in each spectrum to allow determination of the proper dead-time correction.

The half-life of ^{141m}Sm was determined independently from the 196.6-, 431.9-, and 538.5-keV peaks (cf. next section). The results were then averaged to yield a value of 22.1±0.3-min. (The spectra and half-life curves can be found in (Epp 70). The half-life of ^{141g}Sm was determined from the 403.9-keV peak and the result obtained was 11.3±0.3-min.

4.1.3.B. γ-Ray Singles Spectra

Two Ge(Li) detectors were used to cross-check each other in making energy and intensity measurements on the ^{141m}Sm γ rays. These were a five-sided coaxial detector

having 2.5% efficiency (at 1332 keV compared with a 3x3-in. NaI(Tℓ) detector, source distance 25 cm) and a true coaxial detector having 10.4% efficiency. Under typical operating conditions, using a cooled FET preamplifier, an RC linear amplifier with near-Gaussian shaping and DC-coupled base-line restoration, and 12- or 13-bit ADC's coupled to a PDP-9 or Sigma-7 computer, we achieved a resolution of ≈2.2 keV FWHM for the ^{60}Co 1332-keV peak.

The energies of the prominent ^{141m}Sm γ rays were determined by counting the ^{141}Sm source simultaneously with several well-known calibration standards. Above 800 keV, ^{56}Co was the principal standard, (Cam 71) while at lower energies ^{54}Mn, ^{57}Co, ^{141}Ce, ^{137}Cs, ^{207}Bi, and ^{243}Cm (cf. (Epp 70) were used. A number of spectra were taken, and the energies of the stronger ^{141m}Sm γ rays were obtained from the average values. These peaks were then used to determine the energies of the weaker ^{141m}Sm γ rays, which were obscured by the standards. The relative intensities were determined by correcting the net peak areas by using a previously prepared efficiency curve. For more details on the methods of data reduction used, cf. (Epp 70) or (Epp 71). The first and sixth of the successive 5-min singles spectra that were used to determine the energies and intensities and to assign γ rays on the basis of half-life are shown in Figs. 4 and 5.

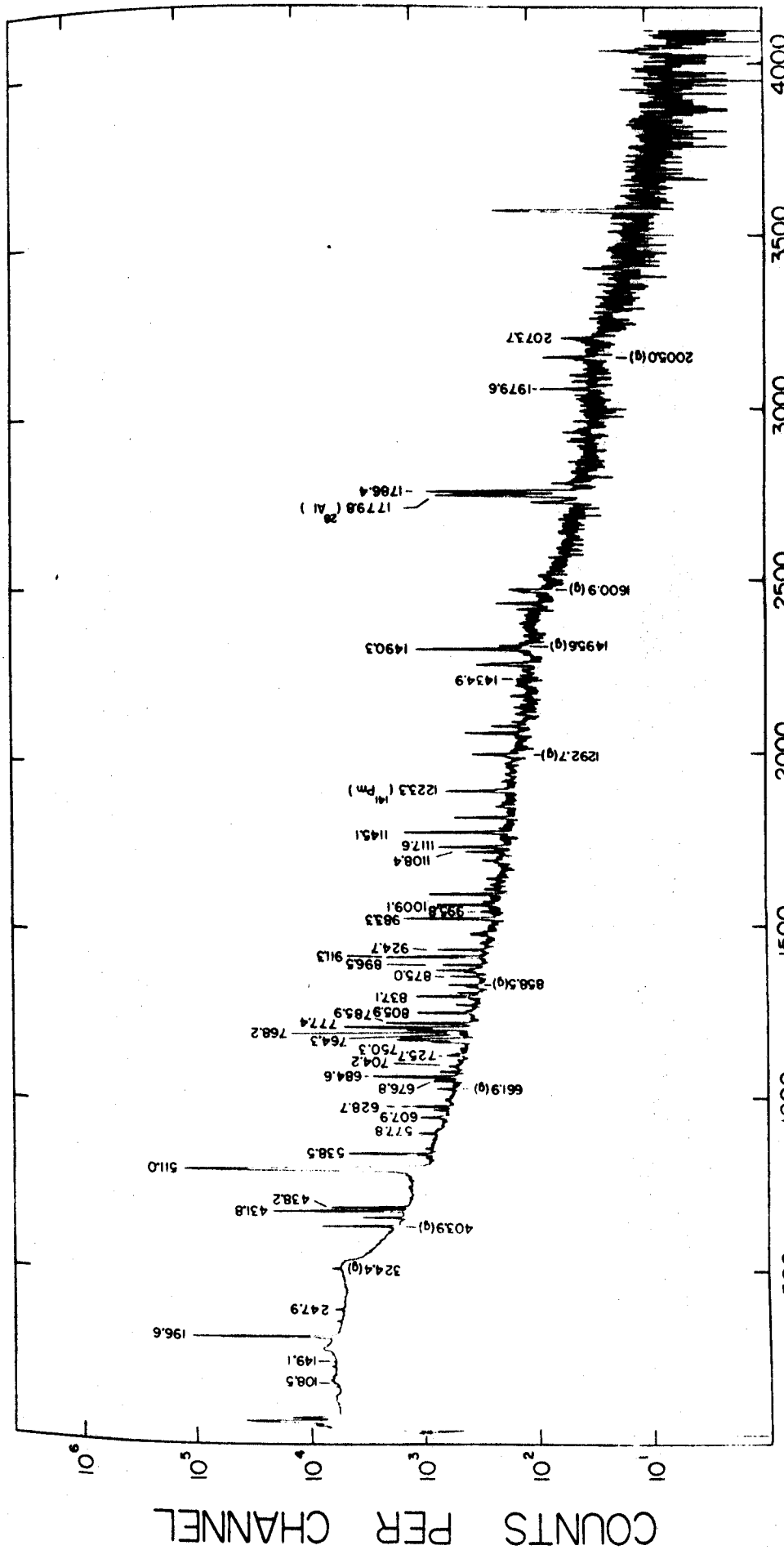

Figure 4. Singles γ-ray spectrum for $^{141m+g}$Sm taken with 10.4% Ge(Li) detector. First of six successive 5 m spectra.

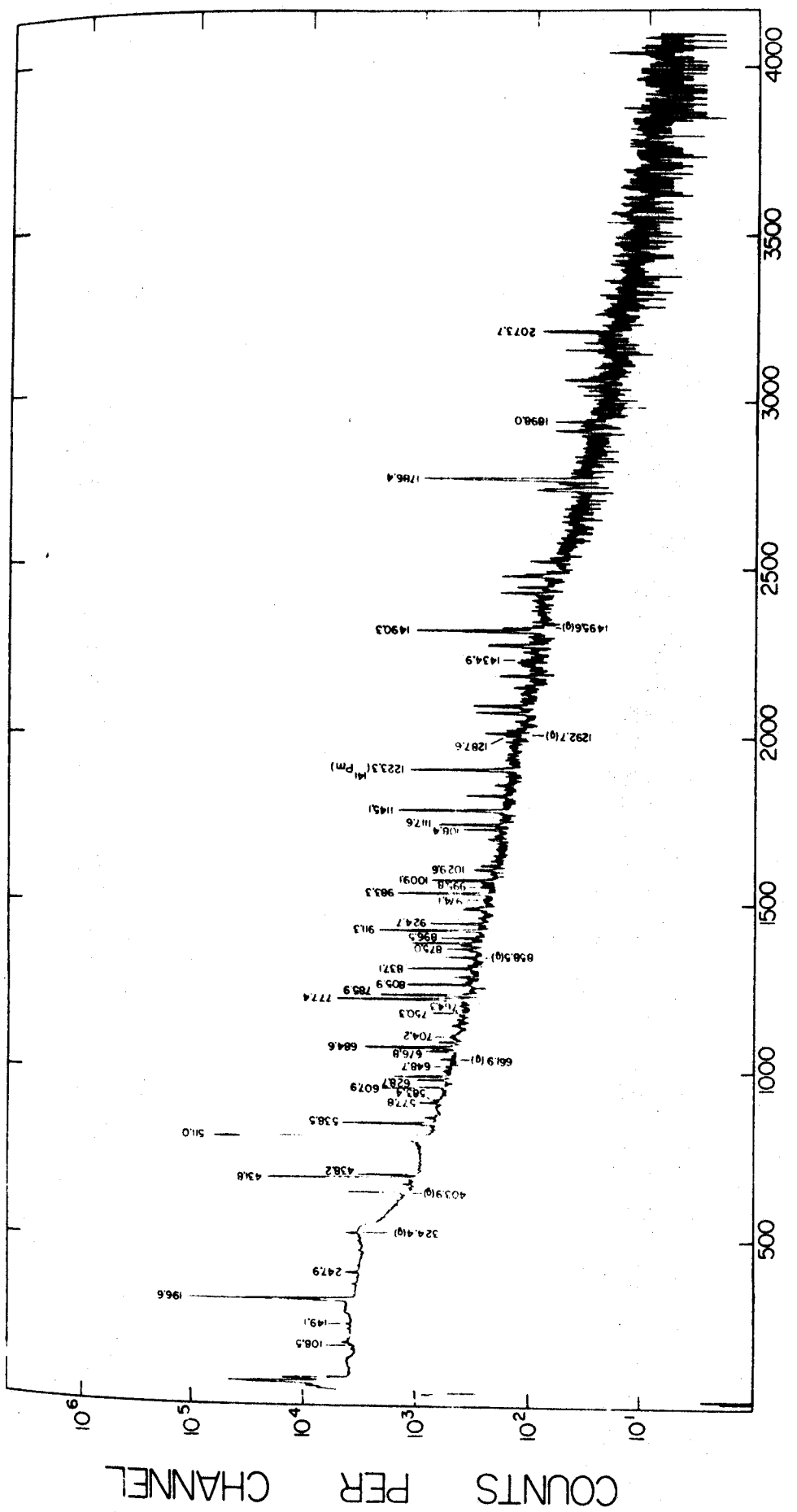

Figure 5. Singles γ-ray spectrum for ^{141mtg}Sm taken with the 10.4% Ge(Li) detector. Last of six successive 5 m spectra.

Table II. Energies and Relative Intensities of γ Rays From the Decay of ^{141m}Sm

This Work		Hesse (Hes69)	
Energy (keV)	Intensity	Energy (keV)	Intensity
108.5±0.3	0.5 ±0.1	---	---
149.1±0.3	0.7 ±0.2	---	---
196.6±0.3	184 ±18	196.5±0.5	260 ±30
247.9±0.2	1.91±0.35	---	---
431.8±0.1	100 ±5	431.7±0.5	100 ±10
538.5±0.3	20.9 ±1.4	538.0±0.5	18 ±5
577.8±0.3	2.2 ±0.6	---	---
583.4±0.3	0.7 ±0.2	---	---
607.9±0.2	2.5 ±0.3	---	---
628.7±0.1	6.6 ±0.20	628.3±0.5	6.8±1.0
648.7±0.3	0.9 ±0.2	---	---
676.8±0.3	3.4 ±0.5	---	---
684.6±0.2	19.6 ±1.5	684.2±0.5	21.8±2.6
704.2±0.3	1.1 ±0.2	---	---
725.7±0.5	3.6 ±0.6	726.3±0.7	9.9±1.7
750.3±0.3	3.9 ±0.60	749.5±0.8	4.6±1.0
764.3±0.3	0.4 ±0.1	---	---
768.2±0.5	0.4 ±0.1	---	---
777.4±0.3	50.3 ±2.0	777.1±0.5	58.2±7.0
785.9±0.1	16.9 ±1.0	785.8±0.5	20.7±2.5
805.9±0.1	8.8 ±1.6	806.0±0.6	10.8±1.6
820.7±0.3	0.4 ±0.1	---	---
837.1±0.2	8.87±0.30	836.7±0.7	11.5±3.0
875.0±0.1	3.1 ±0.1	874.6±0.7	4.6±1.0
882.0±0.3	0.4 ±0.1	---	---
896.5±0.1	3.6 ±0.4	896.2±0.7	5.6±1.5

Table II. - Continued.

This Work		Hesse (Hes69)	
Energy (keV)	Intensity	Energy (keV)	Intensity
911.3±0.3	22.8 ±0.6	911.1±0.5	26.5±3.5
924.7±0.1	5.7 ±0.8	924.4±0.7	6.9±1.3
952.1±0.2	2.2 ±0.1	---	---
955.4±0.5	1.7 ±0.1	---	---
974.1±0.5	0.5 ±0.1	---	---
983.3±0.3	18.0 ±0.8	982.9±0.5	21.6±3.5
995.8±0.5	0.9 ±0.2	---	---
1009.1±0.4	7.2 ±0.6	1008.3±0.5	10.5±2.0
1029.6±0.6	1.3 ±0.3	---	---
1108.4±0.2	3.1 ±0.3	---	---
1117.6±0.2	8.0 ±0.6	1117.2±0.6	11.1±1.8
1145.1±0.2	21.6 ±0.8	1144.9±0.5	27.5±4.0
1287.6±0.4	0.7 ±0.3	---	---
1380.9±0.6	0.5 ±0.2	---	---
1434.9±0.4	0.9 ±0.3	---	---
1463.4±0.6	4.5 ±0.8	1462.1±0.8	5.4±2.0
1490.3±0.1	22.9 ±1.5	1490.2±0.5	27.4±3.5
1786.4±0.4	27.1 ±1.1	1785.9±0.6	33.6±4.0
1898.0±1.0	0.94±1.15	1898.5±1.2	2.5±1.0
1979.6±0.2	0.99±0.12	1979.2±0.8	1.6±0.7
2073.7±0.2	3.53±1.2	2072.9±0.6	11.8±2.0
---	---	1136.6±0.8[a]	5.2±1.5
---	---	1530.7±1.0[a]	2 ±1
---	---	1879.9±0.8[a]	6.3±1.5
---	---	1966.9±0.8[a]	2.5±1.0
---	---	2281.1±1.0[a]	1.5±0.5
---	---	2302.6±1.0[a]	1.1±0.4
---	---	2582.3±1.0[a]	2.9±0.8

[a] These γ rays could not be identified in the present investigation.

On the basis of half-lives and relative intensities we have assigned at least 47 γ rays to ^{141m}Sm decay. The energies and intensities of these are listed in Table II where they are compared with the results obtained by Hesse (Hes 69). The two sets of data are in fair agreement, but we see many weak transitions that he did not observe, and we do not include seven γ rays that he associated with ^{141m}Sm decay.

4.1.3.C. Prompt γ-γ Coincidence Spectra

Several types of prompt coincidence experiments were performed using Ge(Li)-Ge(Li) and Ge(Li)-NaI(Tℓ) spectrometers. These included two-dimensional coincidence experiments, pair spectra experiments, and anticoincidence experiments.

Details of the two-dimensional coincidence experiment can be found in (Epp 70a), (Epp 71), and (Gies 71) so they will not be repeated. Suffice it to say that the 2.5% efficient Ge(Li) detector and another one having 3.6% efficiency (also 2.0 keV resolution FWHM at 1332 keV) were placed in 180° geometry, with a graded Pb shield placed between them to help prevent scattering from one detector into the other. Coincident events (resolving time, 2τ=160 nsec) from both sides were processed, and their addresses were listed in pairs on magnetic tape. This yielded a 4096x4096-channel array of prompt coincidence

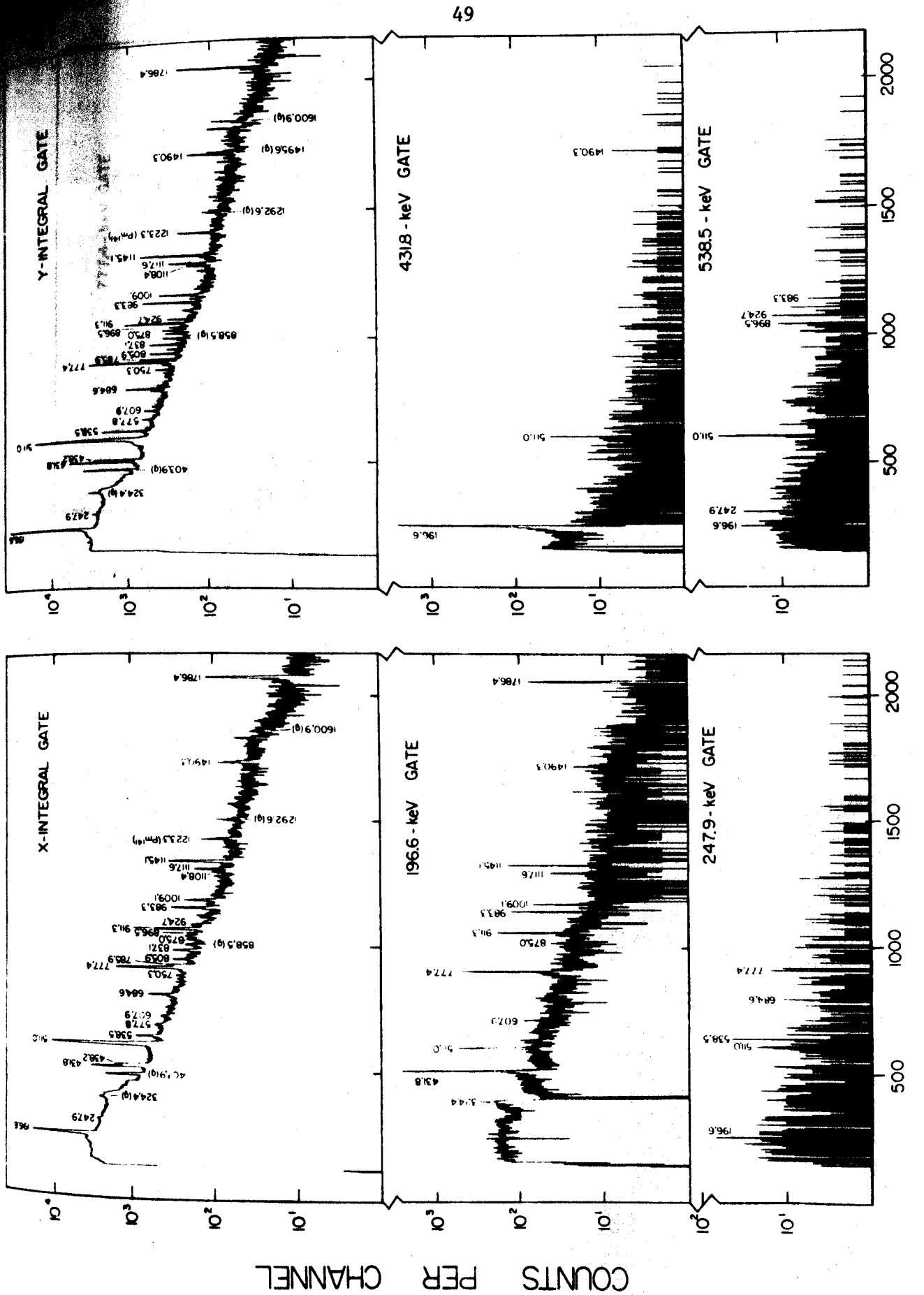

Figure 6. Results of two-dimensional Ge(Li)-Ge(Li) coincidence experiments for ^{141m}Sm.

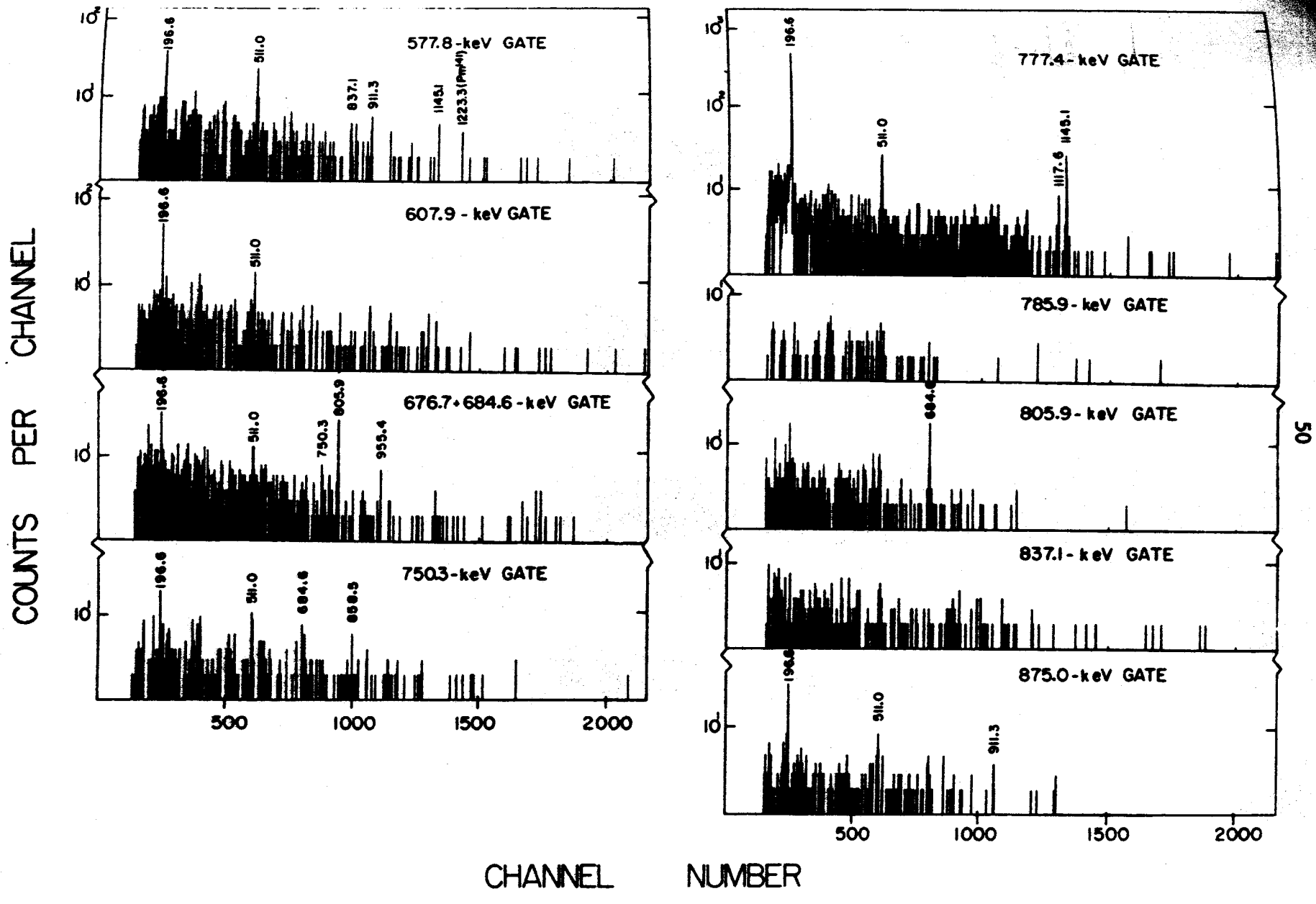

Figure 7. Additional gated slices from the two-dimensional Ge(Li)-Ge(Li) coincidence experiments on ^{141m}Sm.

Table III. Summary of γ-γ Two-Dimensional Coincidence Results for ^{141m}Sm

Gate Energy (keV)	γ-Rays Enhanced (keV)
Integral	196.6, 247.9, 538.5, 577.8, 607.9, 684.6, 750.3, 777.4, 805.9, 837.1, 875.0, 896.5, 911.3, 924.7, 983.3
196.6	431.8, 607.9, 777.4, 875.0, 911.3, 983.3, 1009.1, 1117.6, 1145.1, 1490.3, 1786.4
247.9	538.5
431.8	196.6, (1490.3)[a]
538.5	247.9, 896.5, 924.7
577.8	837.1 (weak)
607.9	196.6
676.7+684.6	(196.6)[a], 750.3, 805.9
750.3	(196.6)[a], 684.6, 858.5[b]
777.4	196.6, 1117.6, 1145.1
785.9	No coincidence in evidence
805.9	684.6
837.1	No coincidence in evidence
875.0	196.6, 911.3
911.3	196.6, 875.0, 983.3
924.7	(196.6)[a], 538.5, (777.4)[a]
952.1	538.5
983.3	196.6, 911.3
1009.1	196.6, 777.4

Table III. - Continued

1117.6	196.6, 777.4
1145.1	196.6, 777.4
1490.3	(196.6)[a]
1786.4	196.6

[a]These intensities are less than expected for these transitions to be in coincidence. They are considered to arise from chance coincidences.

[b]This is not a ^{141m}Sm transition.

events, which could later be sorted off-line in gated slices. The integrated coincidence spectra from each detector are shown at the top of Fig. 6. Some representative gated spectra are shown in the remainder of Fig. 6 and in Fig. 7; the remaining gated spectra can be found in (Epp 70). In these spectra gates were set on the X side (2.5% detector) and the displays were taken from the Y side (3.6% detector). A summary of the two-dimensional coincidence results is given in Table III.

The pair (511-keV-511-keV-γ) coincidence spectrum shown in Fig. 8 was obtained with total annihilation absorbers around the sources and the 2.5% Ge(Li) detector placed inside an 8x8-in. NaI(Tℓ) split annulus (Aub 67). The single-channel analyzer associated with each half of the annulus had its window adjusted to accept only the 511-keV region. A triple coincidence (2τ=100 nsec) was required before the fast coincidence unit would generate a gate signal and allow pulses from the Ge(Li) detector to be stored. Thus, only double-escape peaks and peaks due to transitions from levels fed by β^+ decay appear in the spectrum in Fig. 8. The $\gamma^{\pm}$ peak is a measure of the chance contributions to the spectrum.

Finally, to complement the various coincidence spectra, an anticoincidence spectrum was taken, again employing the 2.5% Ge(Li) detector and the 8x8-in. NaI(Tℓ) split annulus.

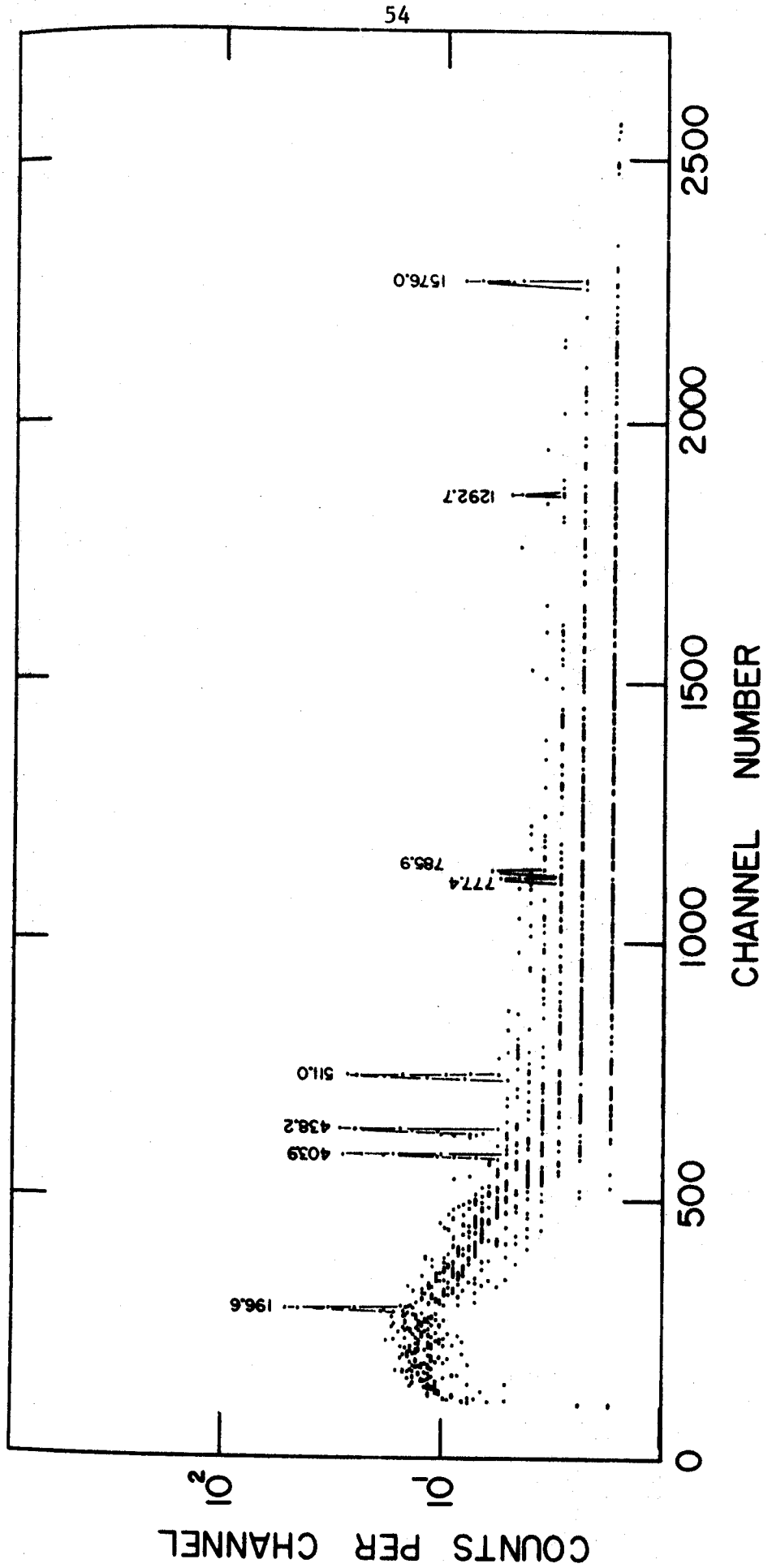

Figure 8. 511-511-keV-γ coincidence spectrum for $^{141m+g}$Sm.

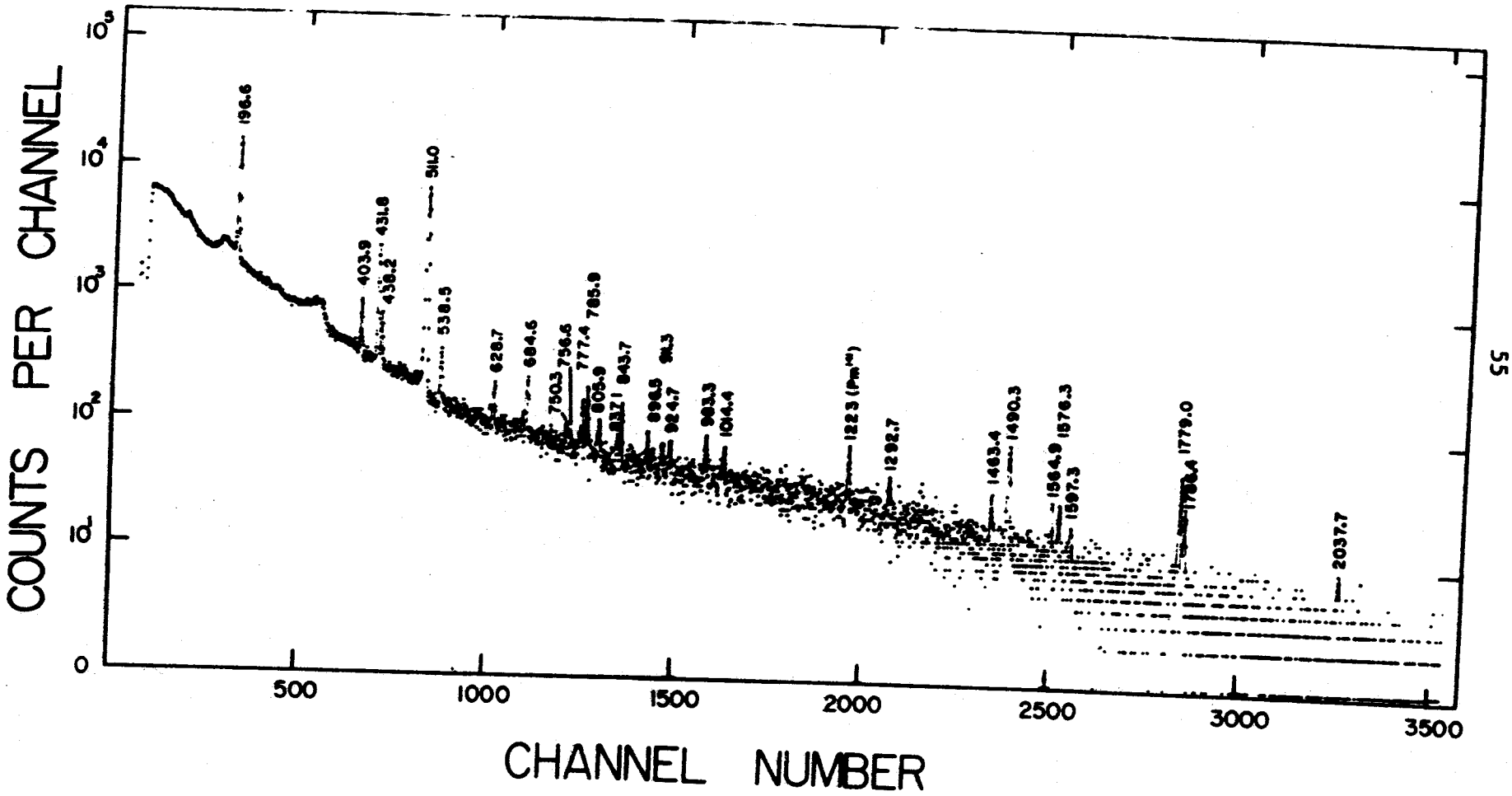

Figure 9. $^{141m+g}$Sm anticoincidence spectrum.

Table IV. γ-Ray Intensities for ^{141m}Sm Coincidence Experiments

Energy (keV)[a]	Relative Intensities				
	Singles[a]	Anti-Coinc.	Integral Coinc.	196.6-keV Gate	Delayed Integral Coinc.
196.6	100	77.1	60.4	---	5.74
247.9	1.04	1.67	0.98	---	1.67
431.8	54.6	2.32	22.3	53.0	2.32
538.5	11.3	11.3	8.81	---	11.3
577.8	1.22	---	1.30	---	---
607.9	1.38	---	1.79	1.90	---
628.7	3.60	---	---	---	---
684.6	10.6	8.32	7.30	---	8.32
725.7	1.95	---	---	---	---
750.3	2.14	1.55	1.70	---	1.55
777.4	27.4	---	27.4	27.4	---
785.9	9.20	10.2	4.99	---	10.2
805.9	4.78	4.50	3.45	---	4.50
837.1	4.82	---	3.99	---	---
875.0	1.68	---	1.64	1.97	---
896.5	1.95	---	1.33	---	---
911.3	12.4	---	12.6	12.3	---
924.7	3.08	1.67	2.06	---	1.67
952.1	1.20	---	0.82	---	---
955.4	0.91	---	---	---	---
974.1	0.27	---	---	---	---
983.3	9.80	---	8.03	7.96	---
1009.1	3.93	---	4.04	4.46	---
1029.6	0.68	---	---	---	---
1108.4	1.67	---	1.64	---	---
1117.6	4.37	---	3.99	3.97	---
1145.1	11.8	---	12.3	14.1	---
1463.4	2.43	---	---	---	---
1490.3	12.5	17.9	3.38	---	17.9

Table IV. - Continued.

Energy (keV)	Relative Intensities				
	Singles	Anti Coinc.	Integral Coinc.	196.6-keV Gate	Delayed Integral Coinc.
1786.4	14.6	---	9.78	17.0	---
1898.0	0.51	---	---	---	---
1979.6	0.54	---	---	---	---
2073.7	1.92	---	---	---	---

[a]The errors placed on these values are given in Table I.

This spectrum is shown in Fig. 9. The ^{141m}Sm source was placed at the center of the annulus tunnel, with the Ge(Li) detector in one end and a 3x3-in. NaI(Tℓ) detector at the other end. The Ge(Li) detector was operated in anticoincidence with γ rays above 100 keV in the NaI(Tℓ) detectors (2τ=100 nsec). The true-to-chance ratio was ≃100/1. This spectrum enhances those transitions that are not in prompt coincidence with the other γ rays or with β^+ emission. It is particularly useful in placing transitions to the ground state or to a metastable state, providing those transitions are primarily EC fed and not β^+ fed.

A summary of the relative intensities of ^{141m}Sm γ rays in some of the more important coincidence spectra is given in Table IV.

4.1.3.D. Delayed Coincidence Spectra

The systematic behavior of states in this nuclear region suggested the presence of a metastable $\pi h_{11/2}$ state in the daughter, ^{141}Pm. In the earlier work on ^{139m}Nd decay (Bee 69b) a delayed coincidence spectrum was essential in elucidating the decay to the higher-lying states, so we felt compelled to perform similar experiments here.

We have identified this state as the state at 628.6-keV in ^{141}Pm and we have determined its half-life to be

700±20 ns. This half-life is long enough to obtain useful integral coincidence information using a resolving time of 100 ns.

Three types of delayed coincidence spectra were obtained. The first two spectra, shown in Figs. 10 and 11 are delayed integral coincidence spectra, the third set of coincidence spectra pertain to the measurement of the lifetime of the 628.6 keV state and are shown in Fig. 12 and 13.

In the first of the delayed integral coincidence spectra, shown in Fig. 10, the gate signal is delayed 250 ns with respect to the linear signal. The result of this is to enhance those transitions that depopulate the state having an appreciable half-life. In the second, shown in Fig. 13, the linear signal was delayed 250 nsec with respect to the gate. Here the result is to enhance those transitions feeding the state having an appreciable half-life. The latter primarily are the transitions that depopulate what we propose as three-quasiparticle states, so this spectrum is crucial in identifying these high-lying, high-spin states.

In order to measure the half-life of the 628.6 keV level we used a modified version of a fast-slow coincidence system, with a 10.4% Ge(Li) detector in the start leg of the system and one-half of the 8x8-in NaI(Tℓ) split annulus in the stop leg. Any pulse above 30-keV in the Ge(Li)

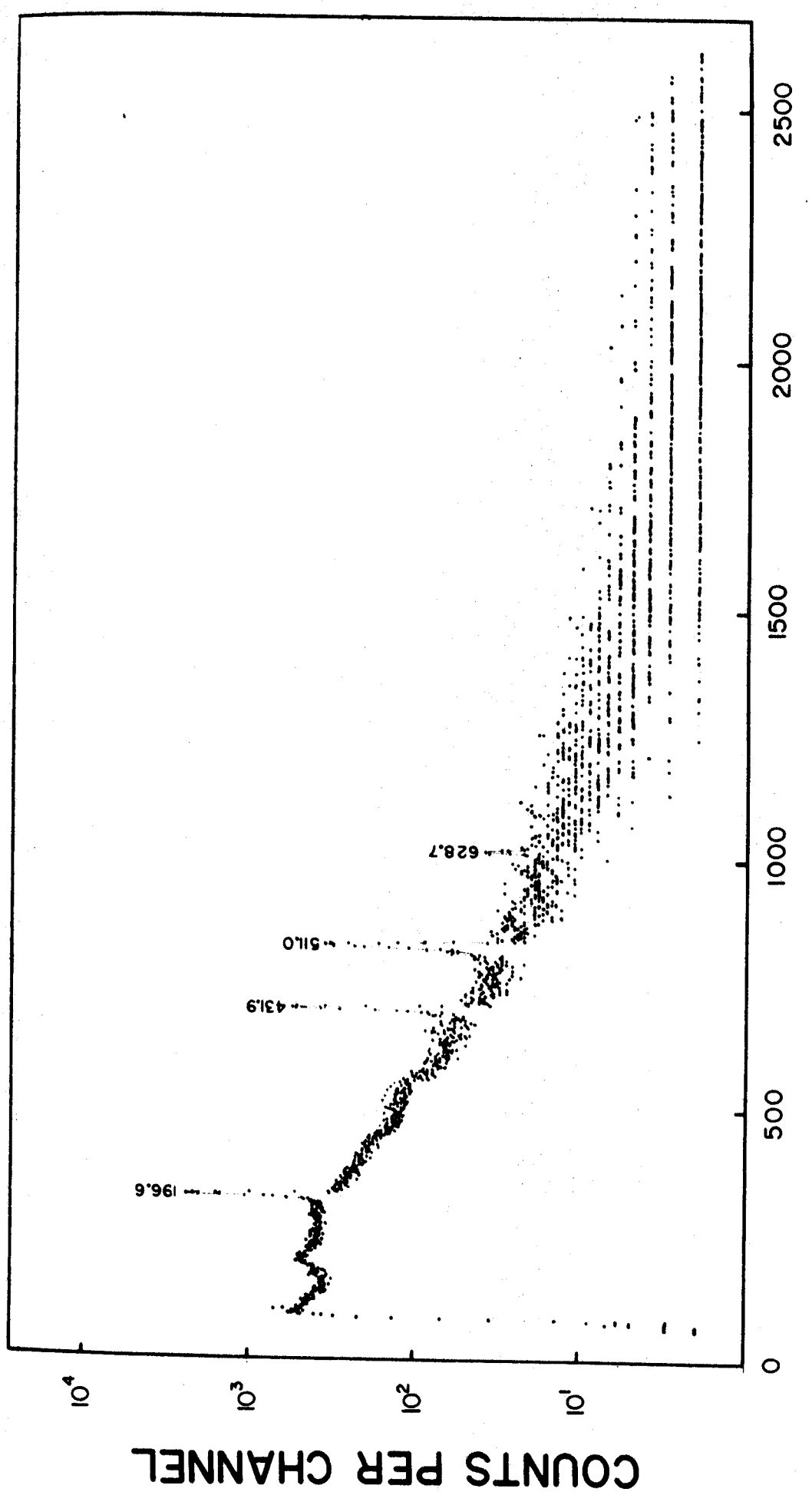

Figure 10. Delayed-gate integral coincidence spectrum for ^{141m}Sm.

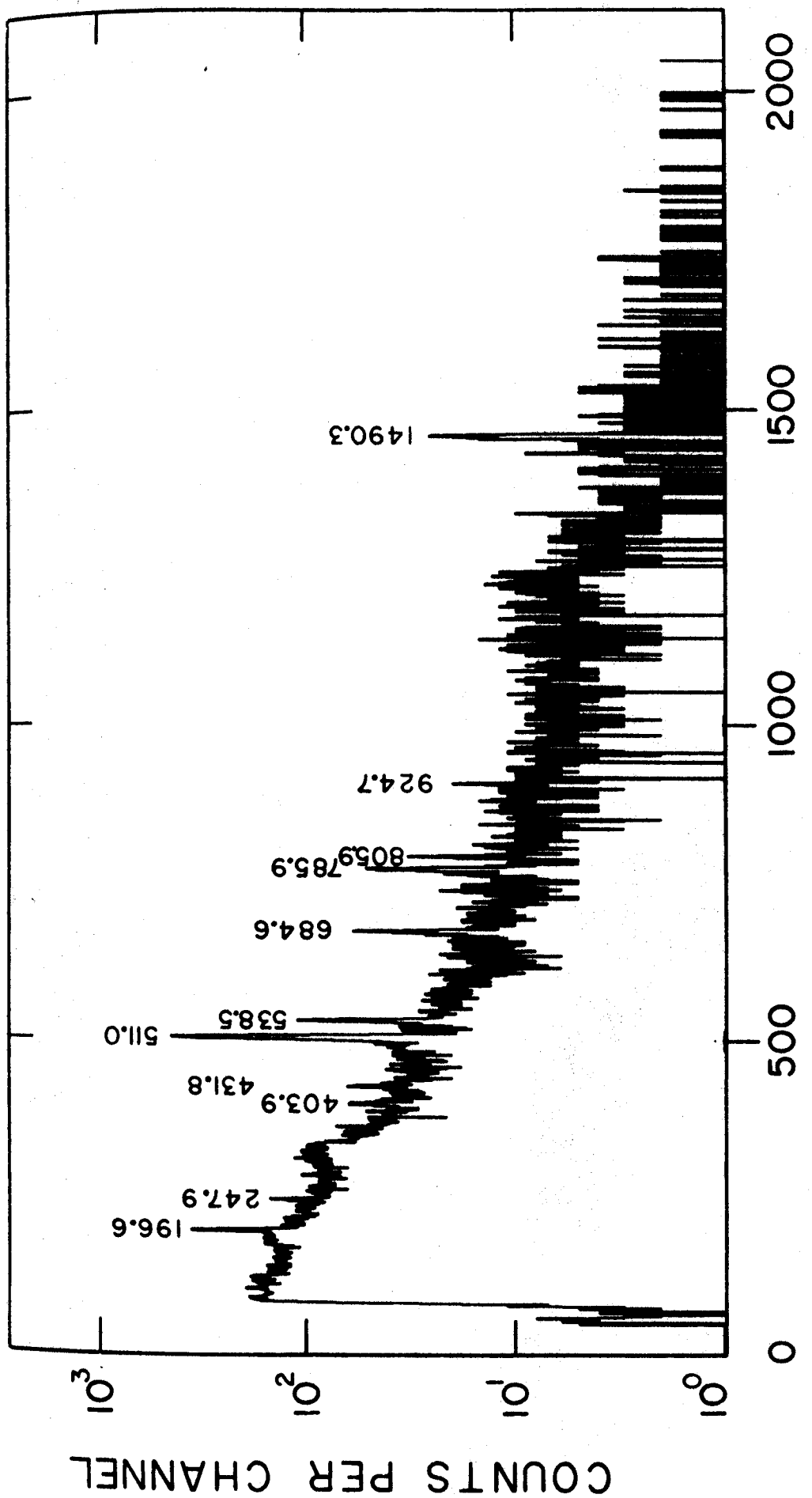

Figure 11. Delayed-signal integral coincidence spectrum for ^{141m}Sm.

detector started the TPHC (time-to-pulse-height-convertor) and any pulse arising in the NaI(Tℓ) detector above the 511.0 keV annihilation peak stopped the TPHC. Two-parameter data were accumulated (time vs. Ge(Li) energy) using TOOTSIE (Bay 71). The data were stored on magnetic tape using the auxiliary program EVENT and recovered off-line.

These experimental results are shown in Figs. 12 and 13. The top spectrum in Fig. 12 is the Ge(Li) integral coincidence spectrum, the center spectrum in Fig. 12 represents pulses generated by the TPHC, while the spectrum at the bottom of Fig. 12 is the calibration spectrum used to test the TPHC linearity. In the TPHC spectrum in Fig. 12 the pulse height is proportional to the time interval between the Ge(Li) pulses and the electronically delayed NaI(Tℓ) pulses—the prompt coincidence peak appears on the right in the TPHC spectra.

The three spectra seen in Fig. 13 were obtained by gating on the peaks at 196.6-, 431.8-, and 628.6-keV, respectively, in the Ge(Li) integral coincidence spectrum and displaying

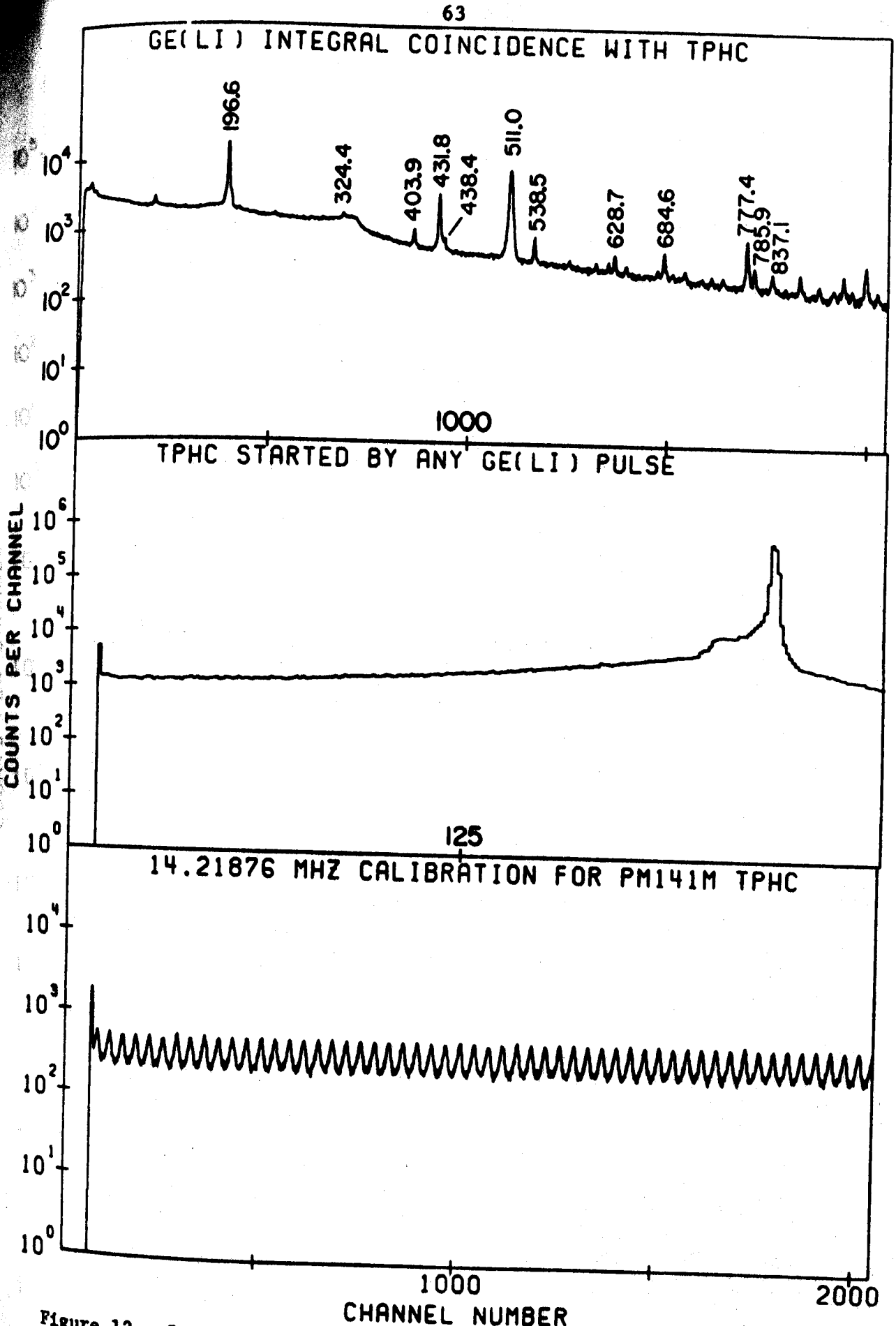

Figure 12. Spectra resulting from two-dimensional coincidence (energy vs. time) measurement of the lifetime of delayed state at 628.6-keV in ^{141}Pm.

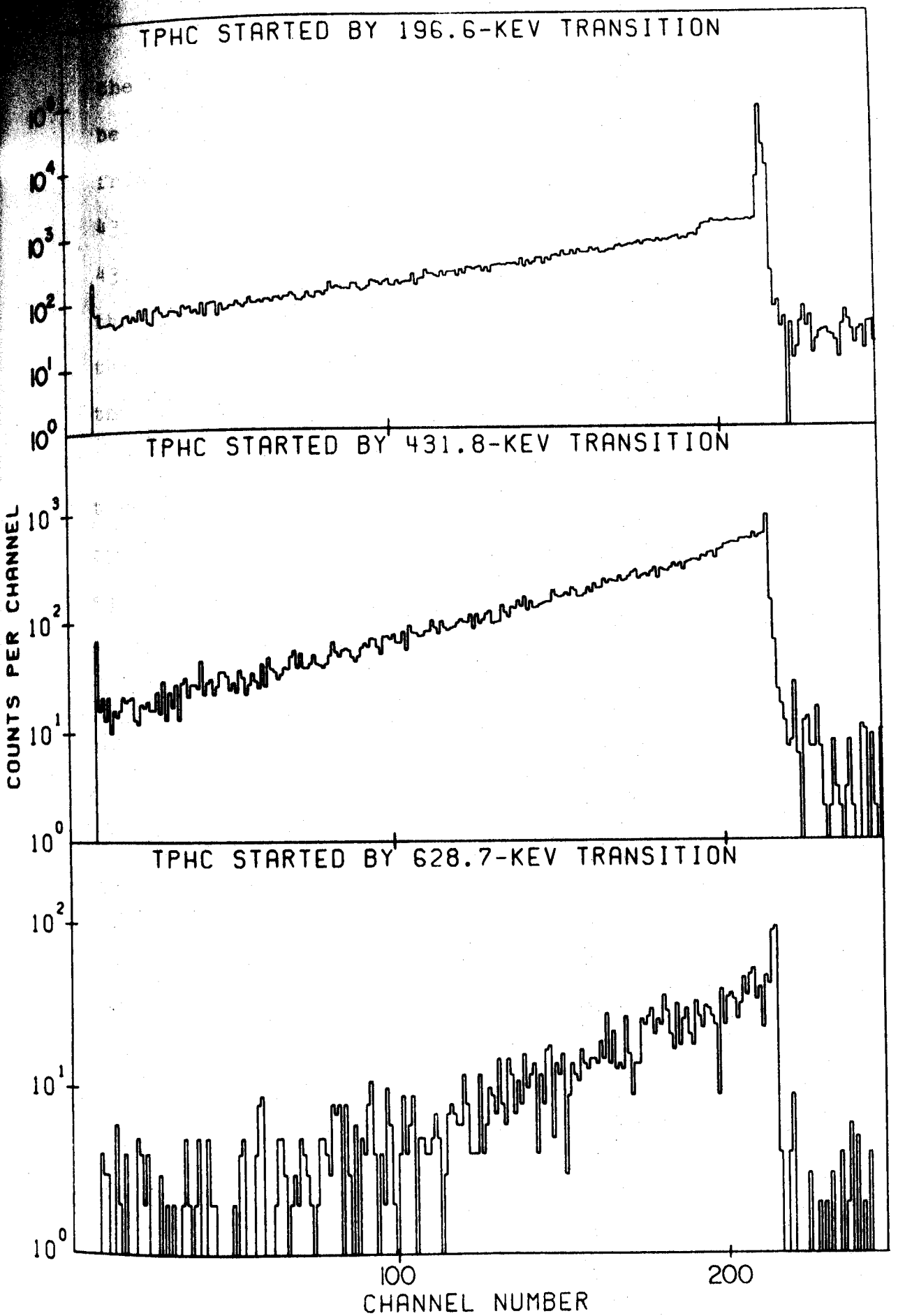

Figure 13. TPHC spectra obtained from half-life measurement of the delayed

the TPHC coincidence pulses. From the decay scheme it can be observed that the 628.6-keV transition represents decay from the isomeric level directly to ground while the 431.8- and 196.6-keV transitions are in cascade. The 431.8 keV transition is from the $11/2^-$ isomeric level to the first excited state. It should be noted that these three spectra are not plotted to the same scale. However, the slope of the three time spectra are essentially the same.

The resolution of the system is 10.0 ns FWHM, and the timing calibration was obtained using RF pulses from the cyclotron. Calculation of the half-life followed a least-squares fit to the logarithms of the data in Fig. 13 (after subtraction for chance coincidences). The value of the half-life was determined to be 700±20 ns. These results indicate the E3 transition from the $11/2^-$ isomeric level to ground is enhanced over the single particle estimate by a factor of 1.6. Correspondingly, the 431.8 keV M2 transition is retarded by a factor of 58. A similar $11/2^-$ state identified in ^{145}Eu at 625.2-keV has been observed to have a lifetime of 800 ns.

It should be noted that the 196.6 keV transition from the $7/2^+$, first excited state to the $5/2^+$ ground state involves $(\nu g_{7/2}) \rightarrow (\nu d_{5/2})$, and hence is an ℓ-forbidden M1. We were unable to determine the lifetime of the 196.6 keV state but we are able to place a limit of, $\tau_{1/2} < 2$ ns, for its half-life from these data.

4.1.3.E. Energy Separation of the Two ^{141}Sm Isomers

Because the ^{141}Sm isomers so admirably meet the requirements of essentially separate decays, it is difficult to determine their energy separation with much precision. Based on a least-squares fit of the previously measured M4 transitions in the other N=79 nuclei, we arrive at an energy of 171.6 keV between the two. An M4 transition of this energy, compared with the EC/β^+ half-life, would be expected to be quite weak. The vicinity of 172 keV is a particularly unfortunate region for the observation of a photon of low intensity, since the backscatter peak from annihilation quanta is 170 keV. We have looked for the isomeric transitions both in γ-ray and electron spectra (using a Si(Li) detector) without success. An M4 transition of this energy should be somewhat easier to see in the electron spectra than in the γ-ray spectra, as the conversion coefficient should be large ($\simeq$4) (Hag 68); however, there is no evidence of any transition peaks above the β^+ continuum. Based on the statistics of our γ-ray spectra, we have placed an upper limit of 0.2% of the total ^{141m}Sm decay for this transition. The results of the different investigating groups who have considered the relations between ^{141m}Sm and ^{141g}Sm are summarized in Table V.

Table V. Published Estimated Relations Between ^{141m}Sm and ^{141g}Sm

Authors	$t_{1/2}(^{141m}Sm)$	$t_{1/2}(^{141g}Sm)$	E_γ (for *M*4)	% *M*4 in decay
Arl't et al. (Arl67)	21.5 min	<10 min	215 keV	---
Bleyl, Münzel, and Pfenning (Bley67)	23.5 min	≈2 min	≈200 keV	<1%
Arl't et al. (Arl70)	22.5 min	9.5±0.5 min	---	---
This work	22.1±0.3 min	11.3±0.3 min	≈171.6 keV	<0.2%

4.1.4. ^{141m}Sm Decay Scheme

We have constructed a decay scheme for ^{141m}Sm from a combination of the foregoing prompt and delayed coincidence spectra, aided only incidentally by energy sums and intensities. This decay scheme is presented in Fig. 14a along with the decay scheme (Bee 69b) of ^{139m}Nd, Fig. 14b, with which it should be compared. Of the 47 γ rays that we concluded belonged to ^{141m}Sm decay, only six very weak ones could not be placed. All energies are given in keV, and since the presence of ^{141g}Sm in our sources prevented a precise measurement of the ^{141m}Sm β^+ spectra, the Q_{EC} of ≈5015 keV is a calculated value (Myr 65). The (total) γ-transition intensities are given in percent of the disintegrations of ^{141m}Sm. The β feedings are also given in percent of ^{141m}Sm disintegrations, and they include both the β^+ and EC decay—the surprisingly small β^+ feedings will be discussed below. The energy assigned to each level is a weighted average based on our confidence in the energy precision of the transitions out of that level. In Table VI we compare our level scheme with those obtained by Hesse (Hes 69) and Arl't *et al.* (Arl 67) and (Arl 70b).

The discussion of the construction of this decay scheme will be broken into two parts: discussion of 1) those levels whose mode of decay bypasses the (metastable) 628.6-keV level and 2) those levels that decay primarily through this metastable level.

Table VI. States in ^{141}Pm Populated by ^{141m}Sm Decay

This Work		Hesse (Hes69)		Arl't et al. (Ar167,Ar170)[a]	
State Energy (keV)	J^{π}	State Energy (keV)	J^{π}	State Energy (keV)	J^{π}
0	$5/2^+$	0	$(5/2^+)$	0	$(5/2^+)$
196.6	$7/2^+$	196.5	$(5/2^+)$	198	$(7/2^+)$
628.6	$11/2^-$	628.3	$(11/2^-)$	629.9	$(11/2^-)$
804.5	$11/2^+,9/2^+$	---	---	---	---
(837.1)	$9/2^+$	---	---	850	$(15/2^+)$
974.0	$9/2^+$	973.6	---	979	$(9/2^+)$
---	---	1033.2	---	---	---
1108.1	$7/2^{\pm},9/2^+,(5/2^-)$	1107.6	---	---	---
1167.2	$13/2^{-(+)},11/2^{-(+)},9/2^{-(+)}$	1166.3	---	---	---
1313.2	$13/2^{-(+)},11/2^{-(+)},9/2^{-(+)}$	1312.5	---	---	---
1414.8	$11/2^-,9/2^-$	---	---	---	---
---	---	1759.4	---	---	---
(1834.0)	$11/2^-,9/2^-$	---	---	---	---
1983.1	$9/2^-$	1982.2	$(9/2^-)$	1982.6	b
2063.5	$11/2^-,9/2^-$	---	---	---	---
2091.6	$11/2^-,9/2^-$	2090.6	---	2091.6	b
2119.0	$11/2^-,9/2^-$	2118.5	---	2119.0	$(9/2^+,11/2^+)$[b]
2702.4	$13/2^-,11/2^-,9/2^-$	---	---	---	---

[a] Hes 69 did not include the 1982.6- or 2091.6-keV states.

[b] Arl 70 includes these plus the revised energy for the 2119.0-keV state and also recognizes that these three states are low-spin members of the three quasiparticle multiplet.

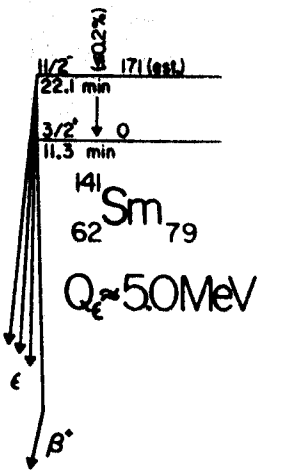

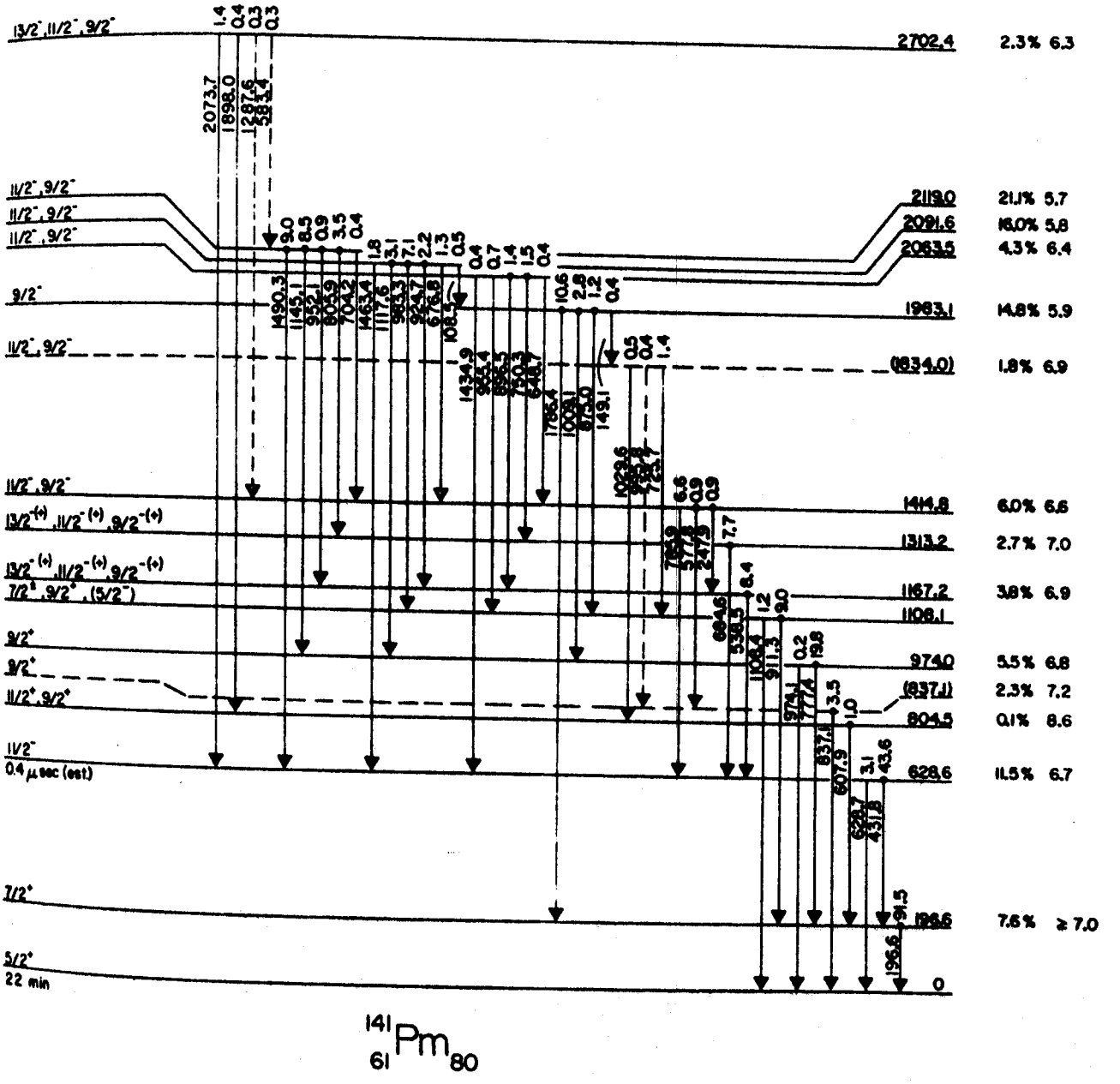

Figure 14a. Decay schemes of ^{141m}Sm.

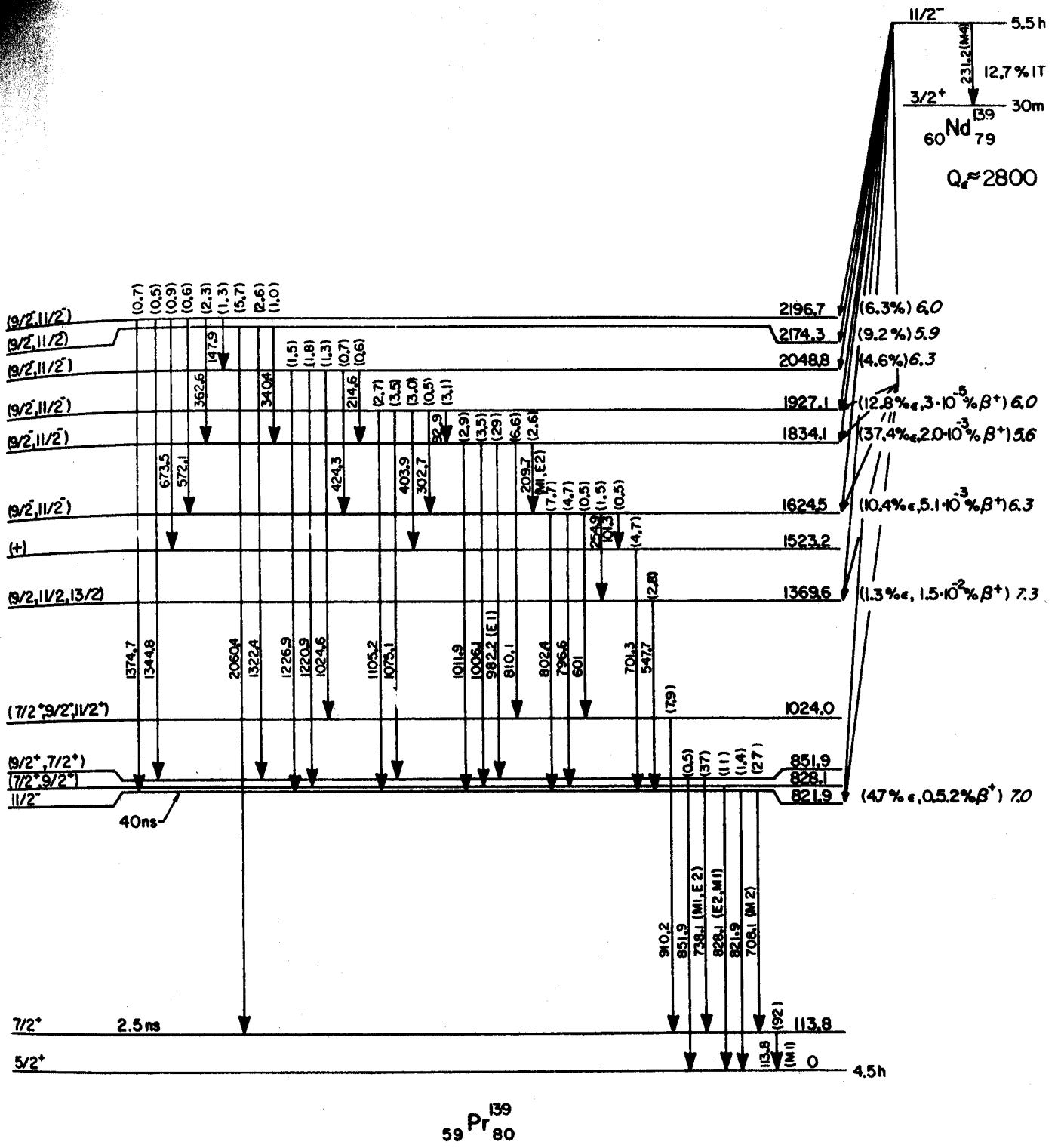

Figure 14b. Decay scheme of ^{139m}Nd.

4.1.4.A. The 196.6-keV and Related Levels

The 196.6-keV transition has been placed as proceeding from the first excited state of ^{141}Pm on the basis of its being the most intense transition in the ^{141m}Sm spectrum. A first excited state at 196.6 keV is completely consistent with the systematics of this region (cf. Section 4.1.6.).

Placement of the 628.6-keV level itself is also straightforward. It decays to ground via the 628.7-keV transition and to the 196.6-keV level via the 431.8-keV transition, as indicated in the prompt coincidence spectra. Expected to be a metastable state on the basis of systematics, this was proven by the delayed coincidence spectra.

Placement of most other levels is not so straightforward and depends on considerable tortuous logic involving the prompt and delayed coincidence spectra. For example, of the eleven γ rays in coincidence with the 196.6-keV γ, only five feed the 196.6-keV level directly. We present only a few crucial points here.

The 804.5-keV level is placed on the basis of a 196.6- and 607.9-keV coincidence and the fact that no γ ray as intense as the 607.9-keV γ was found in the 607.9-keV gated spectrum other than the 196.6-keV γ. Purely on the basis of sums, γ rays at 1029.6 and 1898.0 keV are placed as feeding this level. These are weak transitions that would not show

up in the 607.9-keV gated spectrum. Note that the 805.9-keV γ, which feeds the 628.7-keV level, has no relationship to the 804.5-keV level.

Very similar logic, aided by the presence of a 974.1-keV ground-state transition, places the 974.0-keV level. The two levels at 1108.1 and 1983.1 keV are also placed on the basis of the prompt coincidence data, and the placements are corroborated by multiple energy sums and are consistent with the intensities of the interconnecting γ transitions.

The level placed at 837.1 keV is somewhat of a puzzle. The 837.1-keV γ is enhanced in the integral coincidence spectrum and attenuated in the anticoincidence spectrum. There is weak evidence for coincidence with the 196.6-keV from inspection of the 837.1-keV gated spectrum. However, there is no enhancement of the 837.1-keV peak in the 196.6-keV gated spectrum. Possibly, Compton events from other peaks (e.g., 875.0-keV) could account for the 196.6-keV peak appearing in the 837.1-keV gate spectrum. With this somewhat conflicting evidence, the 837.1-keV transition has been placed as originating from a level of the same energy. This is substantiated to some extent by the placement of the 577.8-keV γ, which we shall see in the next section fits nicely between the 837.1-keV level and a level at 1414.8 keV that will be placed by coincidence data.

4.1.4.B. The 628.6-keV Level and Spin-Related Levels

The 628.6-keV level is almost certainly a $\pi h_{11/2}$ state. This is demonstrated both by the systematics of the region and by the fact that it has a half-life long compared with the typical resolving times ($2\tau \tilde{>} 100$ nsec) of the prompt coincident spectra. That this is in fact the high-spin state is demonstrated by the results of the "delayed gate" coincidence spectrum (Fig. 10). In this spectrum only the peaks at 196.6 and 431.9 keV are present, and that these two transitions are in coincidence is substantiated by the coincidence spectra gated on each one. And further support for the assignment of an isomeric state at 628.6 keV comes from the enhancement of the relatively weak 628.7-keV γ in the anticoincidence spectrum. That ^{141m}Sm is also an $11/2^-$ state means that its primary β^+/EC decay will populate relatively high-spin (9/2, 11/2, 13/2) states in ^{141}Pm and these states should decay by cascades that go through the 628.6-keV state.

The "delayed spectrum" integral coincidence spectrum (Fig. 11) almost immediately places six of the high-lying, high-spin states fed directly by ^{141m}Sm. [This assumes that the six γ rays enhanced in this spectrum feed the 628.6-keV level directly. The absence of sum transitions or observed coincidences and the fact that the resulting decay scheme is the simplest consistent with the experimental data lead us to accept this assumption of direct feeding.]

These six levels lie at 1167.2, 1313.2, 1414.8, 2091.6, 2119.0, and 2702.4 keV. In addition to these six levels, we place a level at 2063.5 keV on the basis of sums—the weak 1434.9-keV γ connects this level with the 628.6-keV level. The 2063.5-keV level is confirmed by the coincidence relations between the 750.3- and 684.6- and between the 896.5- and 538.5-keV γ's.

The remaining level, at 1834.0 keV, is placed only on the basis of energy sums and should thus be considered only tentative.

Numerous corroborations of the placements of most of the states can be found in the coincidence summary of Table III and the coincidence spectra themselves, Figs. 6 and 7.

4.1.5. Discussion

4.1.5.A. The ^{141}Sm Isomers

Ths odd-mass N=79 isotones actually consist of three-hole states, but to a reasonable first approximation their low-lying states can be treated as a single-hole state much in the manner of the N=81 isotones. Among the latter there are now seven known isomeric pairs having $(\nu d_{3/2})^{-1}$ ground states and $(\nu h_{11/2})^{-1}$ metastable states connected by M4 isomeric transitions (Epp 70b). In Fig. 15 we show the energy spacings between the $(\nu d_{3/2})^{-1}$ and $(\nu h_{11/2})^{-1}$ states and also show the squares of the radial matrix elements, $|M|^2$,

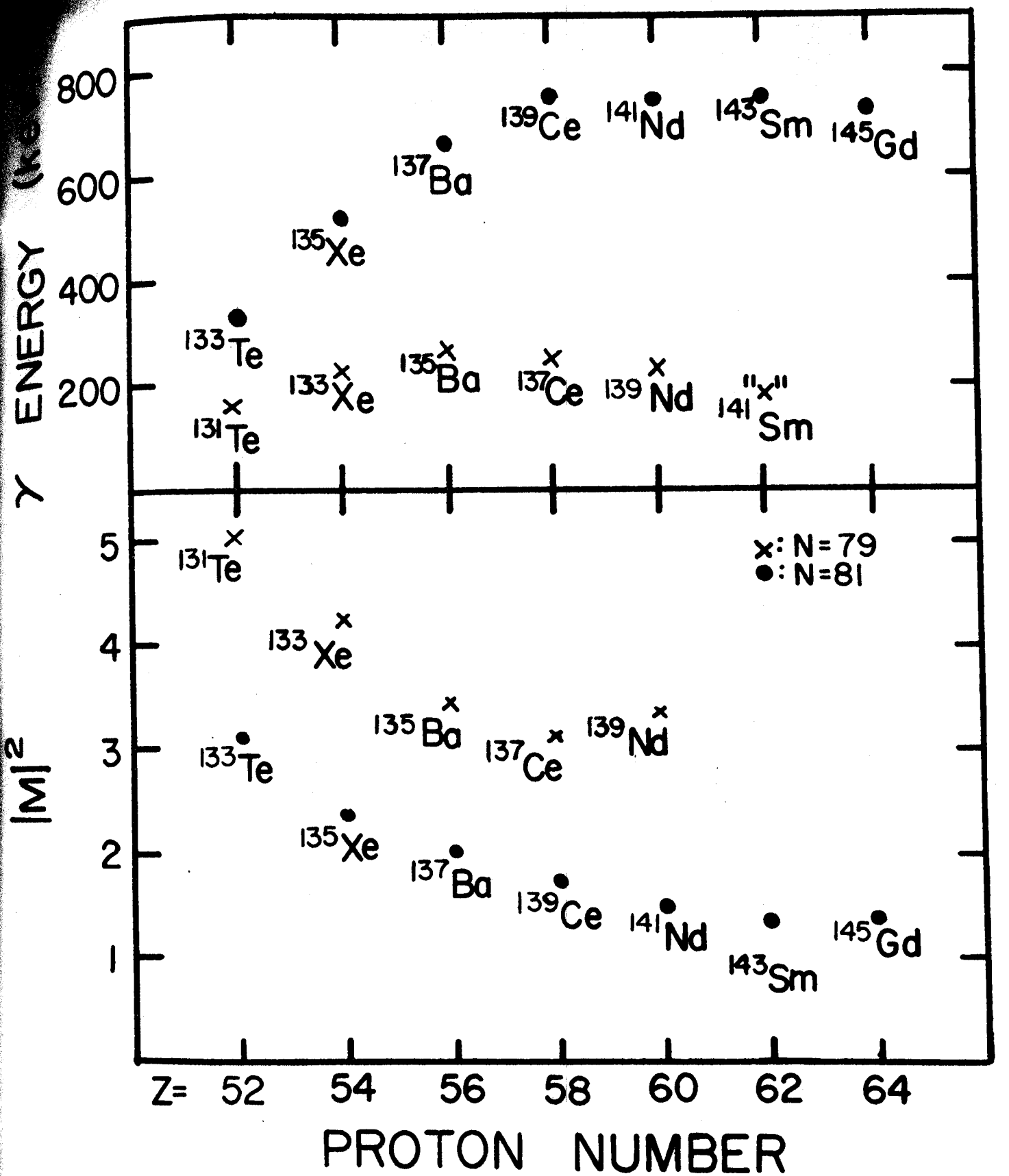

Figure 15. Upper: *M*4 transition probabilities for the *N*=79 and *N*=81 odd-mass isotones. The ^{141m}Sm point is calculated (predicted value.

Lower: Values of the squared radial matrix elements for the single-neutron isomeric transitions for the same nuclei.

for the M4 transitions as calculated using Moszkowski's approximations for single-neutron transitions (Mos 65). Both the energies and matrix elements follow a gentle-enough trend that one has reasonable confidence in extrapolated values, providing the extrapolation is not carried too far. (The fact that the values of $|M|^2$ are not constant is discussed in some detail in (Bee 69b), (Epp 70b), and (Jan 69).)

The $|M|^2$ values for the five known isomeric transitions in the N=79 isotones are somewhat larger than for those in the N=81 isotones. This would indicate that they are less good "single-particle" transitions than the N=81 transitions. However, they are all indubitably M4 transitions and can be described with considerable accuracy as $(\nu d_{3/2})^{-2}(\nu h_{11/2})^{-1} \rightarrow (\nu d_{3/2})^{-3}$. As mentioned in Section 4.1.3.E., we were unable to detect the presence of an isomeric transition between ^{141m}Sm and ^{141g}Sm, but its predicted intensity should be so low that one would not expect to observe it. More to the point, the decay properties, Section 4.1.4., of ^{141g}Sm make it reasonably certain that it has a $3/2^+$ ground state. (The $\nu s_{1/2}$ state crosses the $\nu d_{3/2}$ state in this vicinity, but a ^{145g}Gd ground state of $1/2^+$ has quite different decay properties (Epp 71) from ^{141g}Sm and, in fact, populates three quasiparticle states somewhat analogous to those populated by ^{139m}Nd and ^{141m}Sm.) Also, the analogy of ^{141m}Sm decay

to ^{139m}Nd, where the M4 transition was easily measured, gives us reasonable confidence that the primary configuration of ^{141m}Sm is indeed $[(\pi g_{7/2})^8(\pi d_{5/2})^4]_0[(\nu d_{3/2})^{-2}(\nu h_{11/2})^{-1}]_{11/2^-}$ and that of ^{141g}Sm is $[(\pi g_{7/2})^8(\pi d_{5/2})^4]_0[(\nu d_{3/2})^{-3}]_{3/2^+}$.

4.1.5.B. Single Particle States in ^{141}Pm

For convenience of discussion the states in ^{141}Pm populated by ^{141m}Sm decay can be divided into three classes: 1) single-particle states or states exhibiting appreciable single-particle character, 2) three-particle states, viz., the high-lying multiplet receiving most of the direct β^+/EC population, and 3) the remaining states, most of which appear to contain core-coupled vibrational components. As relatively little has been done in the way of calculations on states in rare-earth nuclei on the neutron-deficient side of N=82, one has to rely rather heavily on parallels with ^{139m}Nd decay and on general systematics of states in this region. As an aid for following the systematics and trends, in Figs. 16 and 17, respectively, we plot the known states in neutron-deficient odd-mass Pm isotopes and in the odd-mass N=80 isotones. Because few reactions studies have been made on nuclei in this region, the number of states reported is very much a function of Q_{EC}.

Between the closed shells at 50 and 82 the available single-particle orbits are $g_{7/2}$ and $d_{5/2}$ lying relatively

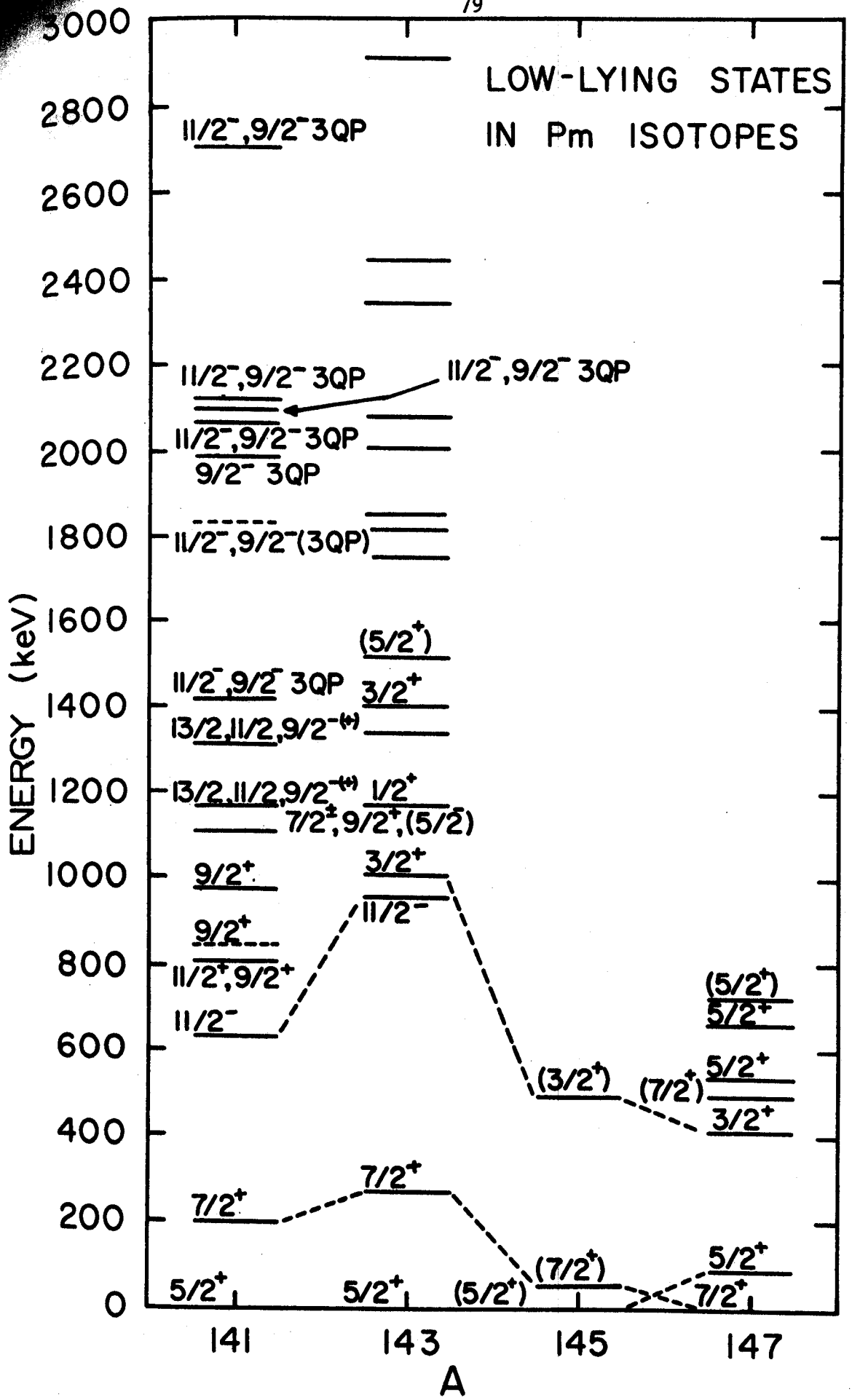

Figure 16. The positions of known states in the odd mass Pm isotopes.

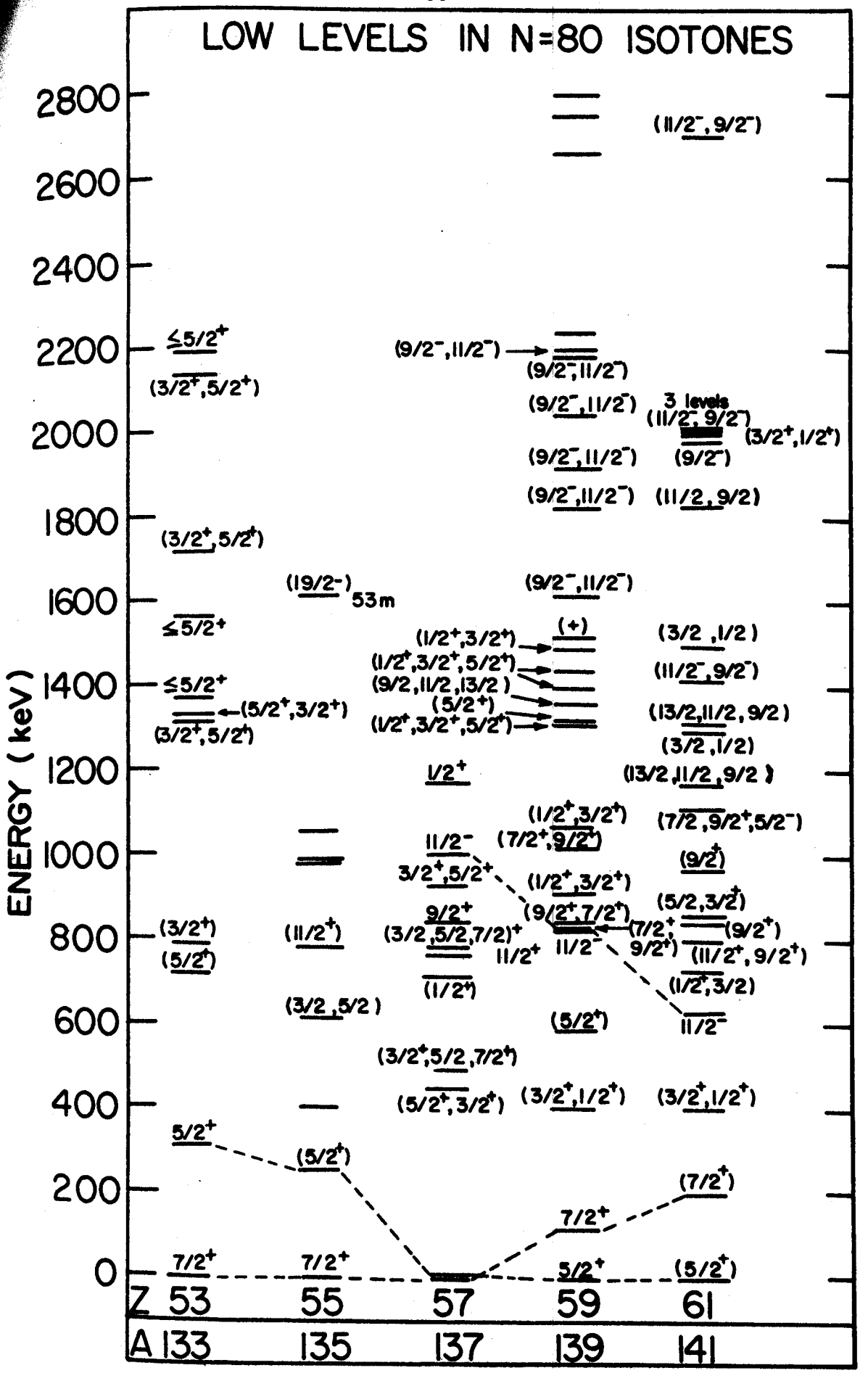

Figure 17. The positions of known states in N=80 odd-mass isotones.

close together and then, after a gap of ~500-1000 keV, $h_{11/2}$, $s_{1/2}$, and $d_{3/2}$ also relatively close together (Wil 71). Systematics as exhibited in Figs. 16 and 17 and extrapolations of the calculations of Kisslinger and Sorensen (Kis 60) suggest $5/2^+$ and $7/2^+$ for the two lowest states in ^{141}Pm. As previously pointed out (Bee 69a) sixteen nuclei in this region have well-characterized ground states and first excited states with $5/2^+$ and $7/2^+$ or $7/2^+$ and $5/2^+$ assignments. In the Pm isotopes there is a change of ground state spin between ^{147}Pm and ^{145}Pm, with ^{147}Pm and the heavier isotopes having $7/2^+$ ground states and ^{145}Pm and ^{143}Pm having $5/2^+$ ground states. Similarly, in the N=80 isotones there is a reversal of these spins between ^{137}La and ^{139}Pr.

In addition to these general arguments, we have three specific arguments for assigning the ground state $5/2^+$ and the 196.6-keV first excited state $7/2^+$. First, the decay properties of ^{141}Pm itself (Section 4.3.) are consistent with a ground state assignment of $5/2^+$ and not $7/2^+$—the decay of ^{141}Pm strongly populates the ground state of ^{141}Nd, which has been quite unambiguously characterized as a $(\nu d_{3/2})^{-1}$ state (Bee 68)(Jol 71)(Fos 71)(Cha 71).

Second, since ^{141m}Sm is undoubtedly an $11/2^-$ state, a β transition between it and a $5/2^+$ ground state of ^{141}Pm would have to be at least third forbidden and hence negligibly

small. This is consistent with our findings. On the other hand, β decay to a $7/2^+$ first excited state would be first forbidden unique. Although only a small branch would be expected, from the γ-ray intensity balance (including corrections for internal conversion) for this state it appears that as much as 7.6% of the decay might populate directly, resulting in a log ft ≥7.0. This compares with ≃3% decay (Bee 69b) from ^{139}Nd to the first excited state in ^{139}Pr with a log ft of ≃7.6. Actually, it would seem reasonable to attribute much of this apparent feeding to errors in the γ-ray intensities and/or to undetected transitions into the state. However, the pair coincidence spectrum (Fig. 8), after correction for chance events and feeding via higher energy states, shows that there is in fact some β^+ decay to the 196.6-keV state. (In both ^{141m}Sm and ^{139m}Nd decays this first forbidden unique transition would involve $\pi g_{7/2} \rightarrow \nu h_{11/2}$, which would be one of the more favorable cases for such a transitions, but we would expect the log ft to be greater than 7.0.) Also, in our measurement (Epp 70a) of the half-life of the 196.6-keV γ we found no evidence for an 11.3-min component, which means that ^{141g}Sm does not populate the 196.6-keV state either directly or indirectly. All of the β feedings are thus consistent with a $7/2^+$ first excited state.

Third, the respective $5/2^+$ and $7/2^+$ assignments are consistent with the branching ratios from the 628.6-keV state, which will be discussed below. We conclude that the ground state of ^{141}Pm is a $5/2^+$ state and the primary component of its wave function is $[(\pi g_{7/2})^8(\pi d_{5/2})^3(\nu d_{3/2})^{-2}]_{5/2^+}$, taken with reference to the closed shells at Z=50 and N=82. Similarly, the primary component of the $7/2^+$ 196.6-keV state is expected to be $[(\pi g_{7/2})^7 x(\pi d_{5/2})^4(\nu d_{3/2})^{-2}]_{7/2^+}$.

That the 628.6-keV state is the $\pi h_{11/2}$ state {complete configuration of primary component $[(\pi g_{7/2})^8(\pi d_{5/2})^2 (\pi h_{11/2})(\nu d_{3/2})^{-2}]_{11/2^-}$} has already been discussed in Section 4.1.3.D. The log ft of 6.7 for the β^+/EC decay from ^{141m}Sm is on the high side for an allowed transition, but this is entirely reasonable when one examines the particle rearrangements necessary. These are included in the stylized diagram presented in Fig. 18. To first approximation the transition would appear to involve the conversion of a $d_{3/2}$ proton into an $h_{11/2}$ neutron, either directly or perhaps through an intermediate state, plus the simultaneous promotion of the $d_{5/2}$ proton remaining from the pair up into the $h_{11/2}$ orbit. Thus the transition undoubtedly goes by smaller components in the wave functions. That the log ft of 6.7 is smaller than that for analogous transition from ^{139m}Nd (there it is 7.0) can be attributed to the $\pi h_{11/2}$ orbit's dropping in energy with increasing Z,

thereby providing larger occupations of $h_{11/2}$ proton pairs. Later we shall show that this is consistent not only with ^{141}Sm and ^{141}Pm behavior, but also with the general trends of single-particle states throughout this region.

Since no conversion-electron data are available for transitions following the decay of ^{141}Sm, we show no multipolarity assignments on the decay scheme. However, the 431.8- and 628.7-keV transitions are expected to be M2 and E3, respectively. We measured the half-life of the 628.6-keV state to be 700 ns. This leads to a partial half-life for the E3 transition of 10.6 μs. Assuming little or no mixing in the transition, the Moskowski single-particle estimate for its half-life (neglecting the statistical factor) is 17 μs. The M2 retardation (a factor of 58) determined here is quite reasonable, since M2's are customarily retarded. However, the E3 is enhanced over the single-particle estimate, and this enhancement appears to be at least by a factor of 1.6. Although most E3's are retarded, this is now the fifth known E3 in this particular nuclear region that is enhanced. The others are in ^{139}Pr, ^{137}La, ^{147}Eu, and ^{149}Eu. These all involve similar

$h_{11/2}$ states. The simplest explanation is for an octupole core-coupled component of the $5/2^+$ ground state to be admixed into the $11/2^-$ states. Unfortunately, the positions of octupole states in neighboring even-even nuclei are not known, and a more quantitative persual of the problem must await such information.

We do not see any states populated by ^{141m}Sm decay that we can identify with the $\pi d_{3/2}$ or $\pi s_{1/2}$ single-particle orbits, nor could we expect to do so. Even from the decay of ^{141g}Sm, Section 4.1.7., it is difficult to associate these orbits with particular states in ^{141}Pm. Both appear to be fractionated and have their strength spread out over many states.

4.1.5.C. A Three-Quasiparticle Multiplet in ^{141}Pm

Some 65% of the β^+/EC decay from ^{141m}Sm populates the multiplet of six states at 1414.8, 1983.1, 2063.5, 2091.6, 2119.0, and 2702.4 keV. (There are seven states if we include the one at 1834.0 keV, which receives about 2% of the population; however, this state is only tentatively placed and thus omitted from the present discussion.) The log ft values range from 5.7 to 6.6 implying that these are all allowed transitions; in fact, they are faster transitions than the $11/2^- \rightarrow 11/2^-$ transition populating the 628.6-keV state.

The explanation for this superficially peculiar behavior of ^{141m}Sm is actually quite straightforward and has been anticipated in the introduction Section 4.1.1. It is given in stylized form in Fig. 18. This multiplet of high-spin, high-lying states is a three-quasiparticle multiplet that the rather unique structure of ^{141m}Sm forces it to populate. ^{141m}Sm, three neutron holes below the N=82 closed shell, undoubtedly has as its primary structure, $[(\pi g_{7/2})^{8}(\pi d_{5/2})^{4}(\nu d_{3/2})^{-2}(\nu h_{11/2})^{-1}]_{11/2^-}$, as depicted in Fig. 18 and discussed in Section 3.1.5.A. Because of its large Q_{EC} it can easily populate states in ^{141}Pm above the pairing gap(s). Now, the most probable form of β transition, given by the above structure, is $\pi d_{5/2} \rightarrow \nu d_{3/2}$, resulting in the structure, $[(\pi g_{7/2})^{8}(\pi d_{5/2})^{3}(\nu d_{3/2})^{-1}(\nu h_{11/2})^{-1}]_{J^-}$, or more simply, $[(\pi d_{5/2})(\nu d_{3/2})^{-1}(\nu h_{11/2})^{-1}]_{J^-}$. Here J^- can be anything from $3/2^-$ to $19/2^-$, but note that allowed transition are limited to $9/2^-$, $11/2^-$, or $13/2^-$. As can be seen from Fig. 14, the analogy with ^{139m}Nd's populating six similar quasiparticle states is striking. Some examples of narrowing down the spin assignments follow.

The 1983.1-keV state is the only one that populates anything lower-lying than the $11/2^-$ 628.6-keV state, and, in fact its 1786.4-keV transition to the $7/2^+$ 196.6-keV state is its strongest mode of deexcitation. The only J^π assignment consistent with this is $9/2^-$. We shall see later

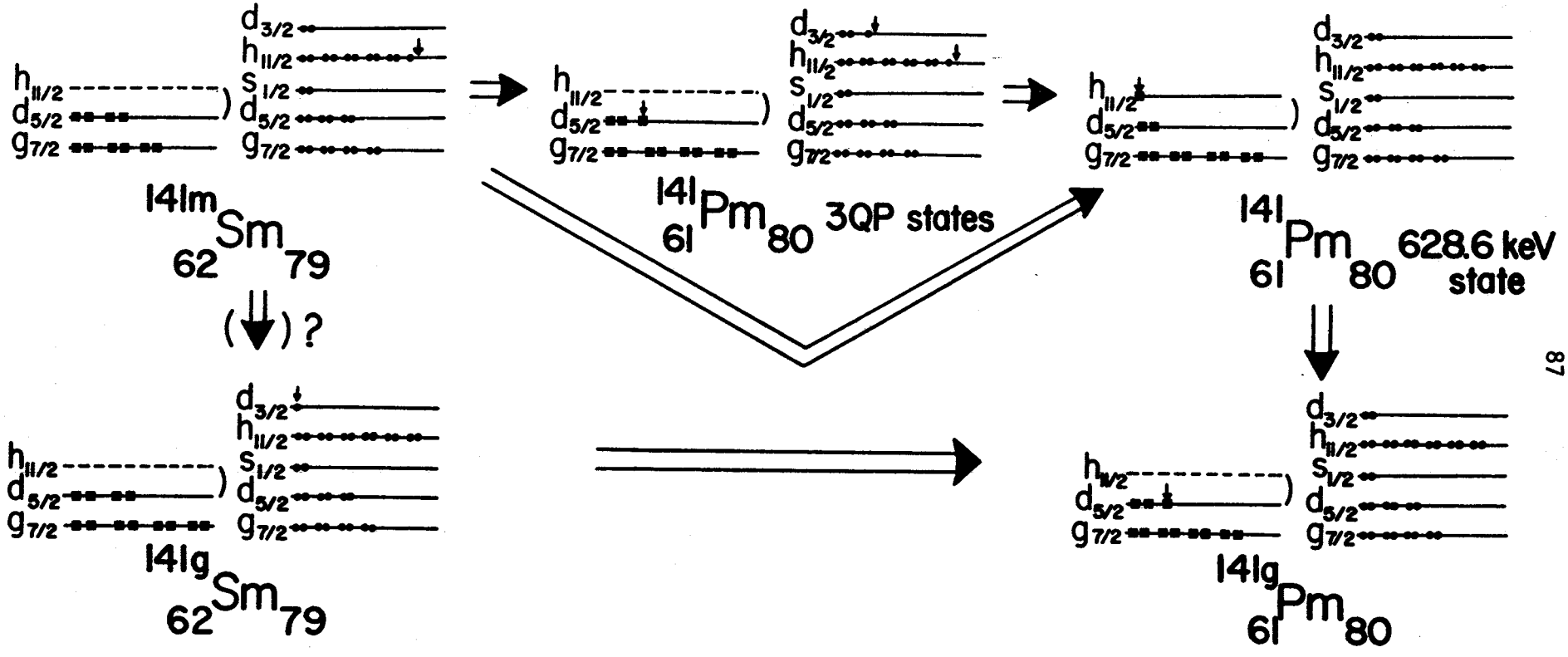

Figure 18. Symbolic shell-model representations of some important transitions between ^{141}Sm and ^{141}Pm states.

(after assigning the 974.0- and 1108.1-keV states) that all three γ transitions depopulating this state are most likely E1, which could be in agreement with the branching ratios. However, we shall not dwell too much on γ-ray branching ratios when speaking to the transitions involving the three-quasiparticle states. By their very nature these states are quite different in structure from the lower-lying states; thus, most γ transitions will proceed primarily via small admixtures in the wave functions, and consequently the branching ratios can be very misleading. For a rather striking demonstration of this the reader is referred to ^{139}Pr (Bee 69b), where many of the multipolarities could be assigned on the basis of conversion coefficients. There it was almost the rule rather than the exception for γ transitions between and out of the three-quasiparticle states to differ from single-particle predictions by orders of magnitude.

Assignments for four of the remaining five states, at 1414.8, 2063.5, 2091.6, and 2119.0 keV, can be narrowed down to $9/2^-$ or $11/2^-$. All except the 2063.5-keV state decay to the 628.6-keV state, indicating some similarities in their wave functions with it, and all four of them also decay to at least one other state that is in the next section assigned $9/2^+$ as its highest possible spin. Assignments of $13/2^-$ would force these branches to be M2 transitions, not likely to compete even with retarded M1's to the $11/2^-$ states.

After our finding the three-quasiparticle multiplet in ^{139}Pr, it seemed worthwhile to perform a shell-model calculation for the states in the multiplet, using as simple and truncated a basis set as possible. This was carried out by Muthukrishnan and Kromminga (Muth 71) who calculated negative-parity states in ^{139}Pr using only the two configurations, $[(\pi d_{5/2})(\nu d_{3/2})^{-1}(\nu h_{11/2})^{-1}]$ (the basic three-quasiparticle configuration), and $[(\pi h_{11/2})(\nu d_{3/2}{}^{-2})]$ (the basic configuration of the 821.9-keV metastable state in ^{139}Pr). Using an exchange mixture postulated by True, they obtained excellent results for energy predictions agreeing with the experimental positions. There was still some problem, however, with transition probabilities, and it appears that configurations of the sort, $[(\pi d_{5/2})^2(\pi g_{7/2})^{-1}(\nu d_{3/2})^{-1}(\nu h_{11/2})^{-1}]$, will have to be added to the basis set. This can be seen empirically by the gradations in the properties of the states of the three-quasiparticle multiplets both in ^{139}Pr and ^{141}Pm, e.g., the γ transitions directly to the $7/2^+$ first-excited states. The main point is that calculations that intentionally used a truncated basis set give approximately correct answers for the three-particle states in ^{139}Pr.

4.1.5.D. The Remaining States in ^{141}Pm

The structure of the remaining six states, at 804.5, (837.1), 974.0, 1108.1, 1167.2, and 1313.2 keV, are not so straightforward and appear to lie somewhere between the single-particle and the three-particle states. They can perhaps be described best as weakly core-coupled states. Their wave functions would thus contain many components, which partly explains why the three-particle states decay down through many of them. It would also be consistent with the γ-ray branching ratios depopulating them and with the fairly large log ft values for the β^+/EC transitions feeding them. Although not completely conclusive, there is evidence that the 2^+ one-phonon quadrupole vibrational state lies at ≈770 keV in both of the adjacent even-even nuclides, ^{142}Sm and ^{140}Nd (Mal 66) and (Rem 63), quite in line with those in the lighter N=80 even-even isotones. Thus, the energies of the six ^{141}Pm states are in the right range for core-coupled states, the lower ones probably involving the $d_{5/2}$ or $g_{7/2}$ single-particle states and the upper ones the $h_{11/2}$ state.

The 804.5-keV state (log ft =8.6) appears to be fed by a first-forbidden transition, implying positive-parity assignments from 9/2 to 13/2. (A first-forbidden unique transition would also allow $7/2^+$ and $15/2^+$, but we hesitate

to include these because all the log ft's are somewhat high, and it is difficult, if not impossible, to concoct a structure for the state that would allow it to be populated by a relatively fast first-forbidden unique transition.) The $13/2^+$ possibility can be eliminated on the basis of the 607.9-keV γ to the 196.6-keV state, for this would force that transition to be an M3. However, neither of the other possibilities can be eliminated. With the $11/2^+$ assignment the 607.9-keV transition would be a pure E2 and with the $9/2^+$ assignment it would be a mixed M1/E2. Either way the E2 component should be collectively enhanced. In fact, an intelligent guess at the nature of the 804.5-keV state would be that it consists specifically of the $g_{7/2}$ single-particle state coupled to a 2^+ quadrupole core vibration—hence the depopulation solely to the 196.6-keV state. $11/2^+$ or $9/2^+$ is also consistent with the feedings to the 804.5-keV state.

We have been rather cautious about using γ-ray branching ratios to predict J^π assignments except when the structures of the states could be corroborated in other ways, viz., the $\pi h_{11/2}$ state at 628.6-keV. It is instructive here to give an example of how such branching ratios could well be misleading. Of the three possible γ transitions depopulating the 804.5-keV state (ignoring the presence of some low-spin states, which lie below it—known from the decay (Section 4.1.7.) of $^{141}g_{Sm}$), one is present. The missing 804.5-keV transition does not tell us much, and it could be

consistent with single-particle estimates. However, the missing 175.9-keV transition to the 628.6-keV state must be an E1. And single-particle estimates (Mos 65) for this E1, a 607.9-keV M1, and a 607.9-keV E2 yield respective half-lives of 4.6×10^{-14}, 1.1×10^{-13}, and 1.5×10^{-10} sec. Obviously the E1 is severely retarded over such estimates. With our inferred structures for the 804.5- and 628.6-keV states this retardation is quite understandable, even expected. However, wrong conclusions could easily have come out of blindly applying these "external" selection rules.

The 837.1-keV state, if correctly placed (Section 4.1.4.A) must be a $9/2^+$ state, probably a coupling of a $d_{5/2}$ single-particle state with the 2^+ core. The log ft implies a first-forbidden transition, and the γ transition to the ground state eliminates the $13/2^+$ and $11/2^+$ possibilities.

Similar logic, involving feedings both into and out of the 974.0-keV state allows us to assign it $9/2^+$.

Within the limits of our γ-ray intensities there is no β feeding to the 1108.1-keV state. The γ transitions into it from above, most specifically the 875.0-keV γ from the $9/2^-$ 1983.1-keV state, limit its J^π to $5/2^-$, $7/2^\pm$, $9/2^\pm$, $11/2^\pm$, $13/2^-$ (assuming E1, M1, or E2 multipolarities). Its depopulating γ rays, especially the ground-state transition, further limit J^π to $5/2^-$, $7/2^\pm$, or $9/2^+$. The fact that this state is not populated by ^{141g}Sm decay (Section 4.1.7.) is a weak argument against the $5/2^-$ assignment, but we cannot justify eliminating it completely. Also, the internal

structure of this state is probably the least certain in the decay scheme.

The states at 1167.2 and 1313.2 keV exhibit similar properties. The log ft's of 6.9 and 7.0 could mean either allowed or first-forbidden (non-unique) decay. The implied $J^{\pm}$ assignments would be $13/2^{\pm}$, $11/2^{\pm}$, or $9/2^{\pm}$. The γ-ray feedings into them from the three-quasiparticle states do not allow any narrowing down of these values. And each state decays by a single γ ray to the 628.5-keV state, again allowing no reduction in the possibilities. It is tempting to think of these states as couplings of the $h_{11/2}$ single-particle state to a 2^+ core. They lie at approximately the expected energies and such a configuration would explain why even with a $9/2^-$ assignment there would be no γ branching to the 196.6-keV or ground state. Also, with such a structure, there should be considerable configuration mixing with the three-particle states (cf., e.g., (Muth 71)), which would explain why the log ft's are only slightly higher than the log ft for β^+/EC decay to the 628.6-keV state itself. Thus, we prefer the negative parity options.

4.1.5.E. EC/β^+ Ratios and Corrected log ft Values

Straightforward EC/β^+ ratios as calculated by the methods of Zweifel (Zwe 57) are not in good agreement with the ratios obtained from the pair coincidence spectrum (Fig. 8). This spectrum shows that the 196.6-, 403.9-, and 438.2-keV transitions (the latter two resulting from ^{141g}Sm decay) are the only ones to receive significant β^+ decay. Now, as the calculated ratios are for "simple" allowed transitions, it is expected that the β^+ components will be much smaller for the first-forbidden transitions. However, it is now becoming apparent that hindrances even to an allowed transition usually reduce the β^+ component much more rapidly than the EC component (Epp 71). Thus, the rearrangement depicted in Fig. 18 for the decay to the $\pi h_{11/2}$ 628.6-keV state would be expected to result in the EC/β^+ ratio being larger than the calculated value. (Note, however, that because of the half-life of this state the pair coincidence spectrum would pick up only a small component of its β^+ feeding.) The log ft values presented on the decay scheme itself are so-called "normal" values, obtained using the calculated EC/β^+ ratios. We used these for ease of later improvements and corrections and also because most people are more familiar with decay scheme logic based on such values. In Table VII we compare these with the log ft values we obtained assuming only EC

Table VII. Comparison of log ft's Assuming Either the Theoretical EC/β^+ Ratios of all EC Decay

energy V)	Normal	EC-decay only
	≥7.0	6.4
	6.7	6.1
	8.6	8.2
	7.2	6.8
	6.8	6.4
	6.9	6.5
	7.0	6.6
	6.6	6.2
	6.9	6.7
	5.9	5.7
	6.4	6.2
	5.8	5.6
	5.7	5.5
	6.5	6.3

decay. The latter are expected to be more realistic. Unfortunately, very little has been done on the quantitative theory of EC/β^+ ratios.

4.1.6. Discussion and Conclusions

The decay schemes of ^{141m}Sm and ^{139m}Nd, presented in Fig. 14, are remarkably similar. However, there are some differences, and these differences allow us to glean some important information about the behavior of shell-model orbits in this region of the nuclidic chart below N=82.

The most striking difference between the two is that whereas in ^{139}Pr there are many low-energy apparently enhanced γ transitions between members of the three-quasiparticle multiplet, in ^{141}Pm such transitions are fewer and weaker. Also, the transitions out of the multiplet to lower-lying states appear to be much more retarded in ^{139}Pr than in ^{141}Pm. Actually, this is more or less what one would expect from the known behavior of shell-model orbits in this region. The retardation of transitions down to the 628.6-keV state, for example, is represented in Fig. 18. With only $g_{7/2}$ and $d_{5/2}$ proton states occupied, these transitions would be formally two-particle transitions. A $d_{5/2}$ or $g_{7/2}$ proton would have to be converted into an $h_{11/2}$ neutron, either directly or perhaps through an intermediate state, and the remaining member of the pair would have to be promoted up to the $h_{11/2}$ orbit. Thus the transitions must proceed instead via small admixtures in the wave functions. Such happens in ^{139}Pr. It is

known, however, both from reactions studies (Wil 71) and from the β^+/EC decay of some N=81 nuclei that the $\pi h_{11/2}$ orbit drops rapidly in energy with increasing Z in this region. For example, the log ft values for the $11/2^- \rightarrow 11/2^-$ transitions in $^{141m}Nd \rightarrow ^{141}Pr$, $^{143m}Sm \rightarrow ^{143}Pm$, and $^{145m}Gd \rightarrow ^{145}Eu$ are >7.0, 6.7, and 6.2, respectively (Fir 71) (Fel 70)(Epp 70b) and the speed of these transitions should reflect sensitively the occupation of the $\pi h_{11/2}$ orbit by proton pairs. At Sm, specifically ^{141}Sm, it has acquired enough population by proton pairs to allow the γ transitions to proceed via this component and be less retarded than those in ^{139}Pr.

The β^+/EC decay of ^{139m}Nd and ^{141m}Sm to the $\pi h_{11/2}$ state in their daughters is another indicator of occupancy of the $\pi h_{11/2}$ orbit by pairs (cf. the transition in Fig. 18). Thus, we would expect the transition to be faster in $^{141m}Sm \rightarrow ^{141}Pm$ than in $^{139m}Nd \rightarrow ^{139}Pr$, quite consistent with our experimental findings.

The decay of ^{141m}Sm thus is important in two respects. 1) Taken by itself it provides information on a whole multiplet of high-lying states in ^{141}Pm. Simple shell-model calculations should provide information on the major components of their wave functions, and a closer scrutiny of the transition probabilities should provide much information about the smaller components. 2) In the context

of this region below N=82, it provides corroboration of the systematic population of low-lying three-quasiparticle multiplets by the β^+/EC decay of some of the $11/2^-$ isomers of the N=79 and 77 isotones. One should next look for this behavior from the decay of $^{137(m)}$Nd and perhaps $^{143(m)}$Gd.

4.1.7. ^{141g}Sm Introduction

As mentioned in Section 4.1.1, the first positive identification of ^{141m}Sm was made at about the same time by two different groups, Arl't et al. (Arl 67) and Bleyl Münzel, and Pfinning (Ble 67). At that time, ^{141g}Sm was not identified, however, its half-life was estimated to be less than 10m (Arl 67). The first positive identification of ^{141g}Sm was made by Eppley and Todd and reported in (McH 70). They determined the half-life to be 11.3±0.3-m and constructed a preliminary decay scheme. Further confirmation of these half-life results was presented by a Russian group (Arl 70) who reported the half-life to be 11±1-m and identified transitions at 403.8- and 438.4-keV as belonging to the decay of ^{141g}Sm.

The study of ^{141g}Sm (11.3 m) is a natural outgrowth of the study of ^{141m}Sm. These results also complement the previous work by Beery, on the N=79 isotones (Bee 69a), who studied the decay schemes of $^{137m+g}$Ce and $^{139m+g}$Nd. Additional interest in ^{141g}Sm concerns the spin of the ground state. A glance at the systematics in the region of $50 \leq Z \leq 65$ and $72 \leq N \leq 82$ indicates the odd mass, odd neutron isotopes possess ground state spins of $1/2^+$ or $3/2^+$. These ground states can be characterized in shell-model terms as $(\nu s_{1/2})$ or $(\nu d_{3/2})$. The spin of the ground state changes from $1/2^+$ to $3/2^+$ somewhere in the vicinity of ^{141}Sm. The ground state spin of ^{139g}Nd is $3/2^+$ while that of ^{145g}Gd

appears to be $1/2^+$. Indications are that the $1/2^+$ and $3/2^+$ levels are very close in ^{141}Sm with either level being equally probable for the ground state. The character of the ^{141g}Sm decay scheme could be expected to exhibit quite different features depending on whether its ground state spin is $1/2^+$ or $3/2^+$. If the spin of ^{141g}Sm is $3/2^+$ its decay scheme should have features in common with that of ^{139g}Nd (Bee 69a). If the spin is $1/2^+$ it might be expected to have features analogous to those of ^{145g}Gd (Epp 71).

4.1.8. Experimental Results for ^{141g}Sm

4.1.8.A. ^{141g}Sm Gamma Ray Spectra

The identification of those gamma-rays associated with the decay of ^{141g}Sm is a rather difficult task, and the results are not as definitive as those from the study of ^{141m}Sm. The difficulties arise from the relatively short half-life of ^{141g}Sm (11.3m) and the character of the ^{141g}Sm decay ($\sim$90% of the EC/β^+ decay is directly to the ground state of ^{141}Pm). As a consequence of its half-life, the transitions of ^{141g}Sm must always be observed in the presence of the longer lived and more intense ^{141m}Sm. This makes identification of the weak lines in the ^{141g}Sm spectra somewhat less than certain.

The transition at 403.9-keV has been identified as the most intense transition belonging to the decay of ^{141g}Sm. This placement is made from the observation that it exhibits approximately the same excitation threshold as the peaks identified with the ^{141m}Sm decay and from consideration of its half-life. In the excitation studies it was determined that two sets of transitions with different lifetimes (11.3m and 22.1m) exhibited approximately the same excitation threshold and they could be assigned to the decay of ^{141}Sm. The longer lived (22.1m) component could be identified with the decay of ^{141m}Sm. This was because it was observed to feed a delayed state in ^{141}Pm at 628.7-keV which was identified

as an $11/2^-$ isomeric level. As a consequence of this identification, the shorter lived (11.3m) component could then be identified with the decay of the ^{141}Sm ground state. After this identification the other transitions of ^{141g}Sm were determined to be those which maintained a constant intensity relative to the 403.9-keV peak intensity in six successive 5 min. spectra.

In order to maximize the presence of ^{141g}Sm relative to that of ^{141m}Sm it is necessary to observe the activity as soon as possible after production. To gain some idea of the problem faced in identifying the ^{141g}Sm activity it is only necessary to compare the relative intensities of the 403.9-keV peak (^{141g}Sm) and the 431.8-keV peak (^{141m}Sm) in the two spectra in Figs. 4 and 5. In the first spectrum counting began 2 min. after the end of the bombardment and continued for 5 min. The ratio of the intensity of the 403.9-keV line to that of the 431.8-keV transition is 100/347. In the second spectrum counting began 27 min. after the end of the bombardment and continued for 5 min. In this instance the relative intensity of the two transitions is now 100/746. The intensity difference points up the difficulty of observing the weaker ^{141g}Sm transitions in the presence of the more intense ^{141m}Sm activity. With very few exceptions, all of the transitions observed in these spectra have been identified. These exceptions are transitions with such short half-lives that they appear in only one or two of the earliest spectra, or

Table VIII. ^{141g}Sm Summary of Singles and Coincidence Intensity Information

Energy	Singles Intensity	Anti Coincidence	Coincidence
324.4±0.2[a]	≤1		
403.9±0.1	100	100	100
438.4±0.1	82.6±3	84.7	82.1
728.0±0.2	7.9±0.5	---	---
854.4±0.2	3.7±0.3	---	10.4
1057.4±0.1	5.5±0.4	---	---
1091.9±0.2	6.1±0.4	---	13.2
1292.7±0.1	16.9±0.5	15.9	19.0
1495.7±0.2	12.3±0.4	---	---
1600.9±0.3	10.3±0.5	---	20.7
2005. ±(0.5)	1.2±0.2	---	---
2037.9±(0.5)	5.4±0.4	2.9	---

[a]This transition is observed to have a small intensity in the ^{141g}Sm decay. It is only possible to estimate its magnitude.

transitions which display such erratic behavior as to preclude any positive identification.

In addition to the results of the $^{142}Nd(^{3}He,4n)^{141}Sm$ reaction previously discussed we have observed ^{141}Sm and its subsequent decay products as it is produced via the β-decay of ^{141}Eu. It was anticipated that ^{141}Eu would not contain a β-emitting isomeric-level and the resulting ^{141}Eu decay would enhance the ratio of ^{141g}Sm to that of ^{141m}Sm. The results tend to confirm this assumption.

The production of ^{141}Eu was via the reaction $^{144}Sm(p,4n)^{141}Eu$, (Q=-36.8 MeV). Targets of enriched ^{144}Sm(95.1%) were bombarded for periods of 1- to 1.5-m with ∿1.5μA of 45 MeV protons from the Michigan State University cyclotron. Counting began within 2m of the end of the bombardment, and continued for approximately 2h. During this time several spectra were accumulated and the counting intervals were varied from 5m for the earliest spectrum to 1 h for the final spectrum.

The resultant enhancement of ^{141g}Sm over that of ^{141m}Sm can readily be seen in the spectra in Figs. 21 and 22. In the second of these spectra the ratio of the relative intensity of the 403.9-keV transition (^{141g}Sm) to that of the 431.8-keV transition (^{141m}Sm) is 100/39.5. This same ratio of relative intensities in the $^{142}Nd(^{3}He,4n)^{141}Sm$ reaction is 100/347.3 for the corresponding time after bombardment and the same duration. In order to reduce the effects of very intense,

high energy positron decay, a block of paraffin 5 cm. thick was placed between the source and the detector.

The intense peaks in the first spectrum at 556.8-, 768.3-, and 1023.6-keV have a half-life of 2.0±0.5m and are tentatively identified as belonging to the decay of ^{142}Eu.

4.1.8.B ^{141g}Sm Coincidence Spectra

As pointed out in the previous section, the (11.3m) ^{141g}Sm activity can only be observed in the midst of the more intense (22.1m) ^{141m}Sm activity. This limitation becomes more serious when trying to obtain meaningful coincidence information relating to ^{141g}Sm.

To obtain the best yield of ^{141g}Sm activity relative to that of ^{141m}Sm in a source, it is necessary to begin counting as quickly as possible after the end of a bombardment. In addition, the counting interval must be kept short since the longer lived ^{141m}Sm activity will eventually overwhelm the shorter-lived ^{141g}Sm activity. With these limitations in mind, a 2-dimensional Ge(Li)-Ge(Li) coincidence experiment was performed. The detectors employed were of 10.4% and 4.5% efficiency with 2.2-keV and 1.9-keV resolution (at 1332-keV) respectively. Counting of the $^{141m+g}Sm$ sample began within 2m of the end of the bombardment and was continued for a period of not more than 30m, with the sample replenished every 5 to 10m. At the end of each 30m period the source was completely replaced with a freshly prepared source, and

the procedure was continued. Statistics were accumulated in this manner for a period of 12 hrs. The results of this effort can be observed in the spectra in Figs. 19 and 20. Though the results of this coincidence experiment seem somewhat meagre they were obtained with some difficulty, and, in conjunction with other evidence such as energy sums and intensity balances, were of significant value in the construction of the ^{141g}Sm decay scheme. A glance at these spectra will emphasize the difficulty encountered in constructing the ^{141g}Sm decay scheme, namely the lack of significant detected coincidences between transitions. This result was somewhat anticipated since the decay scheme of ^{141g}Sm could be expected to exhibit similar overall features with that of ^{139g}Nd. The results of the ^{139g}Nd study (Bee 70) also exhibited few coincidences.

In addition to the above mentioned coincidence data, we were able to use the same 511-511-keV-gamma triple coincidence and anticoincidence spectra for both ^{141m}Sm and ^{141g}Sm. These spectra assisted us in placing those transitions which decay directly to ground and those exhibiting strong positron-feeding. The anticoincidence spectrum is seen in Fig. 9 and the 511-511-keV-gamma triple coincidence spectrum is seen in Fig. 8. A summary of the various coincidence data for ^{141g}Sm is displayed in Table IX.

Table IX. Summary of γ-γ Two-Dimensional Coincidence Results for ^{141g}Sm

Gate Energy (keV)	γ-ray Enhanced (keV)
324.4	196.6, 403.8, 511.0, 777.4
403.9	324.4, 511.0, 1091.9, 1600.9
438.4	854.4, 1057.7 (very weak)
854.4	511.0
1091.9	403.9, 511.0
1292.7	511.0
1600.9	403.9

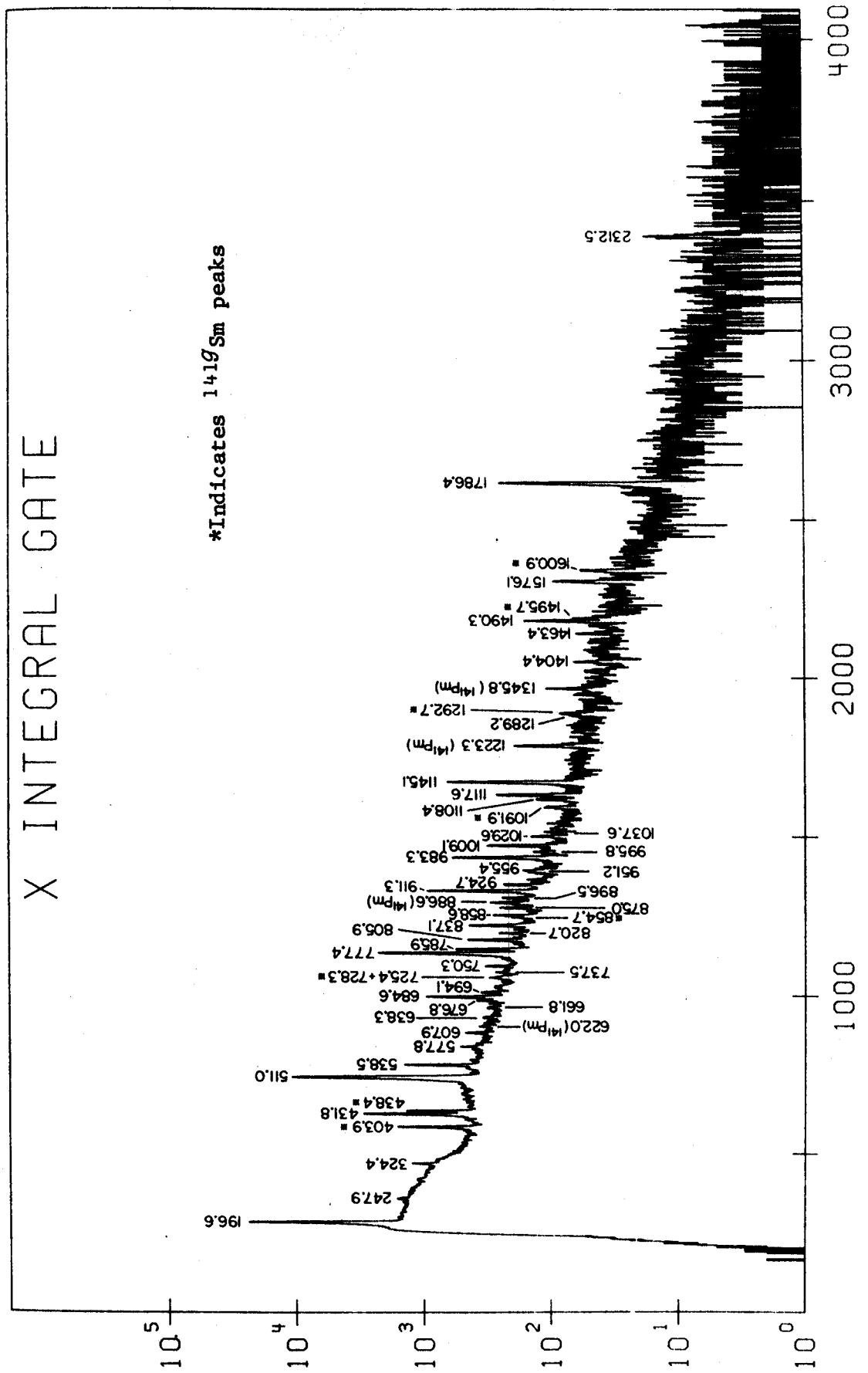

Figure 19a. ^{141m}Pm ^{149}Sm 2-dimensional integral coincidence spectrum taken with 10.4% Ge(Li) detector.

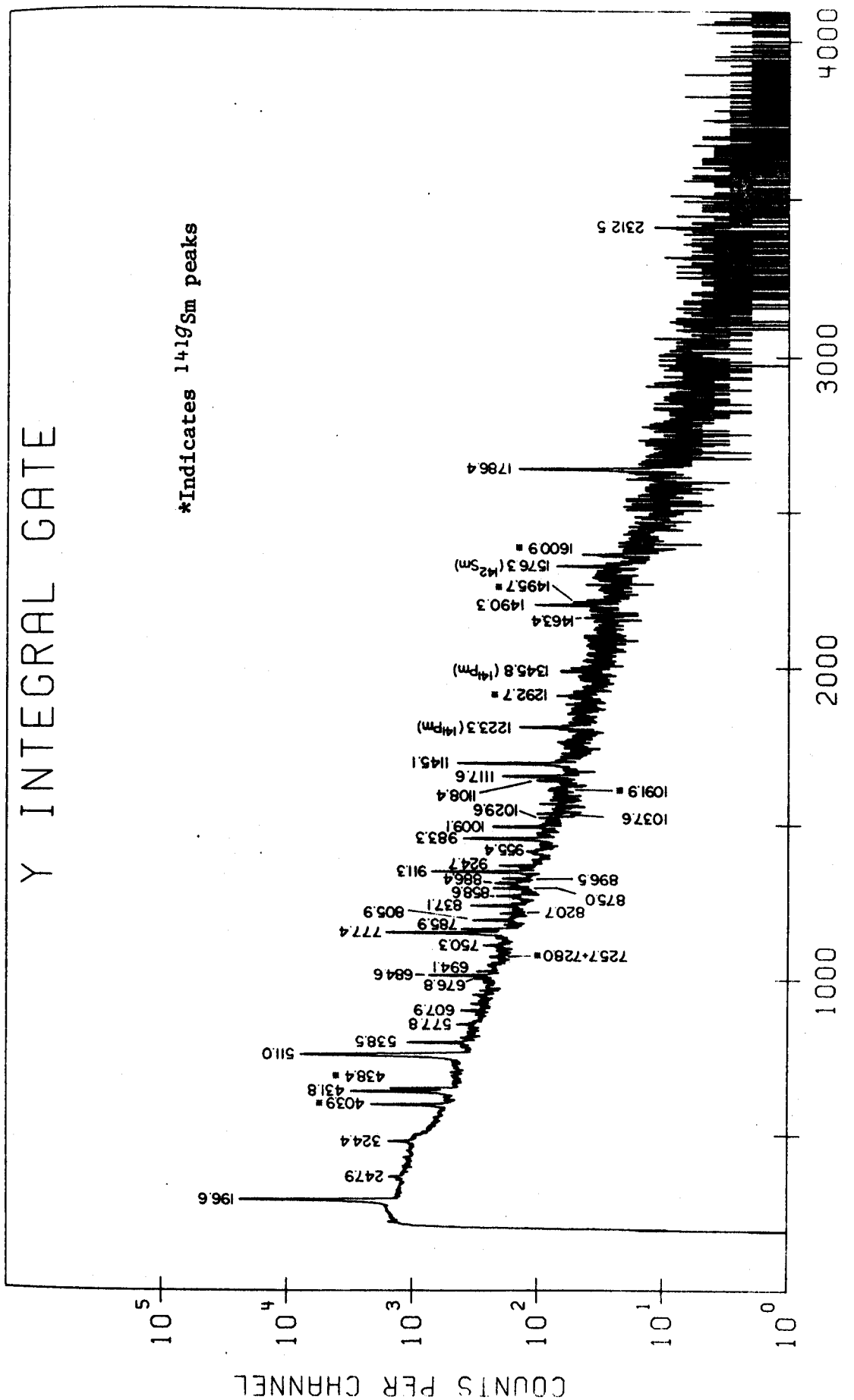

Figure 19b. ^{141m}Sm 2-dimensional integral coincidence spectrum taken with 4.5% Ge(Li) detector.

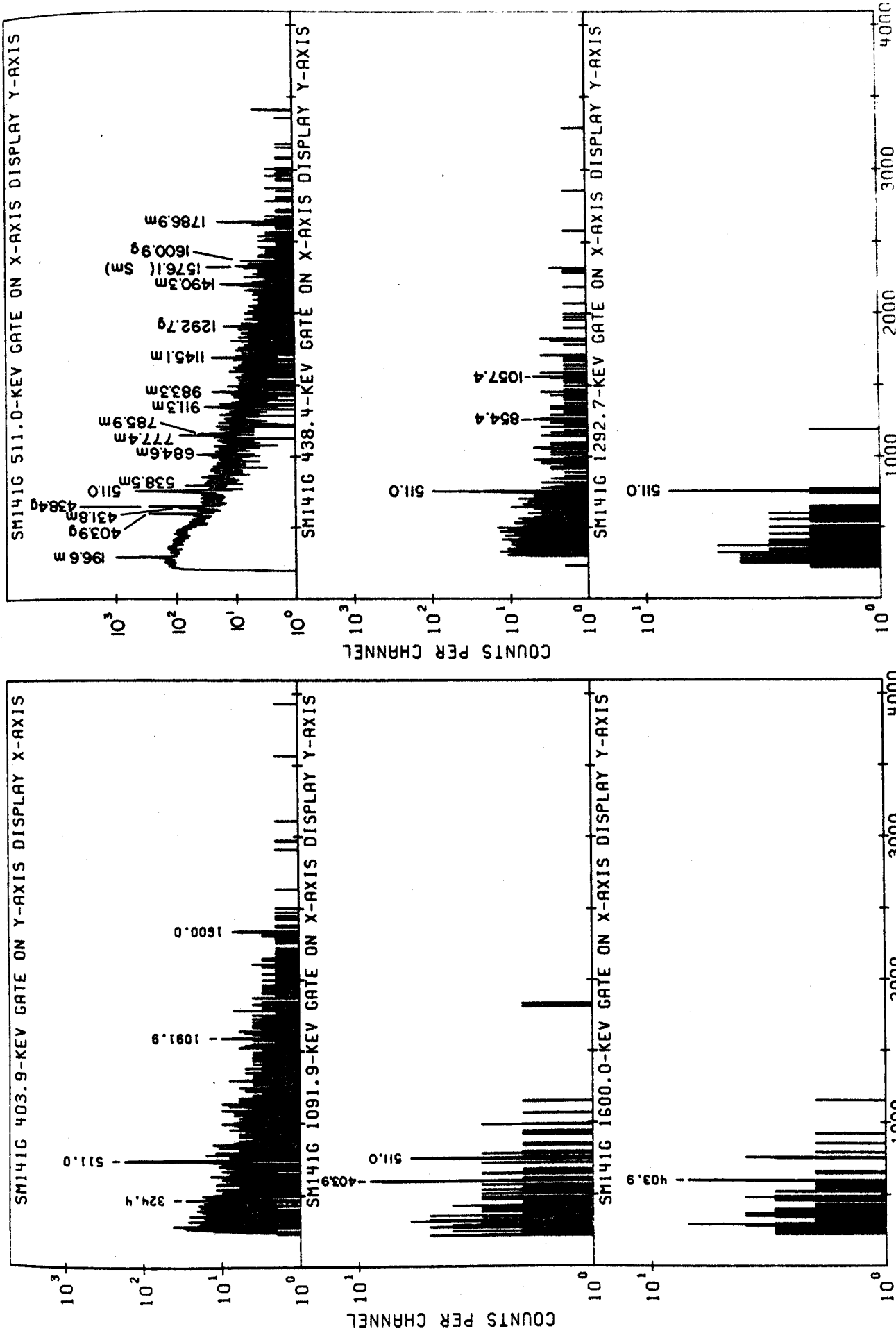

Figure 20. Gated slices from 2-dimensional coincidence spectra for ^{141g}Sm.

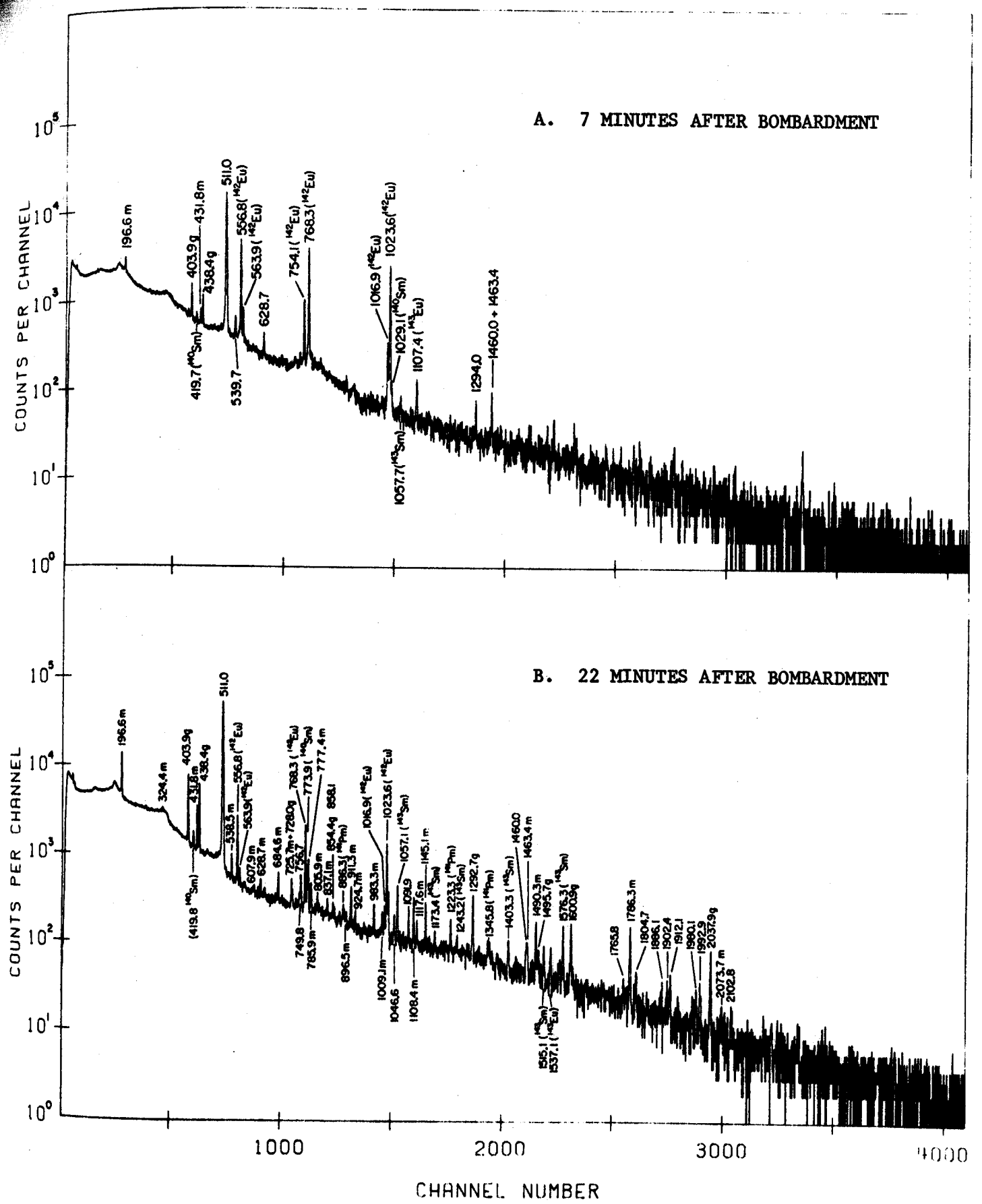

Figure 21. Spectra resulting from bombarding ^{144}Sm with 45 MeV protons.

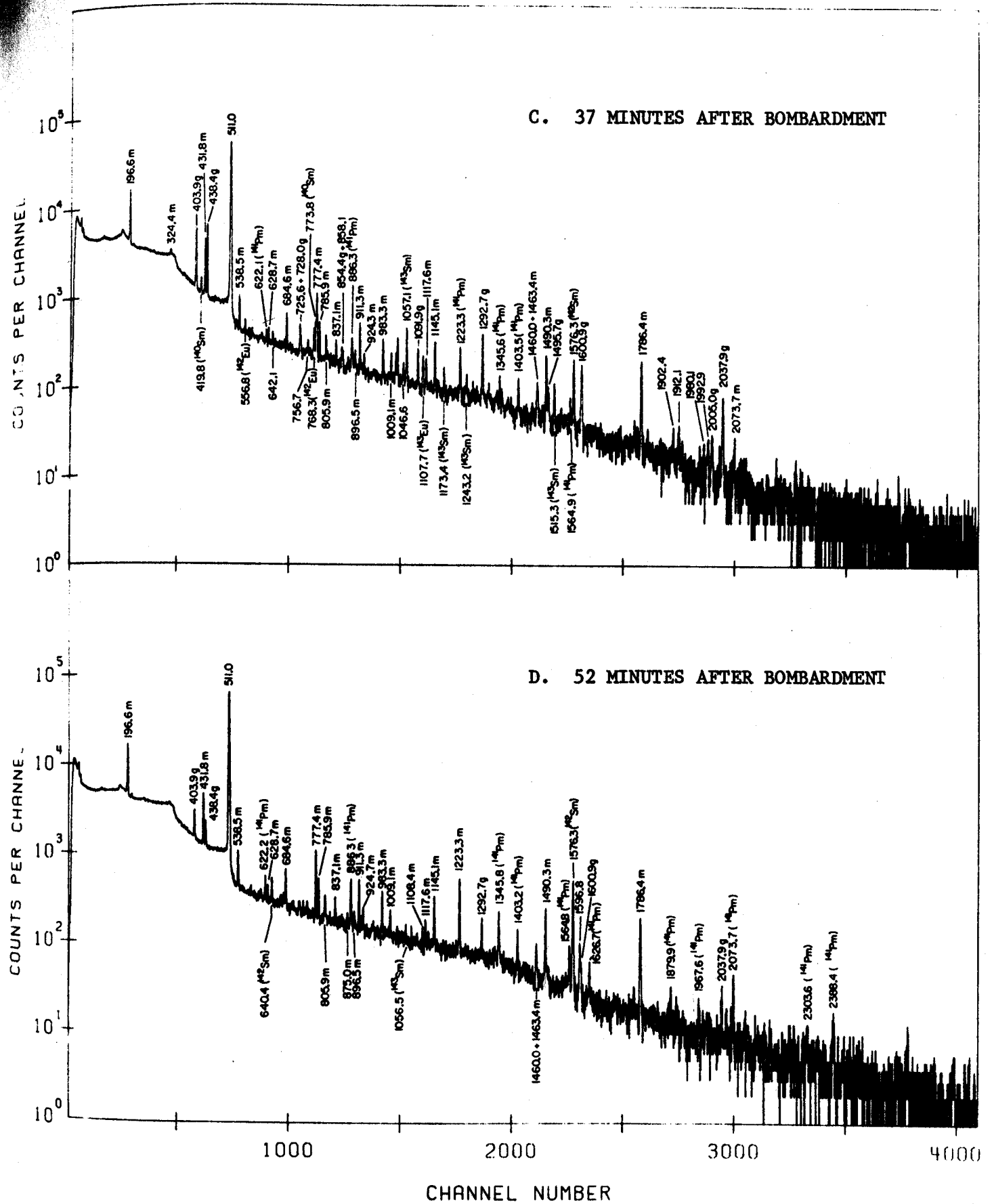

Figure 22. Spectra resulting from bombarding ^{144}Sm with 45 MeV protons for 1m.

4.1.9. ^{141g}Sm Decay Scheme

The decay scheme of ^{141g}Sm we have been able to construct from our measurements is shown in Fig. 23. The transition energies are given in keV, and the Q_{EC} is a calculated value (Myr 65). The (total) γ-transition intensities and the β feeding, both β^+ and EC, are given in percent disintegrations of ^{141g}Sm.

As can be seen from the singles spectra Figs. 4 and 5 the 403.9- and 438.4-keV transitions are the most intense lines arising from the decay of ^{141g}Sm. Together these two transitions account for 71% of the ^{141g}Sm gamma-ray intensity. This evidence seems to support the placement of levels in ^{141}Pm at 403.9 and 438.4 keV. Further evidence supporting these placements comes from the observed enhancement of transitions at 403.9 and 438.4 keV in both the anticoincidence and 511-511-keV-gamma triple coincidence spectra Figs. 8 and 9, indicating strong EC/β^+ feeding to these levels.

The placement of levels at 1495.7 and 2005.0 keV are suggested by the observation of peaks at 1091.9 and 1600.9 keV in coincidence with the 403.9-keV transition. Confirmation of these placements comes from observation of transitions of 1495.7- and 2005.0-keV.

The level at 1292.7 keV is placed on the basis of the enhancement of a peak at this energy in the anticoincidence

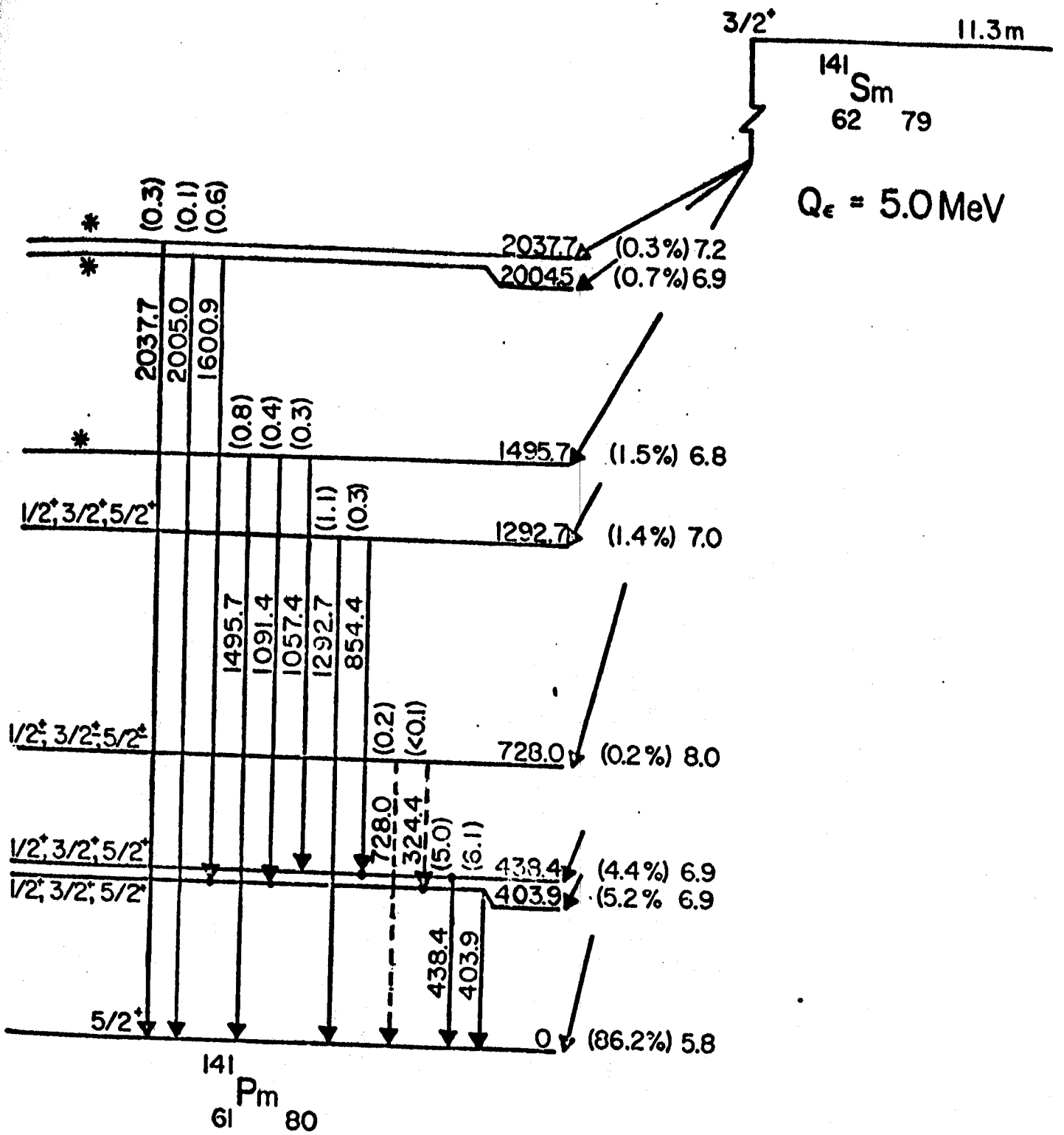

Figure 23. Decay scheme of ^{141g}Sm.

spectrum and the observed coincidences between the 438.4- and 854.4-keV gamma-rays.

The observation of a transition at 2037.7-keV in the anticoincidence spectrum suggests a level at this energy in ^{141}Pm.

Placement of the level at 728.0-keV comes about in the following manner. A transition of this energy has been observed to have the proper half-life and in addition, we have observed an apparent coincidence between the 403.9-keV line and the 324.4-keV peak in the 324.4-keV gated spectrum. The evidence is somewhat hard to reconcile since the 324.4-keV line exhibits decay characteristics closely approximating the 22.1m half-life of ^{141m}Sm. One possible explanation of these coincidence data is that the 324.4-keV peak is in the energy region of the intense compton edge from the 511.0-keV annihilation photons. The possibility exists that these coincidences arise from the very strong underlying compton background. However, this does not completely explain the enhancement of the 324.4-keV line in the 403.9-keV gate. An alternate possibility is that there are two transitions at this energy with the stronger of these exhibiting a 22.1m half-life. As a result we have dashed-in the transitions arising from the 728.0-keV level indicating that the evidence is not conclusive, although it slightly favors placement of a level at this energy in ^{141}Pm.

4.1.10 Spins and Parities of Levels in ^{141}Pm Fed by the Decay of ^{141g}Sm

The log ft values shown on the decay scheme are calculated assuming the total EC plus β^+ feeding to the ^{141}Pm ground state by the decay of ^{141g}Sm is 86.2%. Because of the presence of ^{141m}Sm and the decay of the daughter ^{141}Pm, the positron feeding by ^{141g}Sm to the ground state of ^{141}Pm is difficult to measure directly. We have estimated 86.2% to be an upper limit for the direct decay of the ground state of ^{141}Sm to the ground state of ^{141}Pm. This value of 86.2% was arrived at in the following manner. The total β^+ feeding arising from the decay of ^{141m}Sm was estimated from the EC/β^+ ratios (it was assumed ^{141m}Sm did not feed the ^{141}Pm ground state directly). The EC/β^+ ratios to the states in ^{141}Pm fed via the ^{141g}Sm decay were determined and their resultant (total) β^+ feeding was determined. In addition the 511-keV peak intensity was corrected for the intensity arising from the decay of the daughter ^{141}Pm. This latter correction was made by normalizing the 511-keV peak intensity to the 1223.3-keV peak and subtracting the contribution due to the ^{141}Pm decay as determined in Section 4.2. The intensity of the 511-keV peak after these corrections was assumed to arise solely from the beta-decay of ^{141g}Sm to the ground state of ^{141}Pm. This assumes that there is no β^+ intensity

which might arise from contaminants. This seems reasonable in light of the cleanliness of the target material, and of our observation of the reaction products. The log ft values shown on the decay scheme are calculated assuming the total beta-decay (i.e. EC+β^+) to the ^{141}Pm ground state is 86.2%. These log ft values are not significantly affected by this number, however. An error of 20% in the estimated intensity of the β^+ decay results in a change in the log ft values of 0.1, at the most.

The spin and parity assignments which appear on the decay scheme are arrived at by assuming the ground state spin of ^{141}Sm is $3/2^+$. This assumption is based on the following argument. The ground state spin of ^{141}Pm is $5/2^+$ (arguments substantiating this are presented in Section 4.1.5.B). The log ft value for the beta-decay between ^{141g}Sm and ^{141}Pm is 5.8. This value is somewhat higher than the log ft of 5.1 for the decay between ^{139g}Nd and the ^{139}Pr ground state, however it is certainly an allowed transition. This limits the possible spin of ^{141g}Sm to $3/2^+$, $5/2^+$, or $7/2^+$. The values of $5/2^+$ and $7/2^+$ seem unlikely, from the systematic behavior of other nuclei in this region. The odd neutron, odd mass nuclei with $56 \leq Z \leq 63$ are characterized by ground state spins of $1/2^+$ or $3/2^+$. The $1/2^+$ assignment is ruled out because the log ft value of 5.8 indicates an allowed transition between ^{141g}Sm and the ^{141}Pm ground state.

In addition to the preceding argument, further evidence tending to favor the $3/2^+$ assignment for the ground state of ^{141g}Sm is the overall character of the decay scheme. The ^{141g}Sm decay is similar to that of ^{139g}Nd and ^{143}Sm, whereas, if the ground state spin of ^{141}Sm were $1/2^+$, the resultant decay scheme might resemble that of ^{145g}Gd (Epp 71). ^{145g}Gd was observed to populate several high lying low-spin states but no direct decay to the ^{145}Eu ground state was observed.

Apart from the ground state, the remaining seven levels are all populated by β^+/EC decay from $3/2^+$ ^{141g}Sm with log ft values ranging from 6.9 to 8.0. Because of the total absence of any direct population of the $7/2^+$ first excited state from these levels, it is difficult to narrow down the spin assignments .

The two levels at 403.9- and 438.4-keV both appear to be populated strongly in the 511-511-keV-gamma triple coincidence spectrum, and the log ft value of 6.9 for both levels indicates they are fed by allowed beta decay. This limits each of their possible spin assignments to $1/2^+$, $3/2^+$, or $5/2^+$. It is tempting to limit these assignments to $3/2^+$ or $5/2^+$ because of the absence of an observed transition to the $7/2^+$ first excited state. However, the $1/2^+$ can not be ruled out, without more positive evidence.

The level at 728.0-keV is populated with a log ft of 8.0. This is high for an allowed transition, and, as a result, the

possibility of a first forbidden decay can not be ruled out. Consequently we have assigned spin possibilities to the 728.0-keV level of $1/2^{\pm}$ or $3/2^{\pm}$ or $5/2^{\pm}$.

The remaining levels at 1292.7-, 1495.7-, 2004.5-, and 2037.5-keV all have log ft values between 6.8 and 7.2. These are probably fed by allowed beta decay. In fact, these log ft values compare favorably with those arising from decay to the high lying levels in ^{141}Nd. As a result, we can assign these states spins of $1/2^{+}$, $3/2^{+}$ or $5/2^{+}$.

4.1.11. Discussion of Levels Populated by ^{141g}Sm Decay

It is interesting to attempt a brief comparison between the decay schemes of ^{141g}Sm and its nearest odd neutron neighbors, i.e. ^{139g}Nd and ^{143}Sm. All three decays populate the ground state strongly via beta decay 88%, 86%, and 96% for ^{139g}Nd, ^{141g}Sm, and ^{143}Sm, in that order. The corresponding log ft values are 5.1, 5.8, and 4.8. None of these β^{+}/EC decays exhibits any measureable feeding to the $7/2^{+}$ first excited state in the daughter.

The decay of ^{139g}Nd populates two low-lying states at 405.0 and 589.2 keV both with log ft values of 6.4. The state at 405.9 keV in ^{139}Pr [spin ($3/2^{+}$, $1/2^{+}$)] decays directly to ground, bypassing the $7/2^{+}$ first excited state at 113.8 keV. The ^{139}Pr state at 589.2 keV is assigned ($5/2^{+}$) and is observed to populate the $5/2^{+}$ ground state, the $7/2^{+}$ first excited state and the level at 405.0 keV.

In the case of ^{141g}Sm the decay populates two levels at 403.9 and 438.4-keV, both with log ft values of 6.9. These states both decay to the $5/2^+$ ground state bypassing the $7/2^+$ first excited state at 196.6-keV in ^{141}Pm. Their energy separation is 34.5 keV, too low to observe possible feeding from the 438.4 keV to the level at 403.9 keV.

The decay of ^{143}Sm populates three low-lying states at 1056.5-, 1173.4-, and 1403.2-keV with spins of $3/2^+$, $1/2^+$, and $3/2^+$, respectively, (Wil 71) and (DeF 70). The corresponding log ft value for beta decay to these levels are 5.9, 6.4 and 6.4, respectively.

It is interesting to note that these three levels in ^{143}Pm all decay directly to ground bypassing the $7/2^+$ first excited state at 271.8-keV.

From this comparison, the similarities seem to imply that the levels fed in the decay of ^{141g}Sm have more in common with the levels populated by the decay of ^{143}Sm than those populated in the decay of ^{139g}Nd. However, without more evidence it is difficult to reach any definite conclusions.

4.2. The Decay of ^{141}Pm

4.2.1. Introduction

^{141}Pm is twice removed from stability on the neutron deficient side of the N=82 closed shell and decays with a 20.9m half-life to 2.5h ^{141}Nd. The character of $^{141}_{60}Nd_{81}$ is such that the decay of ^{141}Pm might be expected to populate low-lying neutron hole states in the daughter, which are of a fairly pure single-quasiparticle nature. This is indeed the case, and it is possible to compare the beta decay results with those of recent particle transfer studies. These include ^{142}Nd(p,d)^{141}Nd by Jolly and Kashy (Jol 71) and a similar (p,d) study by Chaumeau et al. (Cha 71). In addition, Foster et al. (Fos 71) have reported on their studies of the ^{142}Nd(d,t)^{141}Nd reaction.

Our interest in the decay of ^{141}Pm arises from several directions. The decay of ^{141}Nd has been studied previously by the gamma ray spectroscopy group at MSU (Bee 68), and this study constitutes the next link in the A=141 decay chain. In addition we have been pursuing the identification of three-quasiparticle multiplets in the odd mass N=80 isotones. The first such multiplet was identified in the decay of ^{139m}Nd and the next decay expected to exhibit these characteristics is that of ^{141m}Sm. We report on the results of the $^{141m+g}$Sm decay in Section 4.1.

Because the half-life of ^{141m}Sm (22.1m) decay is very similar to that of the daughter decay ^{141}Pm (20.9), it was essential to the ^{141m}Sm study that we be able to distinguish between the transitions associated with the decay of each isotope. In order to avoid confusion it is very advantageous to produce the ^{141}Pm activity separately from that associated with $^{141m+g}$Sm. In carrying out this study of the decay of ^{141}Pm we have been able to obtain more information than has been available heretofore.

The first positive identification was made in 1952 by V. Kistiakowsky Fischer (Fis 52). ^{141}Pm was produced by bombarding isotopically enriched samples of $(^{142}Nd_2)O_3$ with 20-30 MeV protons. The half-life was determined to be 22±2m, in good agreement with our results of 20.9±0.2m. Prior to 1967 little else had been reported about the decay of ^{141}Pm. At that time Bleyl et al. (Ble 67) reported the half-life to be 20.90±0.05m and identified several of the strong transitions and compared their results with a Russian study (Bon 66); no attempt was made to construct a decay scheme. More recently Hesse (Hes 69) observed 11 transitions that he identified with the decay of ^{141}Pm. These transitions were identified as a by-product of his study of the decay of ^{141m}Sm. To date the most complete study has been performed by Charvet et al. (Char 70). This study identified 24 transitions arising from the decay of ^{141}Pm. Of these 24 transitions 19 were placed in a decay scheme containing 11 levels.

As a result of this current study we have identified 50 transitions belonging to the ^{141}Pm decay. Our proposed decay scheme (Fig. 29) places 43 of these transitions and contains 23 levels.

4.2.2. ^{141}Pm Source Preparation

The 21 min. ^{141}Pm activity was produced primarily by the very clean ^{142}Nd(p,2n)^{141}Pm reaction on targets of $^{142}Nd_2O_3$ (enriched to ≳90% ^{142}Nd). The bombarding times were typically 1-2m with ≳1μA beams of 24-MeV protons from the MSU cyclotron. Counting began within 2m of the end of the bombardment and a particular source was not counted longer than 50m.

A study of the excitation function was made by varying the incident beam energy in ∿3 MeV steps from below 14 MeV, the -Q value of the (p,2n) reaction, to 30 MeV, which is 5 MeV above the -Q value for the (p,3n) reaction. This allowed us to determine that our targets were free of the 6m ^{140}Pm activity and other possible contaminants.

In addition to the above experiments, ^{141}Pm sources were also produced via the reaction ^{141}Pr(^{3}He,3n)^{141}Pm (Q=-14.7 MeV) at 25 MeV as a check on the identification. The ^{141}Pm peaks were observed in the same intensity ratio and to have the same decay rates, but this reaction was not as clean as the (p,2n) reaction. The ^{141}Pm activity has

also been observed in the ^{141}Sm experiments where it is the daughter of ^{141}Sm. Comparison of the strong gamma-rays in the spectra with the results of reaction studies, has allowed us to confirm the identity of several levels in ^{141}Nd.

4.2.3. Experimental Results ^{141}Pm

4.2.3.A. ^{141}Pm Gamma-Ray Singles Spectra

Gamma-ray energies and intensities observed in the decay of ^{141}Pm were determined with the aid of a Ge(Li) detector having a counting efficiency of 2.5% with a cooled FET, and a typical resolution of 2.2-keV FWHM for the 1332.48-keV line of ^{60}Co.

With the exception of the 193.8-keV transition, the energies of the stronger lines in the ^{141}Pm spectrum were determined by observing them in the ^{141m}Sm spectra. These lines were in turn used to determine the energies of the weaker transitions. The previously measured ^{141m}Sm energies were used as standards for the determination of the ^{141}Pm energies. The results of this method were checked by subsequently observing the strong lines in the ^{141}Nd decay (Bee 68), and using ^{141}Pm to determine these energies. These results proved accurate to within the quoted error limits. The energy of the 193.8-keV transition was determined by counting the ^{141}Pm activity in the presence of ^{57}Co, ^{192}Ir, and ^{243}Cm (Epp 70a). The results from several different spectra were then averaged to arrive

at the value of 193.8-keV for the energy of the first excited state in ^{141}Nd.

Transitions belonging to the decay of ^{141}Pm were identified by their intensities in successive spectra relative to the 1223.3-keV line. Starting 2m after bombardment, 5 successive 10m spectra were accumulated. The process was repeated several times with the spectra in the corresponding time intervals added. Those gamma-rays which maintained a constant intensity relative to the 1223.3-keV in each of the five 10m spectra were identified as belonging to ^{141}Pm. The first and fifth of these spectra are displayed in Fig. 24. We have identified 50 gamma-rays associated with the decay of ^{141}Pm and incorporated 43 of these into the current decay scheme. Table X contains a complete list of the energies and intensities of the transitions observed in this study.

4.2.3.B. ^{141}Pm γ-γ Prompt Coincidence Studies

Several prompt coincidence experiments were performed using two germanium detectors. These included two-dimensional megachannel coincidence experiments using Ge(Li)-Ge(Li) spectrometers, and anticoincidence and electron-positron annihilation triple coincidence experiments utilizing Ge(Li)-NaI(Tℓ)-annulus spectrometers. Results of the different two-dimensional coincidence combinations are summarized in Table X. The results of the other coincidence experiments appear in Table XII.

Table X. Energies and Relative Intensities of γ Rays From the Decay of ^{141}Pm.

This Work		Charvet et.al (Char70)		Hesse (Hes69)	
Energy (keV)	Intensity	Energy (keV)	Intensity	Energy (keV)	Intensity
180.2±0.2	0.6±0.2				
193.8±0.1	34.9±1.7	193.7±0.3	32±3		
289.4±0.1	3.6±0.6				
538.2±0.1	1.7±0.4				
544.7±0.2	1.4±0.4				
597.2±0.1	1.2±0.3				
622.2±0.2	18.9±1.0	622.0±0.1	20±2	621.2±0.5	19.8±2.3
647.2±0.1[a]	1.3±0.3				
706.0±0.6	1.0±0.3				
756.7±0.1	1.7±0.4				
886.3±0.1	52.5±2.6	886.1±0.2	52±5	886.0±0.5	56.7±7.0
901.2±0.2	1.1±0.5				
958.7±0.1[a]	1.3±0.4				
966.3±0.1[a]	2.0±0.5				
1022.8±0.1	2.8±0.5				
1029.9±0.1	7.8±0.5	1029.6±0.5	7±0.7	1028.5±0.8	7.8±3.1
1080.7±0.4	1.0±0.2				
1223.3±0.2	100.	1223.3±0.1	100.	1222.9±0.5	100.
1345.8±0.1	27.6±1.4	1345.4±0.2	30±3	1345.0±0.7	49.4±11
1371.0±0.3	2.2±0.7	1370 ±1.0	3±0.5		
1403.2±0.1	16.0±1.0	1403.2±0.3	16±2	1403.1±0.7	17.7±4
1564.8±0.1	17.9±1.0	1564.7±0.2	17±2	1563.7±0.5	21.3±4.7
1596.8±0.1	16.1±1.0	1596.9±0.2	13.6±1.5	1597.7±0.7	20.6±4
1626.7±0.1	5.8±0.6	1626.5±0.7	6±1		
1703.8±0.2	1.2±0.2	1703.3±1	1±0.2		
1820.4±0.3	1.6±0.4	1820.2±1	1.7±0.3		

Table X - continued

1872.6±0.1	0.5±0.2				
1879.9±0.1	6.9±0.7	1879.8±0.5	8±2	1879.9±0.8	9.8±2.3
1897.1±0.1	1.1±0.3	1897.0±1	0.9±0.2		
1967.6±0.1	3.6±0.4				
2052.8±0.1	2.6±0.4	2053.3±1	2.4±0.5		
2066.2±0.2	1.3±0.2				
2073.7±0.1	13.4±1.0	2073.5±0.4	12±2	2072.9±0.6	18.4±3.1
2109.6±0.1	1.8±0.2				
2145.2±0.7	0.3±0.1				
2246.4±0.2	1.5±0.4	2247 ±1.5	1.4±0.3		
2265.3±0.3	0.7±0.1	2266 ±1.5	1±0.2		
2303.6±0.2	2.4±0.2	2305 ±1.5	1.5±0.5		
2311.6±0.2	0.5±0.1				
2354.4±0.2	1.0±0.2	2355 ±2	0.8±0.2		
2388.4±0.1	1.3±0.2	2389 ±2	1 ±0.2		
2419.1±0.5[a]	0.2±0.1				
2429.8±0.5	0.6±0.1				
2505.0±0.5	0.6±0.2	2505 ±2	0.5±0.1		
2602.1±0.5[a]	0.1±0.05				
2612.3±0.5	0.3±0.1				
2619.6±0.5	0.4±0.1				
2690.3±0.5[a]	0.2±0.1				
2804.9±0.5	0.5±0.1	2804 ±2	0.4±0.1		
2985.5±0.5	0.9±0.2				

[a] These transitions belong to ^{141}Pm but we were unable to place them in the decay scheme.

302.9[b]

788.9[b]

1037.7[b]

1043.2[b]

[b] These transitions were observed to have a half-life slightly longer than that of ^{141}Pm. ($\tau_{1/2}$ est. ~ 30 min.)

Table XI. γ-Ray Intensities for ^{141}Pm Coincidence Experiments

Energy (keV)	Relative Intensities				
	Singles	Anti-Coinc.	Integral Coinc.	193.8-keV Gate	511-511-keV Coinc.
180.2	0.6				
193.8	34.9	26.4	574.1		7.5
289.4	3.6		39.6	1.9	
511.0	2385				65.5
538.2	1.7		7.4		
544.7	1.4				
597.2	1.2		4.7		
622.2	18.9	7.3	58.7		4.6
647.2	1.3				
706.0	1.0				
886.3	52.5	20.5	114.3	3.3	4.2
901.2	1.1				
958.7	1.3		2.1		
966.3	2.0		3.4		
1022.8	2.8		4.7		
1029.9	7.8	1.9	17.3	6.9	5.3
1051.9	2.0				12.6
1080.7	1.0				
1223.3	100	56.1	100		100
1282.1	0.9				3.3
1345.8	27.6	9.0	39.3		8.6
1371.0	2.2		2.7	2.8	
1403.2	16.0	5.8	17.5	16.0	6.6
1564.8	17.9	13.9	6.5		16.9
1596.8	16.1	16.1	3.2		19.4
1626.7	5.8		7.1	5.8	
1703.8	1.2		0.7	0.6	
1820.4	1.6	2.0	1.0		
1872.6			0.8	1.3	

Table XI Con't.

Energy (keV)	Singles	Anti-Coinc.	Integral Coinc.	193.8-keV Gate	511-511-keV Coinc.
1879.9	6.9	3.8	4.2	6.0	
1897.1	1.1				
1967.6	3.6	3.4			
2052.8	2.6			2.5	
2066.2	1.3				
2073.7	13.4	16.0			1.8
2109.6	1.8	2.5			
2145.2	0.3				
2246.4	1.5	2.5			
2265.3	0.7				
2303.6	2.4	2.5			
2311.6	0.5				
2354.4	1.0	1.1			
2388.4	1.3	1.5			
2429.8	0.6	0.3			
2505.0	0.6	0.5			
2602.1	0.1				
2619.6	0.4	0.3			
2690.3	0.2	0.1			
2804.9	0.5	0.3			
2985.5	0.9				

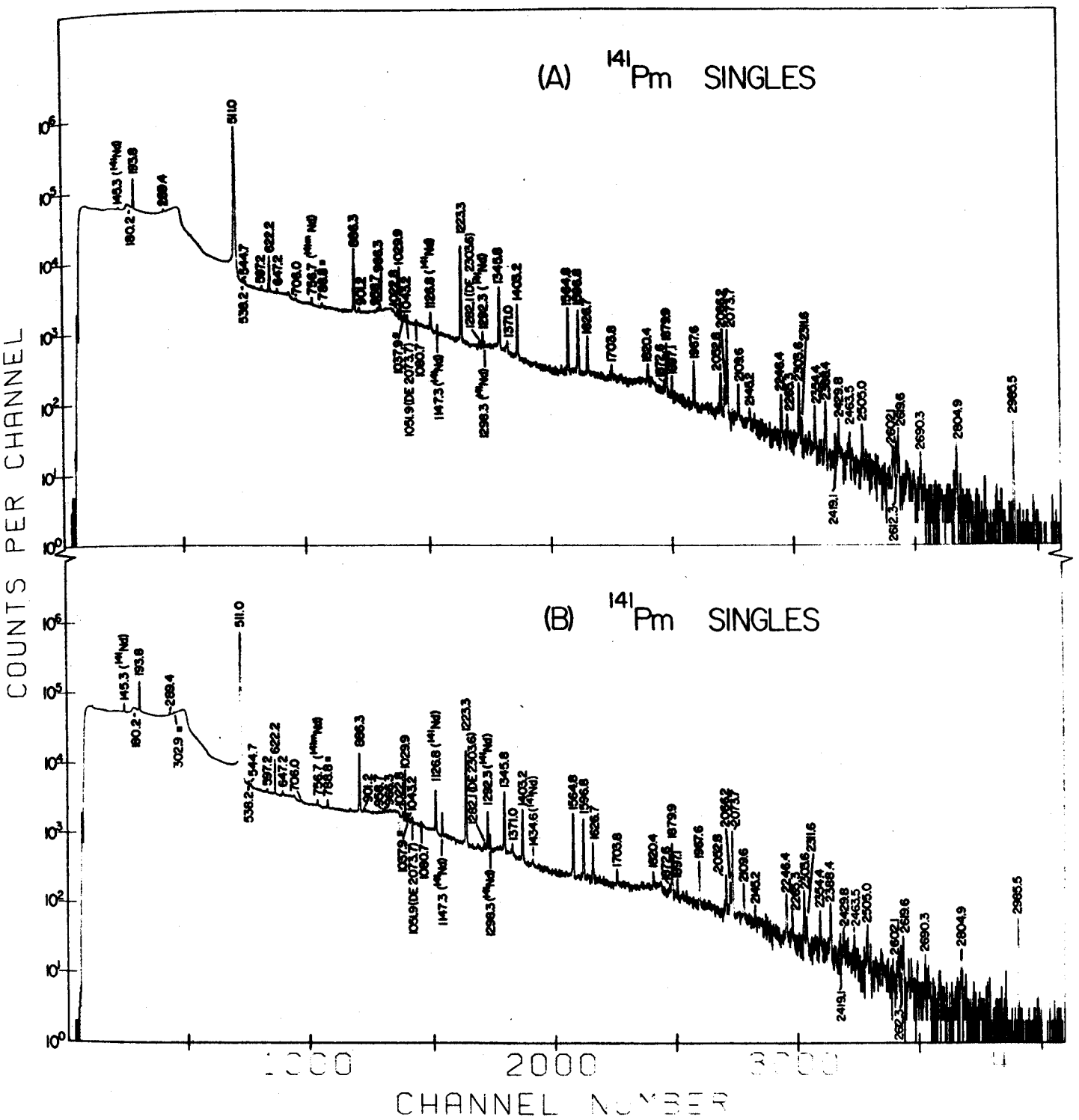

Figure 24. Singles γ-ray spectra for ^{141}Pm.

Upper: First of five successive 10m spectra.
Lower: Fifth of five successive 10m spectra.

Details of the two-dimensional megachannel coincidence experimental set-up are outlined in Section 2.1.2.A. The detectors used were the 4.5% efficient and 10.4% efficient Ge(Li) detectors with 2.0-keV and 2.2-keV resolution FWHM, respectively, at 1332.48-keV. The detectors were placed in 180° geometry with a graded Pb absorber between them to help prevent scattering from one detector into the other. The source was placed off-center as shown in Fig. 3 in order to reduce the 180° coincidences between the 511-511-keV annihilation photons. Coincidence events were recorded on magnetic tape using the data taking program EVENT and the Sigma-7 computer. This yielded a 4096x4096 channel array of prompt coincidences with a resolving time 2τ=120 ns, typically. The integrated (total) coincidence spectrum is shown in Fig. 25, and the various gated spectra are shown in Figs. 25 and 26. Because the ^{141}Pm EC/β^+ decay is ~90% to the ground state of ^{141}Nd and the half-life is 21m, the 2-dimensional Ge(Li)-Ge(Li) coincidence experiment is difficult and information is hard to obtain. This two-dimensional experiment represents a counting time of 12 hrs with very frequent replenishment of the sample and replacement of the old source by a new source every 40-50m in order to achieve higher counting efficiency. Despite the low statistics involved, these spectra were invaluable in construction of the decay scheme and their

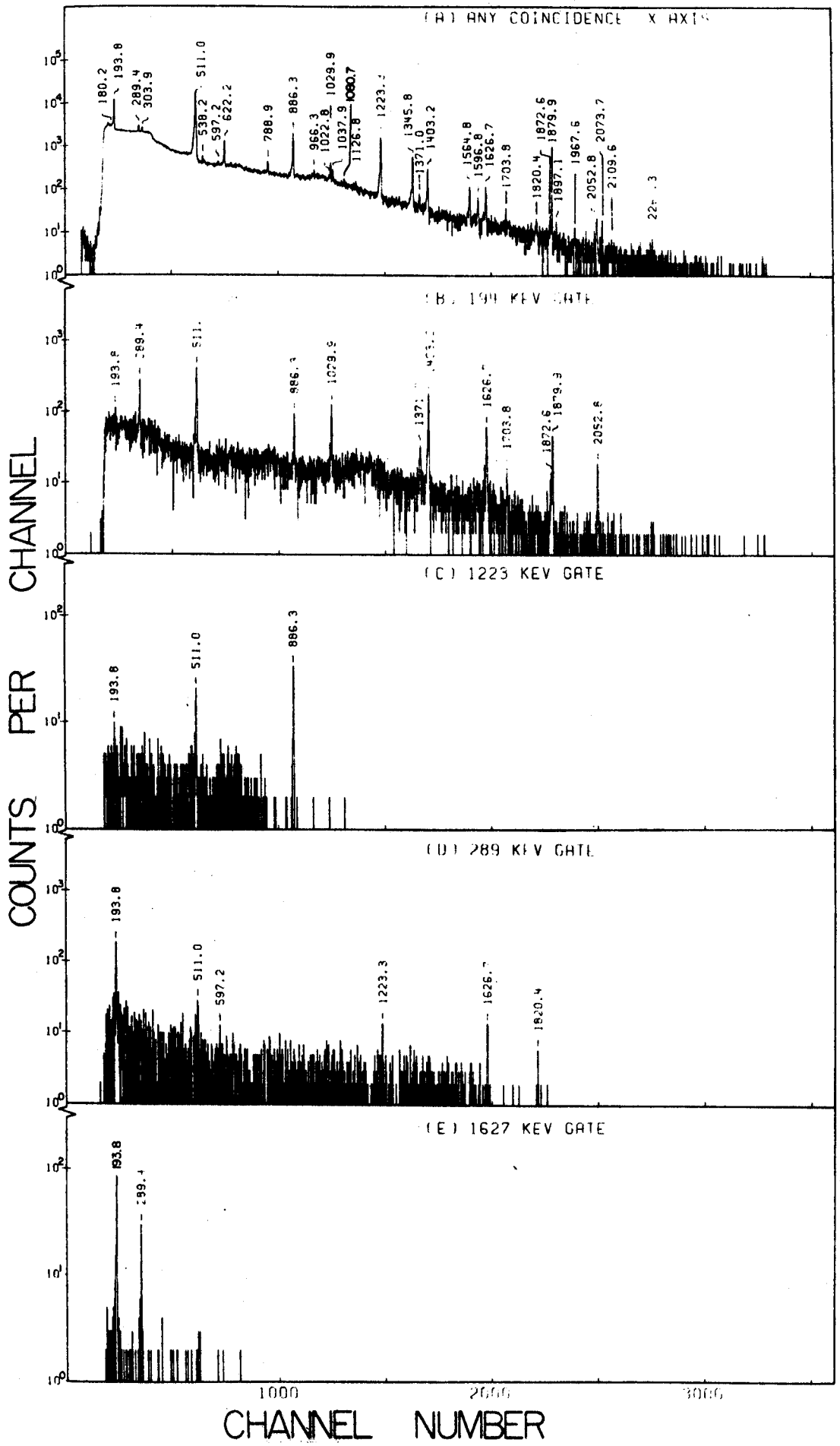

Figure 25. Results of 2-dimensional Ge(Li)-Ge(Li) coincidence experiment for ^{141}Pm.

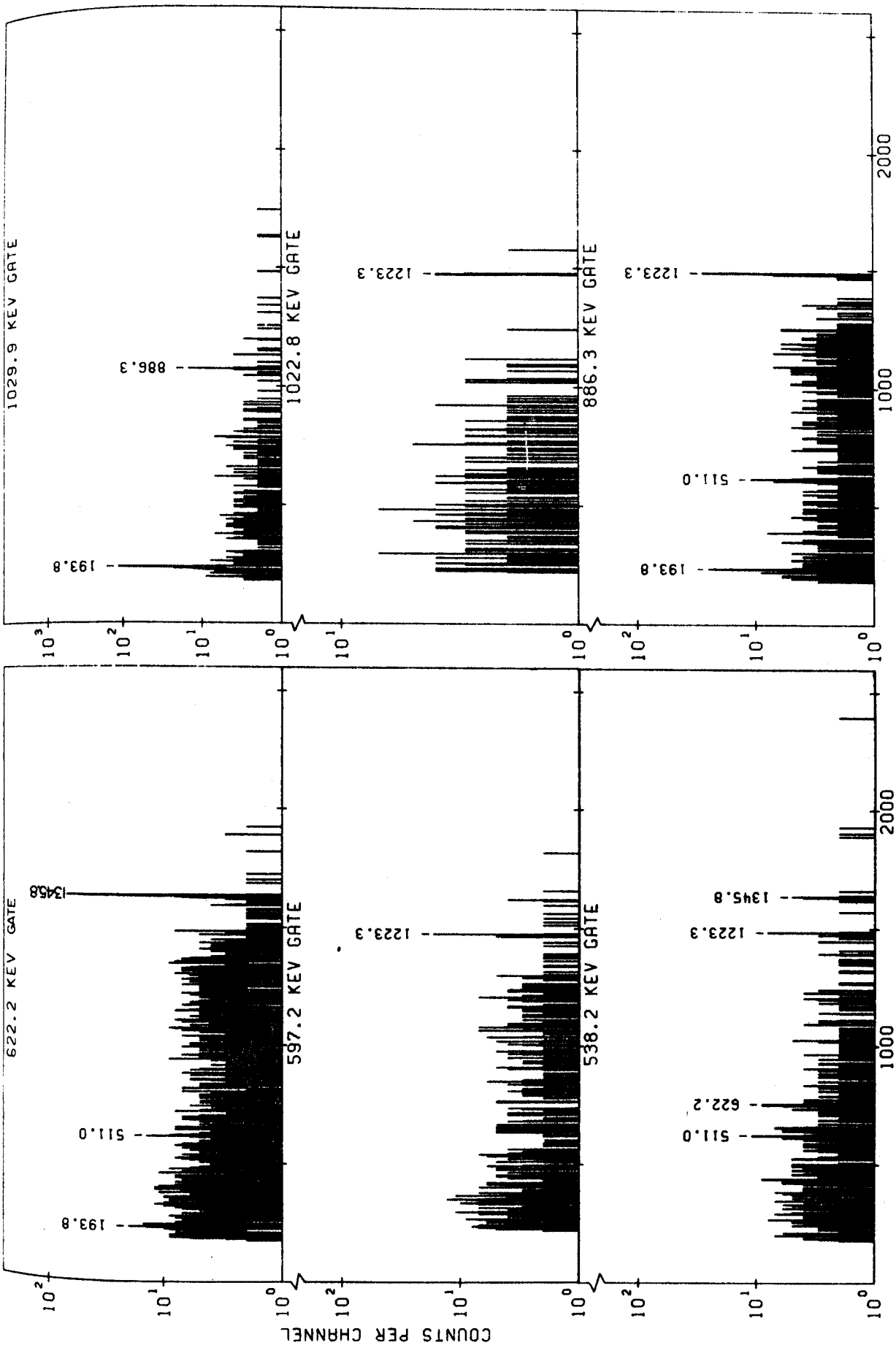

Figure 26a. Additional gated slices from the 2-dimensional Ge(Li)-Ge(Li) coincidence experiments on ^{141}Pm.

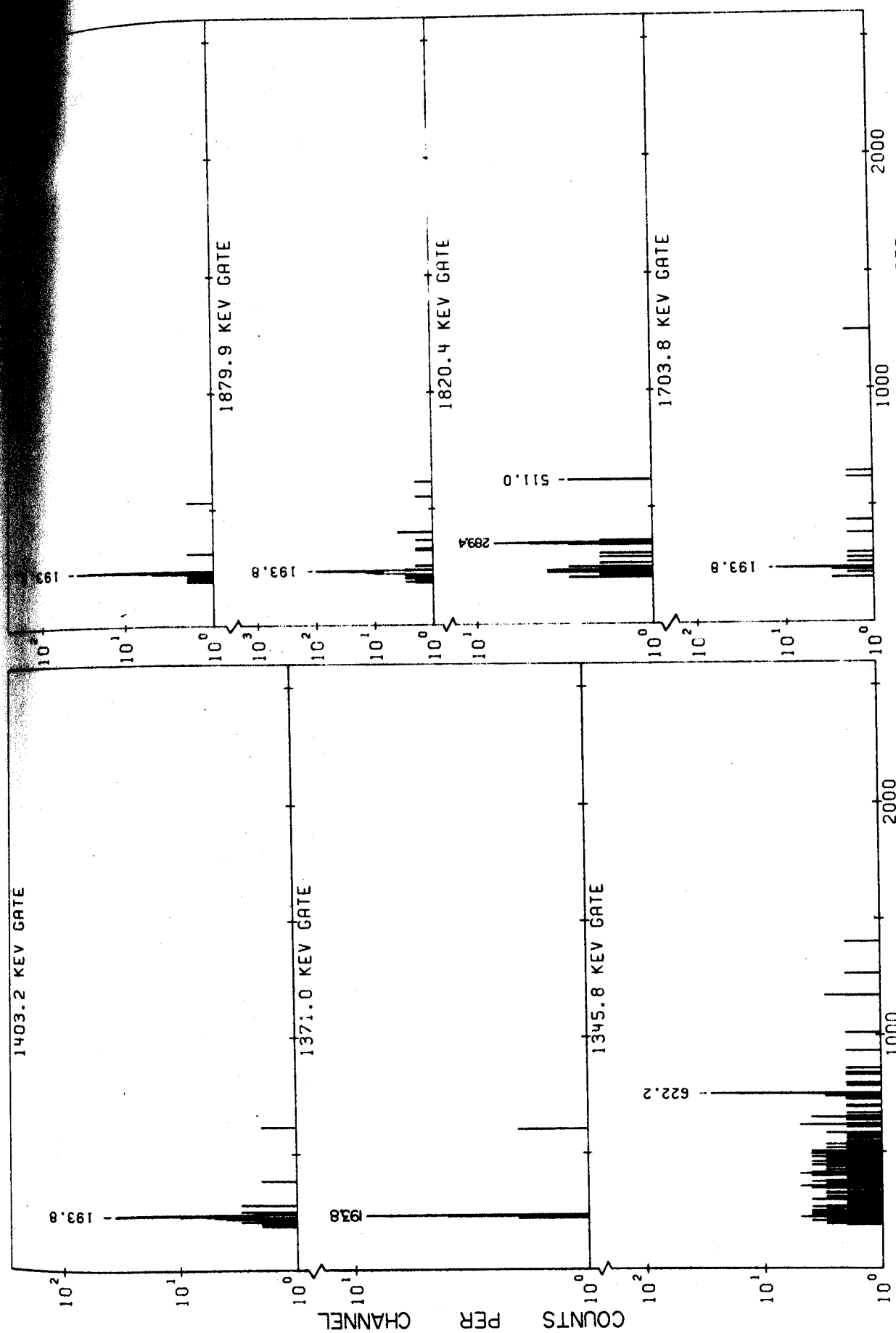

Figure 26b. Additional gated slices from the 2-dimensional Ge(Li)-Ge(Li) coincidence experiments on ^{141}Pm.

results were confirmed by other independent evidences (Char 70) and charged particle reactions (Jo 71), (Cha 71), and (Fos 71).

Additional coincidence data were obtained using the NaI(Tℓ) annulus and a Ge(Li) detector. The anticoincidence spectrum shown in Fig. 27 was obtained under the experimental conditions described in Section 2.1.2.B. This spectrum was taken with a 0.4% Ge(Li) detector (having a 3.0-keV resolution FWHM at 1332-keV) placed in the tunnel of the 8x8 in NaI(Tℓ) annulus with the ^{141}Pm source in the center of the annulus. The Ge(Li) detector was operated in anticoincidence with γ-rays above 100-keV in the NaI(Tℓ) detectors (2τ=100 ns), and a true-to-chance ratio of ~100/1, resulting in the enhancement of those transitions not in prompt coincidence with other γ-rays, x-rays or with β^+ emission. This was particularly useful in placing transitions to the ground state or to a metastable state providing these transitions are fed primarily by EC and not β^+.

The pair (511-keV-511-keV-γ) coincidence spectrum shown in Fig. 28 was obtained using absorbers to enclose the sample to assure total annihilation of the positrons. The experimental details are described in Section 2.1.2.B. In this experiment the single channel analyzers associated with each half of the annulus had their windows adjusted

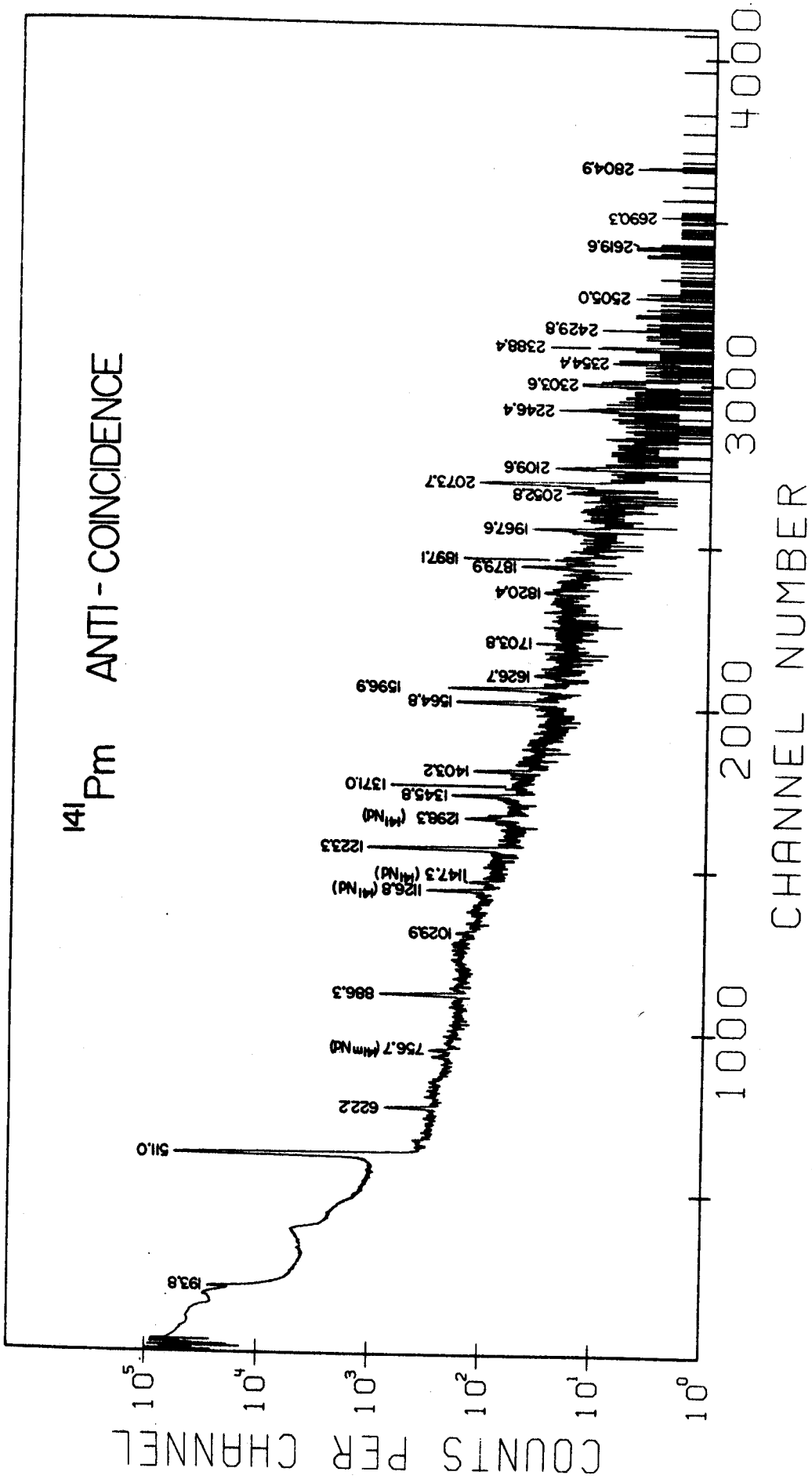

Figure 27. ^{141}Pm anticoincidence spectrum.

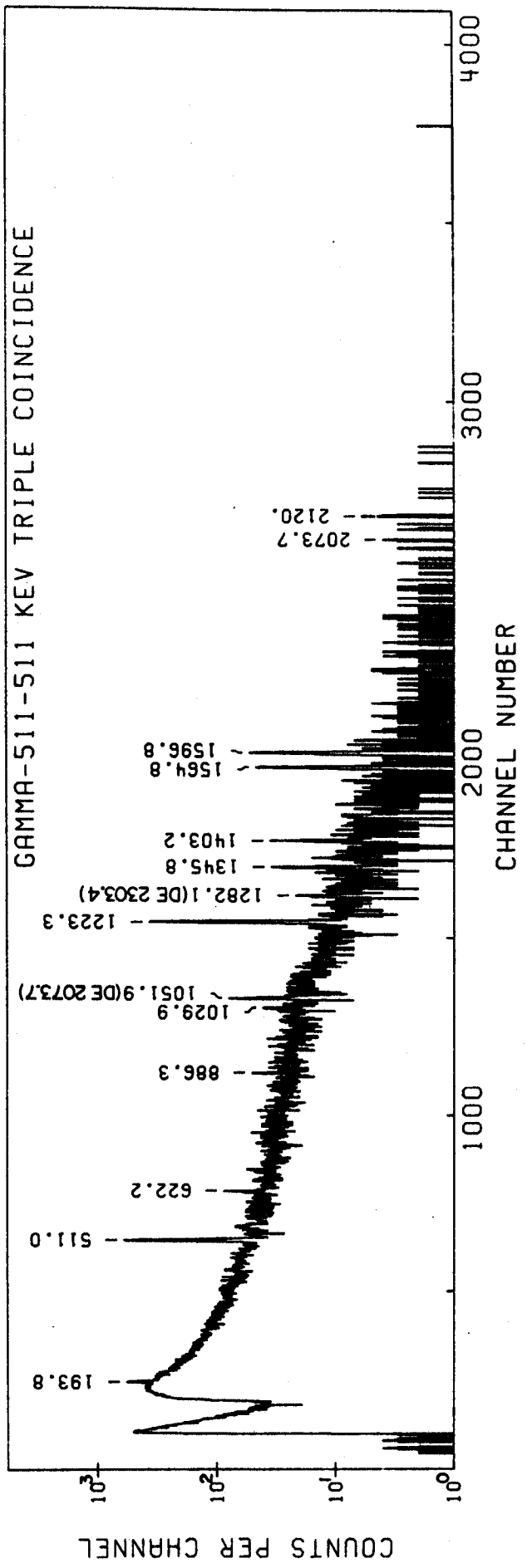

Figure 28. 511-511-keV-γ coincidence spectrum for ^{141}Pm.

to accept only the 511-keV region. A triple coincidence (resolution ~100 ns) was required in order for the fast coincidence unit to generate a gate signal and allow signals from the Ge(Li) detector to be analyzed by the ADC and stored in the analyzer. The result is that only double-escape peaks and transitions from levels fed by β^+ decay appear in the spectrum. The various coincidence results are summarized in Table XII.

4.2.4. ^{141}Pm Decay Scheme

The ^{141}Pm decay scheme we have constructed from our current measurements is illustrated in Fig. 29. All energies are given in keV and Q_{EC}=3.73 MeV is the value determined by Charvet et al. (Char 70). This compares with the theoretical value of 3.622 MeV (Myr 65). The (total) γ-transition intensities, as well as the total beta feeding, are given in percent disintegrations of ^{141}Pm. The log ft values were calculated using 20.9-m for the half-life of ^{141}Pm.

Placement of the level at 193.8-keV is straight-forward and is based on a number of facts. It is the third strongest gamma-ray in the spectrum and is not observed in coincidence with the two strongest lines at 1223.3- and 886.3-keV. Other evidences include the observation of a large number of transitions in coincidence with it, Figs. 25 and 26, complemented by the observation of 7 transitions whose

Table XII. Summary of γ-γ Two-Dimensional Coincidence Results for ^{141}Pm Decay

Gated Energy (keV)	Energies of γ-rays in the Gated Spectra	
	Strong	Medium to Weak
193.8	289.4, 1029.8, 1371.4, 1404.3, 1626.7, 1703.6, 1879.9, 2052.7	886.3
289.4		193.8, 597.2, 1223.3, 1626.7, 1820.3
538.2		622.1, 1345.5
597.2		1223.4
622.2	1345.8	
886.3		193.8, 1223.3
1022.8		1223.3
1029.9		193.8, 886.3
1223.3	886.3	
1345.8	622.2	
1371.0		193.8
1403.2	193.8	
1626.7	289.4	193.8
1703.8		193.8
1820.4		289.4
1879.9	193.8	
2052.8		193.8

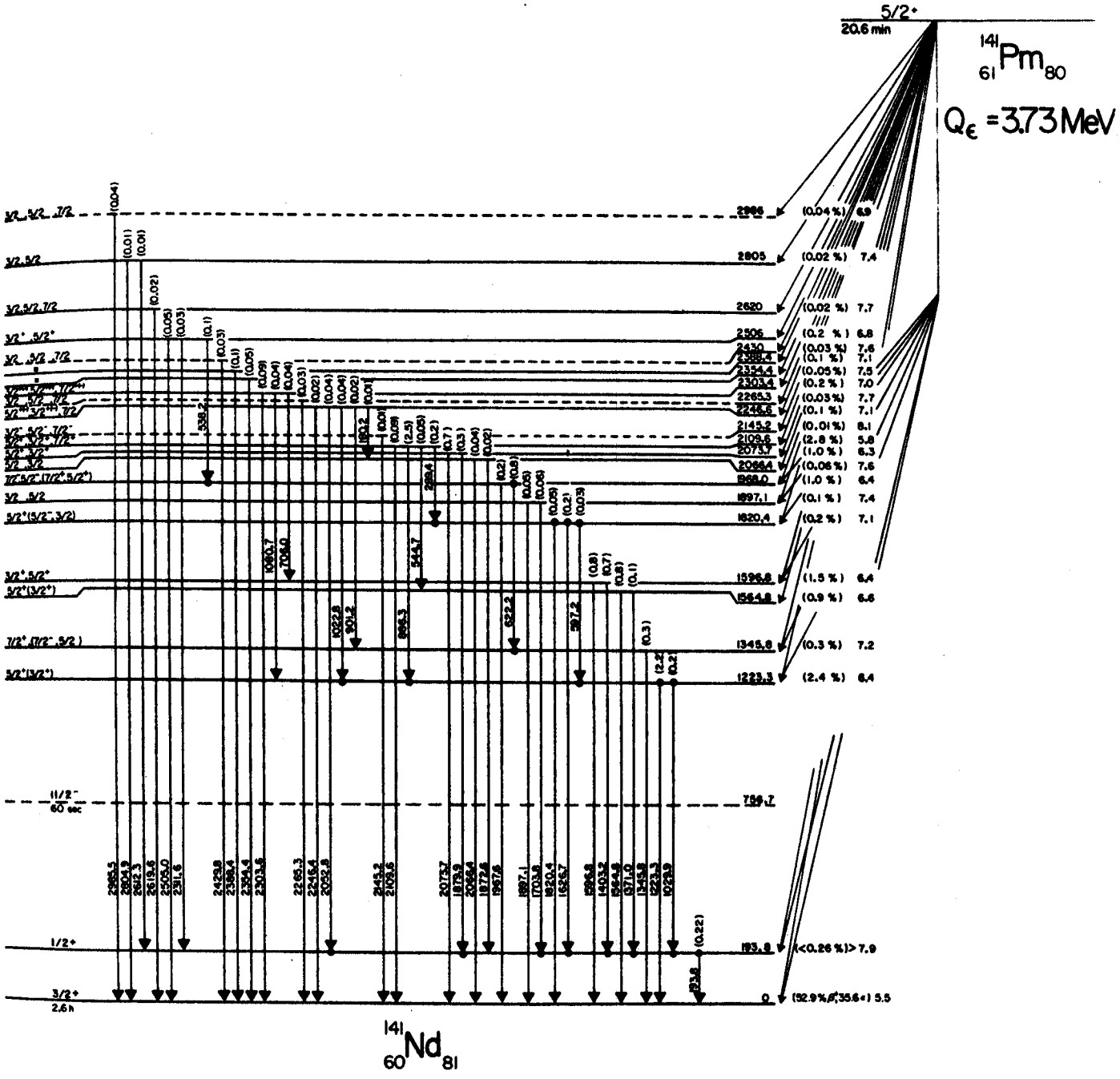

Figure 29. Decay scheme of ^{141}Pm.

energy is equal to the sum of 193.8-keV and the energy of a corresponding transition observed in the 193.8-keV gated spectrum. In addition, this level has been observed in (p,d) and (d,t) reaction studies (Jol 71), (Cha 71), and (Fos 71).

The placement of levels at 1223.3-, 1345.8-, 1564.8-, and 1596.8-keV is suggested by the enhancement of gamma-rays at these energies in both the anticoincidence Fig. 27 and 511-511-keV-gamma triple coincidence spectra (Fig. 28). The levels at 1820.4-, 1968.0-, 2073.7-, 2109.6-, 2246.6-, 2303.4-, 2354.4- and 2388.4-keV can be placed from the fact that peaks at these energies are enhanced in the anticoincidence spectrum.

Levels at 1820.4-, 1897.1-, 2066.4-, and 2265.3-keV are placed by observing that transitions from these states are in coincidence with the 193.8-keV transition and transitions from these levels to the ground state are enhanced in the anticoincidence spectrum.

By relying on energy sums we can postulate levels at 2506- and 2805-keV. Transitions of 2505.4- and 2804.9-keV have been observed, and corresponding transitions of 2311.6- and 2612.3-keV are observed to add with the 193.8-keV transition to give 2506 and 2805. The low efficiency of the Ge(Li) detectors for high energies, prevented these coincidences from being readily observed.

The remaining levels at 2145.2-, 2620-, and 2986-keV are placed solely on the observation of transitions of these energies in the singles experiments and our inability to observe possible sums with other transitions. These transitions are of sufficiently low intensity, that it would be very hard to observe them in either the anticoincidence or triple coincidence experiments.

In addition to these levels, we show the level at 756.7-keV which is the well known 60 sec $11/2^-$ isomeric state in ^{141}Nd. Referring to the first spectrum in Fig. 10, which began 6m after bombardment and was accumulated for 10m, the 756.7-keV transition appears quite intense. This is attributed mostly to the direct production of ^{141m}Nd via the reaction ^{142}Nd (p,p'n)^{141}Nd (Q=-7.1 MeV). The 756.7-keV intensity drops quite rapidly in subsequent spectra, in agreement with this assumption. However, the second spectrum in Fig. 10, which was taken for an elapsed time of 10m beginning 54m after bombardment, shows that the 756.7-keV transition still has a measureable intensity. One would normally expect that the intensity of this peak would have decreased by a factor of $\simeq 2^{54}$ in this amount of time. In fact the relative intensity of this line in the last four of the five successive ten minute spectra is relatively constant, with an average value of 1.7 (normalized to the 1223.3-keV line). This would seem to indicate that there is some indirect feeding of this level in the decay,

Table XIII

^{141}Nd Level-Scheme Comparison

Present Work		Charvet et al.[a]		Jolly and Kashy[b]		Chameux et al.[c]		Foster et al.[d]	
Energy (keV)	Assignment	Energy (keV)	Assignment	Energy (keV)	Assignment	Energy (keV)	Assignment	Energy (keV)	Assignment
0	$3/^+$	0	$3/^+$	0	$3/^+$	0	$3/^+$	0	$3/^+$
193.8	$1/^+$	193.7	$1/^+$	190	$1/^+$	222	$1/^+$	193	$1/^+$
[756.7[e]	$11/^-$	756.8[e]	$11/^-$]	760	$11/^+$	755	$11/^-$	756	$11/^-$
1223.3	$5/^+(3^+/)$	1223.3	$5/^+$	1200	$5/^+$	1220	$5/^+$	1221	$(5/^+)$
1345.8	$7/^+(7/^-,5/^\pm)$	1345.4	$7/^-(5/^-)$	1330	$(7/^+)$	1370		1343	$(7/^+)$
1564.8	$5/^+(3/^+)$	1564.7		1560	$(5/^+)$	1560	$5/^+$	1561	$(5/^+)$
1596.8	$5/^+,3/^+$	1596.9	$3/^+(5/^+)$	...		...		...	
1820.4	$5^+/,(5/^-,3/^\pm)$	1820.2		1800	$(5/^+)$	1840	$5/^+$	1817	$(5/^+)$
...		...		1870	$1/^+$	...		1887	$1/^+$
1897.1	$5/^\pm,3/^\pm$	1897.0		...		...		...	
1968.0	$7/^-,5/^-$, $(5/^+,7/^+)$	1967.4	$(7/^+)$	...		...		...	
2066.4	$5/^\pm,3/^\pm$	...		2050	$(5/^+)$	...		...	
2073.7	$3/^+,5/^+$	2073.5	$3/^+(5/^+)$	2090	$(5/^+)$	2090	$5/^+$	...	
2109.6	$3/^+,5/^+,7/^+$	2109.4	$(5/^+)7/^+$	...		...		...	
2145.2	$3/^-,5/^-,7/^-$	...		...		...		...	
...		...		2190	$11/^-$	...		...	

Table XIII Con't.

Present Work		Charvet et al.[a]		Jolly and Kashy[b]		Chameux et al.[c]		Foster et al.[d]	
Energy (keV)	Assignment	Energy (keV)	Assignment	Energy (keV)	Assignment	Energy (keV)	Assignment	Energy (keV)	Assignment
...		...		...		2210	$7/^+$	...	
2246.6	$3/^\pm,5/^\pm,7/^\pm$	...		...		...		...	
2265.3	*	...		...		...		...	
2303.4	*	...		2300	$(7/^+)$	2310		...	
2354.4	*	...		...		...		...	
2388.4	*	...		...		...		...	
2430	*	...		...		...		...	
2506	$3/^+,5/^+$	...		...		...		...	
2620	$3/^-,5/^-,7/^-$	...		2590		...		...	
2805	$3/^\pm,5/^\pm$	2804		2800		...		...	
...		...		2910		2910	$5/^+$	...	
2986	$3/^\pm,5^\pm/,7/^\pm$	...		...		...		...	
...		...		3090	$7/^+$	3100		...	
...		...		3370	$5/^+$	3350		...	

[e] ^{141m}Nd is not populated in the decay of ^{141}Pm.
This has been well characterized as one of the N=81 M4 isomers. (Bee 68)(Jan 69)

[a] (Char 70)
[b] (Jol 71)
[c] (Cha 71)
[d] (Fos 71)

of ^{141}Pm, or another γ-ray of this same energy. By adding a level at 1403.9-keV we could place the 607.9- and 706.0-keV transitions between the level at 2109.6-keV and the level at 756.7-keV. The intensity of 607.9-keV transition does not balance with that of the 756.7-keV transition, and we have placed it elsewhere on the basis of other energy sums. However, these transitions have intensities low enough to have an error of 10-20% associated with them. Consequently it is difficult to determine whether these are the only transitions which might possibly feed the level at 756.7-keV. Others may have gone unobserved.

This decay scheme (Fig. 29) is in good agreement with that reported by Charvet et al. (Char 70). However, we have added ten levels to the 13 initially proposed by Charvet and placed an additional 25 transitions for a total of 43. The only significant disagreement between our results and those of Charvet concern the spin of the levels at 1345.8- and 1968.0-keV (discussed in Section 3.2.4.). In Table XIII we compare our results with those of Charvet et al. and include the results of the (p,d) and (d,t) reaction studies (Jol 71), (Cha 71), and (Fos 71).

4.2.5. Spin and Parity Assignments of Levels in ^{141}Nd Populated by the Decay of ^{141}Pm

4.2.5.A. ^{141}Pm Ground State

The ground state spin of ^{141}Nd has been determined by the atomic beam method to be 3/2 (Alp 62), and in shell-model terms it is predicted to be a $(d_{3/2})^{-1}$ neutron state. Results of (p,d) and (d,t) reaction studies have confirmed a $3/2^+$ assignment for this state (Jol 71), (Cha 71), and (Fos 71). This evidence, coupled with our data, indicates the ground-state spin of ^{141}Pm is $5/2^+$, as described below.

Our results show that 89% of the EC/β^+ decay of ^{141}Pm populates the $3/2^+$ ground state of ^{141}Nd. The log ft value for the transition is 5.5, and this certainly suggests an allowed beta decay. This implies the spin assignments of $1/2^+$, $3/2^+$, or $5/2^+$ for the ground-state spin of ^{141}Pm. We can narrow down the possible spin by observing the systematics of odd-proton odd-mass nuclei in the $51 \leq Z \leq 63$ region. These nuclei all exhibit ground-state spins of $5/2^+$ or $7/2^+$. In the Pm isotopes the ground-state spins of ^{143}Pm and ^{145}Pm are $3/2^+$ while the heavier isotopes, beginning with ^{147}Pm, exhibit $7/2^+$ ground state spins. The possibility of a $7/2^+$ spin for the ^{141}Pm ground state can be eliminated because this would require a second-forbidden non-unique β-transition. This clearly is in conflict with the observed value of 5.5 for the log ft. Hence we will assume in our following arguments that the ground state spin of ^{141}Pm is $5/2^+$.

4.2.5.B. The 193.8-keV and Higher States

We observed no direct population ($\lesssim$0.26%) of the 193.8-keV state in ^{141}Nd. This figure could certainly be much less since it is based on intensity balances of the gamma rays feeding this level, and these could be in error by as much as ±10%. As a result of this situation, we have calculated a minimum value of the log ft for decay to this level of 7.9. We feel the actual value is certainly no lower than this and quite probably much higher. These observations are consistent with this state being assigned $s_{1/2}$ from the (p,d) and (d,t) reaction studies. This state has also received careful study from Charvet et al. (Char 70). The lifetime of this state was found to be 1.17±0.15 ns and the E2/M1 mixing ratio was determined to be: δ^2=0.15±0.04.

The log ft values for the remaining states in ^{141}Nd range from 6.3 to 7.7. This immediately suggests either allowed or, at most, first forbidden non-unique transitions and limits their possible spins to 3/2, 5/2, or 7/2. In the following we try to narrow down the spin assignments by making comparisons with the (p,d) and (d,t) studies (Jol 71), (Cha 71), and (Fos 71) and the conversion electron work of Charvet et al. (Char 70).

For reference, we include the electron work of Charvet et al. (Char 70) in Table XIV. In Fig. 30 we graphically compare these experimental results with the theoretical calculations of Hager and Seltzer (Hag 68).

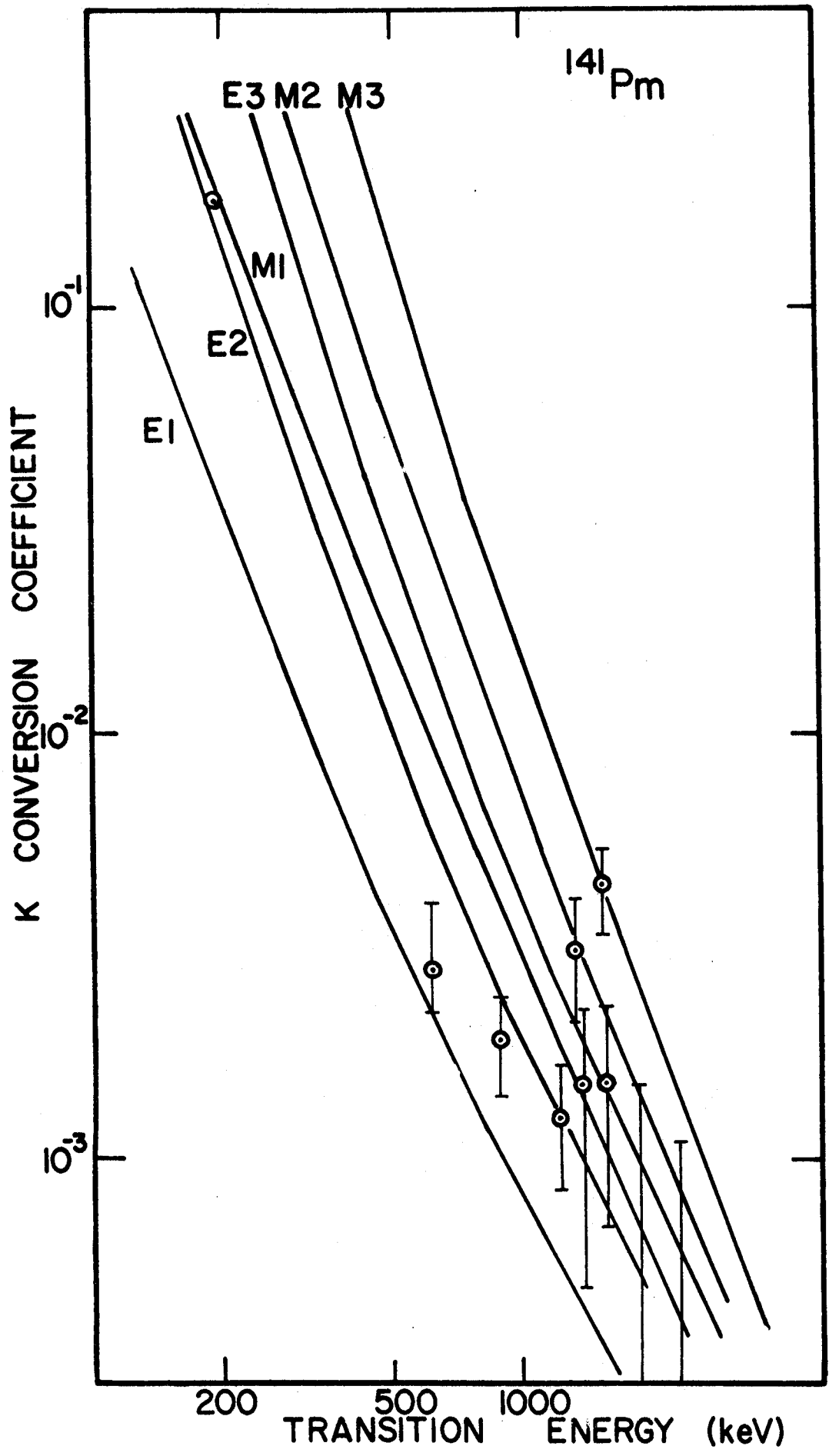

Figure 30. Comparison of experimental and theoretical K-conversion coefficients for some of the γ-transitions following the ^{141}Pm decay.

Table XIV. The ^{141}Pm Conversion Electron Results of Charvet et al. (Char 70).

Energy (keV)	Photon Relative Intensity	K-Conversion Relative Intensity	Experimental $\alpha_K \times 10^3$	Multipolarity Assigned
193.7±0.3	32 ±3	100[a]	180[b]	M1+E2
622.0±0.1	20 ±2	$1.2^{+0.5}_{-0.3}$	$2.8^{+1.2}_{-0.6}$	E1
886.1±0.2	52 ±5	1.7 ±0.2	1.9 ±0.5	E2(+M1)
1223.3±0.1	100	2.1 ±0.6	1.25±0.4	E2,M1
1345.4±0.2	30 ±3	1.6 ±0.3	3.1 ±1.0	M2
1403.2±0.3	16 ±2	0.4 ±0.2	1.5 ±1	(E2,M1) or E3
1564.7±0.2	17 ±2	1.4 ±0.3	4.4 ±1.0	M3
1596.9±0.2	13.6±1.5	0.36±0.2	1.5 ±0.8	(E2,M1)
1879.8±0.5	8 ±2	<0.2	<1.4	(E2,M1) or E1
2073.5±0.4	12 ±2	<0.25	<1.1	(E2,M1) or E1

[a]The value of $I_K(193.7)=100$ serves as the fiducial value for the determination of electron intensities.

[b]The value of $\alpha_K=180$ serves as the fiducial value for the determination of conversion coefficients.

In Table XIII we compare the levels identified and our spin and parity assignments with those of Charvet and the (p,d) and (d,t) studies.

The 1223.3-keV State

The level we have placed at 1223.3-keV has a log ft of 6.3. This implies an allowed transition and suggests spins of $3/2^+$, $5/2^+$, or $7/2^+$. Because this state feeds both the $1/2^+$ state at 193.8-keV and the $3/2^+$ ground state, this would tend to rule out the possibility of $7/2^+$ as a spin assignment. The intensity ratio of the 1223.3-keV γ to the 1029.9-keV from the 1223.3-keV state is 11. If the spin of this level were $7/2^+$, the multipolarity of the 1223.3-keV transition could be expected to be E2 and that of the 1029.9-keV transition would be M3. The single-particle estimate (Mos 65) predicts a ratio (E2/M3) of 41×10^5, and for a spin of $5/2^+$ we would have a predicted ratio (M1/E2) of 840. For a possible spin of $3/2^+$ (both M1's) we obtain a ratio of 1.7. It is clear from the comparison of the results that the $7/2^+$ assignment is unlikely. Experimentally it is common to find that E2's are enhanced, (i.e. their transition probability is greater than that predicted theoretically) and M1's are retarded (their transition probability is less than theoretically predicted). It would not require much E2 enhancement or M1 retardation to be consistent with the $5/2^+$ assignment.

The conversion electron work of Charvet et al. indicates the multipolarity of the 1223.3-keV gamma is E2+M1 (Table XIV), suggesting a $3/2^+$ or a $5/2^+$ assignment. The spin and parity of this level have been assigned $5/2^+$ because of the observation of $\ell=2$ momentum transfer in the reaction studies. The interpretation of these data is straightforward and relatively unambiguous. The results of Chameaux et al. include the use of a polarized proton beam to study the $3/2^+$ ground state and the lowest $5/2^+$ state in ^{143}Sm (Cha 71). Comparing our results with with the reaction data, it seems probable that this is the same $5/2^+$ level that is observed at this excitation in the (p,d) and (d,t) reactions.

The 1345.8-keV State

The level at 1345.8-keV is observed to decay via a single transition to the $3/2^+$ ground state. The fact that it fails to populate the $1/2^+$ first excited state suggests this level possesses a possible spin of 5/2 or 7/2. However, it should be recognized that this is a weak argument and that 3/2 could also be possible. If this were the case there would probably be certain internal selection rules that would be operative—and we have no information available about these selection rules. It is difficult to draw any conclusions concerning the parity of this level because the log ft value of 7.2 does not allow a definite distinction between an allowed

or first forbidden beta decay. As a result of this evidence, the spin assignments could be $5/2^{\pm}$ or $7/2^{\pm}$ (with $3/2^{\pm}$ being less likely).

The conversion electron results of Charvet et al. indicate the experimental K conversion coefficient of this transition is $\alpha_K=(3.1\ 1.0)\times10^{-3}$. Theoretical conversion coefficients for M2, E2, or E3 transitions of this energy are $\alpha_K(M2)=3.4\times10^{-3}$, $\alpha_K(E2)=1.05\times10^{-3}$ and $\alpha_K(E3)=2.04\times10^{-3}$, and these results suggest the multipolarity of the transition is M2 (as seen in Fig. 30). Since this state decays to the $3/2^+$ ground state and M2 transitions involve a parity change, this evidence implies the spin of the 1345.8-keV level could be $5/2^-$ or $7/2^-$. (If the multipolarity of the transition were either E2 or M3, no parity change would be involved and the level would have positive parity.)

A state has been observed at this excitation energy in the (p,d) and (d,t) reaction studies on ^{142}Nd, and the results seem to suggest $7/2^+$ for the spin and parity. Jolly and Kashy have suggested ($7/2^+$) and Foster et al. also indicate ($7/2^+$), while Chameaux et al. have given no spin assignment.

Evidence from the systematics of energy levels in the even proton N=81 nuclei can also be considered. A $7/2^+$ state has been identified at 1347.7-keV in ^{139}Ce (Ful 62) (Bee 69c), and a $7/2^+$ state is seen at 1360-keV in ^{143}Sm (Jol 71). From the similarity of these results, one might expect this level in ^{141}Nd to be a similar $7/2^+$ state.

At the present time the evidence pertaining to the spin of this level is not definitive and an unambiguous assignment cannot be made. Our preference is to slightly favor $7/2^+$ as the most likely choice, but $7/2^-$ and $5/2^\pm$ cannot be ruled out.

The State at 1564.8-keV

The level at 1564.8-keV is populated by beta decay with a log ft of 6.6. This indicates an allowed transition, suggesting possible spins of $3/2^+$, $5/2^+$, and $7/2^+$. This state is observed to feed both the 193.8-keV, $1/2^+$ state and the $3/2^+$ ground state. The $7/2^+$ possibility can be ruled out because this would require the 1371.0-keV γ to the first excited state to be a M3 and the 1564.8-keV γ to the ground state an E2. The experimental ratio of the intensity of the 1564.8-keV γ to the intensity of the 1371.0-keV γ is 8. The theoretical single-particle estimate predicts a ratio (E2/M3) of 2.4×10^5. This is clearly in disagreement with the experimental results and there would have to be truly unusual enhancements (and retardation) to obtain this ratio. In the case of a $5/2^+$ spin the theoretical predictions indicate an (M1/E2) ratio of 352, while for a $3/2^+$ assignment (both M1's) the predicted ratio is 1.5. As a result of these estimates we can rule out the $7/2^+$. However we conservatively retain both $5/2^+$ and $3/2^+$, noting it would require reasonable amounts of E2 enhancement or M1 retardation (both experimentally observed in other nearby nuclei) to favor the $5/2^+$ spin and parity.

The conversion electron results of Charvet indicate the multipolarity of the 1564.8-keV transition is M3. This spin change is somewhat large for a gamma transition, and as a result, this level might be expected to exhibit a measureable half-life. Theoretical single-particle estimates for a M3 transition of this energy suggest a possible lifetime of 700 ns for this state. We have made no special effort to determine a lifetime for this level, however we are able to place a limit on its possible magnitude. We have observed this transition in the 511-511-keV-gamma, triple coincidence experiment (resolving time ~100 ns). If this state were delayed, it would not be expected to exhibit many coincidences with the positrons feeding it (within the resolving time of the experiment) and as a result its intensity in this experiment might be expected to be noticeably less than in the singles experiment. In fact however, these intensities are very nearly the same—suggesting a half-life less than a two hundred ns. In general, except for E2 multipoles, the other multipolarities are hindered (i.e. they exhibit partial half-lives longer than the single particle estimates), hence, if anything we would anticipate a half-life longer than 700 ns for this state.

The (p,d) and (d,t) studies populate a level at this excitation characterized by an $\ell=2$ angular momentum transfer, and they are assigned spin and parity of $5/2^+$. This is quite probably the same level as we observe in the beta decay. As a result of the evidence, a $5/2^+$ assignment seems most likely, although $3/2^+$ remains a possibility.

The 1596.6-keV State

The level at 1596.8-keV (log ft=6.4) populates the $5/2^+$ level at 1223.3 keV, the $1/2^+$ first excited state and the $3/2^+$ ground state. The log ft value suggests an allowed transition limiting the parity to positive. The results of Charvet indicate the 1403.2-keV transition from this level to the $1/2^+$ first excited state may have either E2, M1, or E3 multipolarity because of the uncertainty in their measurement. The 1596.8-keV ground-state transition is an E2 or M1. The evidence tends to indicate either $5/2^+$ or $3/2^+$ are equally likely. A $7/2^+$ assignment can be ruled out because it would require the 1403.2-keV transition to be an M3. As pointed out earlier this would not be expected to compete favorably with the E2 feeding the ground state.

The Remaining States in ^{141}Nd

We have observed a level at 1820.4-keV (log ft=7.1). This level populates three lower lying levels: the $5/2^+$ 1223.3-keV state, the $1/2^+$ 193.8-keV state, and the $3/2^+$ ground state. The log ft value makes it difficult to determine the parity, hence both + and - must be considered. The spin can be limited to 3/2 or 5/2 on the basis that 7/2 would require the 1626.7-keV transition to the $1/2^+$ state at 193.8-keV to be an M3 or E3 (considered unlikely). A

level is observed at this excitation in both the (p,d) studies and the (d,t) work and all three groups favor $5/2^+$ for the spin. It seems likely this is the same level. As a result, $5/2^+$ seems to be consistent with the available evidence but we do not completely rule out $(5/2^-)$ or $(3/2^\pm)$.

At 1968.0-keV we have observed a level with a log ft=6.4 implying a spin of 3/2, 5/2, or 7/2. This level feeds the 1345.8-keV state strongly and also populates the $3/2^+$ ground state. The conversion electron data indicate the multipolarity of the 622.2-keV transition to the 1345.8-keV state is E1. This would imply a parity change between the levels. If the 1345.8-keV level is $7/2^+$, this would require the 1968.0-keV state to be $5/2^-$ or $7/2^-$. If the 1345.8-keV level is $7/2^-$ it would require spins of $5/2^+$ or $5/2^-$. Since we favor $7/2^+$ for the level at 1345.8-keV, we then prefer a $7/2^-$ or $5/2^-$ assignment for the 1968.0-keV level. However, we cannot rule out either $5/2^+$ or $7/2^+$.

The levels at 1897.1, 2066.4 and 2805 keV have log ft values of 7.4, 7.6 and 7.4 respectively. The decay characteristics of these two levels are similar in that they decay to the same states—the $1/2^+$ state at 193.8 keV and the $3/2^+$ ground state. Consequently we can limit the possible spin assignments to 3/2 or 5/2 (7/2 is ruled out because this would require E3 or M3 multipolarities for deexcitation to the $1/2^+$ first excited state). The parity remains uncertain, however.

The levels at 2073.3 and 2206 keV are beta fed with log ft's of 5.8 and 6.8 respectively. The log ft values indicate they are fed by allowed beta transitions and suggest positive parity. We are able to limit their spins and parities to $3/2^+$ and $5/2^+$ because feeding from $7/2^+$ states to the $1/2^+$ level at 193.8-keV would require M3 transitions, which would be expected to be very weak.

The level at 2109.6 keV (log ft=5.8) populates lower lying states of possible spin $5/2^+$ or $3/2^+$. The log ft value indicates an allowed transition favoring positive parity, however the spins and parities could be either $3/2^+$, $5/2^+$, or $7/2^+$ with any of these choices being equally likely.

With a log ft=8.1 the level at 2145.2 keV is probably fed by a first forbidden beta decay indicating possible spins and parities of $3/2^-$, $5/2^-$, or $7/2^-$.

The level at 2246.6 keV feeds levels with spins and parities of $1/2^+$, $3/2^+$, and $7/2^+$ (or possibly $7/2^-$). The log ft value of 7.1 indicates either allowed or first-forbidden beta decay. This indicates its spin could be either $3/2^\pm$, $5/2^\pm$, or $7/2^\pm$.

With the exception of the level at 2303.4 keV, the remaining levels at 2265.3, 2354.4, 2388.4, 2430, 2620, and 2986 keV have log ft's ranging from 6.9 to 7.7. These

results are uncertain enough to prevent any definite statements about the parities of these levels. Hence we can only say that their spins are 3/2, 5/2, or 7/2.

The level at 2303.4 keV is fed with a log ft=7.0 and, as a consequence, we tend to favor a positive parity assignment.

4.2.6. Discussion of the States in ^{141}Nd

The $3/2^+$ ground state and the two lowest excited levels in ^{141}Nd at 193.8-keV and 756.7-keV can be characterized in shell-model terms as $(\nu d_{3/2})^{-1}$, $(\nu s_{1/2})^{-1}$, and $(\nu h_{11/2})^{-1}$, respectively. These states appear to be of a rather pure single quasiparticle nature as characterized by the large spectroscopic factors associated with their population in the (p,d) and (d,t) studies (Cha 71) and (Fos 71). Our results appear consistent with these findings, although we cannot say anything about the parity of the states.

We observed that 88.5% of the β^+/EC decay of ^{141}Pm populates the ground state of ^{141}Nd with a log ft of 5.5. This appears consistent with the transformation of a $d_{5/2}$ proton into a $d_{3/2}$ neutron. A similar $(\pi d_{5/2}) \rightarrow (\nu h_{3/2})$ decay is observed in the case of ^{139}Pr $\xrightarrow[EC]{\beta^+}$ ^{139}Ce, (Bee 69c) in which 98.8% of the β decay is observed to be directly to the ground state of ^{139}Ce with a log ft of 5.6.

The first excited state at 193.8-keV receives no apparent β^+/EC feeding (<0.26%), and the log ft value >7.9 is consistent with its being an $(s_{1/2})^{-1}$ neutron state. The 193.8-keV γ transition from this $1/2^+$ first excited state is primarily an ℓ-forbidden M1 multipole transition ($s_{1/2} \rightarrow d_{3/2}$). Charvet et al.'s results (Char 70) indicate the multipolarity is (87% M1+13% E2). These values correspond to an M1 retardation of 51 spu (Moskowski single particle units), and an E2 enhancement of 4 spu. The experimental lifetime (1.17 ns) of this odd neutron state is the same order of magnitude as similar ℓ-forbidden, low energy transitions ($g_{7/2} \rightarrow d_{5/2}$) in the odd proton N=82 nuclei (Gei 65).

The level at 756.7-keV is the well known isomer ^{141m}Nd ($\tau_{1/2}$=60s) (Bee 68). This state is one of a series of $11/2^-$ isomeric states found in the odd neutron N=81 isotones (Jan 69). These isomers are characterized as $(\nu h_{11/2})^{-1}$ neutron states and all are of a relatively pure single quasiparticle character. These isomeric states are characterized by lifetimes ranging from 410m for ^{133m}Te to the order of 60s for the isotones ^{139m}Ce, ^{141m}Nd, and ^{143m}Sm. The decay of these states is via an M4 transition directly to the ground state. In this study we have discussed, in Section 3.2.4., the apparent observation of indirect feeding to this level from states at higher excitation in ^{141}Nd. It will be of interest to see if a

similar effect is observed in the beta-decay of ^{143}Eu to states in ^{143}Sm.

The state at 1223.3-keV appears to contain approximately one-half to one-third of the $(2d_{5/2})$ single-particle strength, from the reaction studies, indicating that the $(d_{5/2})$ single particle state is considerably fractionated. In the ^{141}Pm decay the 1223.3-keV state is fed by four higher lying states in ^{141}Nd at 1820.4-, 2109.6-, 2246.6-, and 2303.4-keV, with the 886.3-keV γ transition from the level at 2109.6-keV being the second strongest line in the gamma-ray spectrum. This would seem to indicate that these states have some common features in their wave functions. A $5/2^+$ state is observed in the (p,d) studies at 2.09 MeV (Jol 71)(Cha 71), and it could correspond to the level seen at 2109.6-keV in the beta decay. However the energy resolution is not good enough to make a positive identification.

The level at 1345.8-keV (log ft=7.2) is somewhat of a puzzle. From the results of the (p,d) and (d,t) data of Jolly and Kashy and Foster et al. it is tempting to assume it contains some $(\nu g_{7/2})^{-1}$ component in its wave function. Similar $7/2^+$ states have been observed in ^{139}Ce at 1347.4-keV and at 1369.5-keV in ^{143}Sm with log ft values of 7.0 (Bee 69c) and 6.5 (Fir 71), respectively. It should be noted that this $7/2^+$ assignment depends on large

ℓ transfer in the reaction studies, and angular distributions of this kind are difficult to interpret unambiguously. The results of Charvet et al. (Char 70) indicate it deexcites via an M2 multipole transition to the ground state, thus favoring a negative parity assignment (probably $7/2^-$). If it is indeed a $7/2^-$ state, it could result from the coupling of $h_{11/2}$ to a 2^+ vibrational state, or a less likely alternative might be that the unpaired neutron is populating the $f_{7/2}$ orbit. This is the next shell to be populated after the closure at N=82. Population of the $f_{7/2}$ has been observed below the N=82 shell in the reaction $^{138}Ba(d,t)^{137}Ba$ (Ful 62) and more recently via the reaction $^{136}Ba(p,d)^{137}Ba$ (Von Ehr 70); the energy of this state is 1.8 MeV. Such a state is not expected to be observed in a pickup reaction such as (p,d) or (d,t). The 7.2 log ft value makes it difficult to distinguish between an allowed or first forbidden beta decay. In light of the various results, the spin and parity of this level remains somewhat uncertain, but the evidence slightly favors $7/2^+$.

The levels at 2109.6-keV and 2246.6-keV seem to have some features of their wave functions in common with the lower lying states. The 2109.6-keV state feeds 4 low lying states, the 1820.4-, 1564.8-, and 1223.3-keV levels and the ground state. The level at 2246.6-keV feeds states 5 lower lying states at 2066.4-, 1345.8-, 1223.3-, 193.8-keV and the ground state.

At the present time little is available in the way of theoretical calculations with which to compare our results. Heyde and Vander Berghe (Heyd 69) have calculated the ^{139}Ce energy spectrum in a unified model with intermediate coupling. These results appeared before decay work of D. Beery on ^{139}Pr (Bee 69c) and they also were done prior to the appearance of the (p,d) and (d,t) studies mentioned earlier. Preliminary calculations (Ree 71) of the states in ^{141}Nd using the pairing plus quadrupole Hamiltonian of Kisslinger and Sorensen (Kis 63) have been done. The results are for states up to 2 MeV of excitation, and they indicate the three lowest states are very much single quasiparticle states. The lowest $5/2^+$ state seems to have significant admixture of $1/2^+$ and $3/2^+$ coupled to one phonon. Similarly the lowest $7/2^+$ appears to arise mainly from coupling $3/2^+$ to one phonon (2^+) and has little single particle character. The character of the higher lying states apparently arises from coupling $1/2^+$ and $3/2^+$ to one phonon (2^+).

Chapter V

Discussion of Results and Systematics

The previous chapter includes descriptions of the states investigated along with some comparisons with states in neighboring nuclei. One of the results of this study has been the identification of a three-quasiparticle multiplet of high-lying, high-spin, odd-parity states in ^{141}Pm. The character of these states is discussed in some detail in Chapter IV. In this Chapter the results of the studies of ^{141}Sm and ^{141}Pm are related to other nuclides in the region. This thesis then concludes with a survey of energy level systematics of odd proton ($52 \leq Z \leq 65$), odd mass nuclei and odd neutron, odd mass nuclei in the immediate vicinity of the N=82 closed shell.

5.1. Three-Quasiparticle Multiplets in Other Nuclei

Well characterized three-particle states in nuclei are relatively rare and their recognition has most often been dependent upon the isomeric properties of a few high-lying, high-spin states. As a result, the excitation of a multiplet of such states in one nucleus, with each state feeding a number of low-lying states, is of some theoretical interest.

The particular three-quasiparticle multiplet mentioned in Section 3.1.5.C. has some stringent requirements placed on the mechanism involved in its population via the electron capture decay of ^{141m}Sm. These requirements include, (1) a

high-spin parent (e.g. an $h_{11/2}$ isomer), and (2) sufficient energy to populate states well above the pairing gap in the daughter nucleus. In addition, the ability of the parent nucleus to decay by other modes must be severely hindered. For example, an isomeric transition, if present, must be sufficiently low in energy to allow the β^+/EC decay to compete favorably with it. Finally the nucleus must have an intrinsic configuration that forces the preferred path of decay into the three-quasiparticle states. These particular requirements seem to be satisfied for β^+/EC decay of some nuclides with N<82.

The other possible regions where these three-quasiparticle multiplets might be observed are discussed in (Bee 69b). It is possible the decay of ^{137m}Nd may populate such a multiplet in ^{137}Pr, however, no data are currently available for this case.

A comparison of the three-quasiparticle multiplets populated in the decay of ^{139m}Nd and ^{141m}Sm has been made in Section 3.1.6. Here these states are compared with similar states identified in the N=82 region. These involve different particle configurations. The beta decay of ^{145g}Gd (Epp 71) has been observed to populate a quasiparticle multiplet in ^{145}Eu and a multiplet has been populated in ^{139}La via the reaction ^{138}La(d,p)^{139}La (DuB 71).

The structure of the three-quasiparticle multiplet in ^{141}Pm is basically $[(\pi g_{7/2})^{8}(\pi d_{5/2})^{3}(\nu d_{3/2})^{-1}(\nu h_{11/2})^{-1}]_{J^-}$, where J^- is restricted to values of $9/2^-$, $11/2^-$, and $13/2^-$ for states populated by allowed beta decay. The multiplet in ^{145}Eu populated by the ^{145g}Gd decay has the structure

$$[(\pi h_{11/2})^{2n-1}(\nu h_{9/2})(\nu s_{1/2})^{-1}]_{J^+}$$

where J^+ is restricted to $1/2^+$ or $3/2^+$ for allowed beta decay (the spin of the parent is thought to be $1/2^+$). The multiplet in ^{139}La is populated via a stripping reaction and the structure of the multiplet involves $(g_{7/2})$ and $(d_{5/2})$ proton orbitals and $(s_{1/2})$, $(d_{3/2})$, $(f_{7/2})$, and $(p_{3/2})$ neutron orbitals. It can be seen that in each instance a somewhat different group of states is involved.

5.2. Levels in the N=80 and N=82 Odd Proton Nuclei

Figures 17 and 31 show the positions of the low-lying (<4 MeV) levels in the odd mass N=80 and N=82 isotones. The data for N=90 are from the beta decay studies of (Par 68), (Alex 68), (Bee 71), (Fra 64), and (Bee 69b) and Chapter 4 of this thesis; the results of the reaction study ^{141}Pr(p,t)^{139}Pr (Gol 70) have also been included. The N=82 data are from the reaction studies of (Wil 71), (Jon 71), (Dav 70), and (Bae 71) and the beta decay results of (Bee 68), (Ber 69), and (DeF 70).

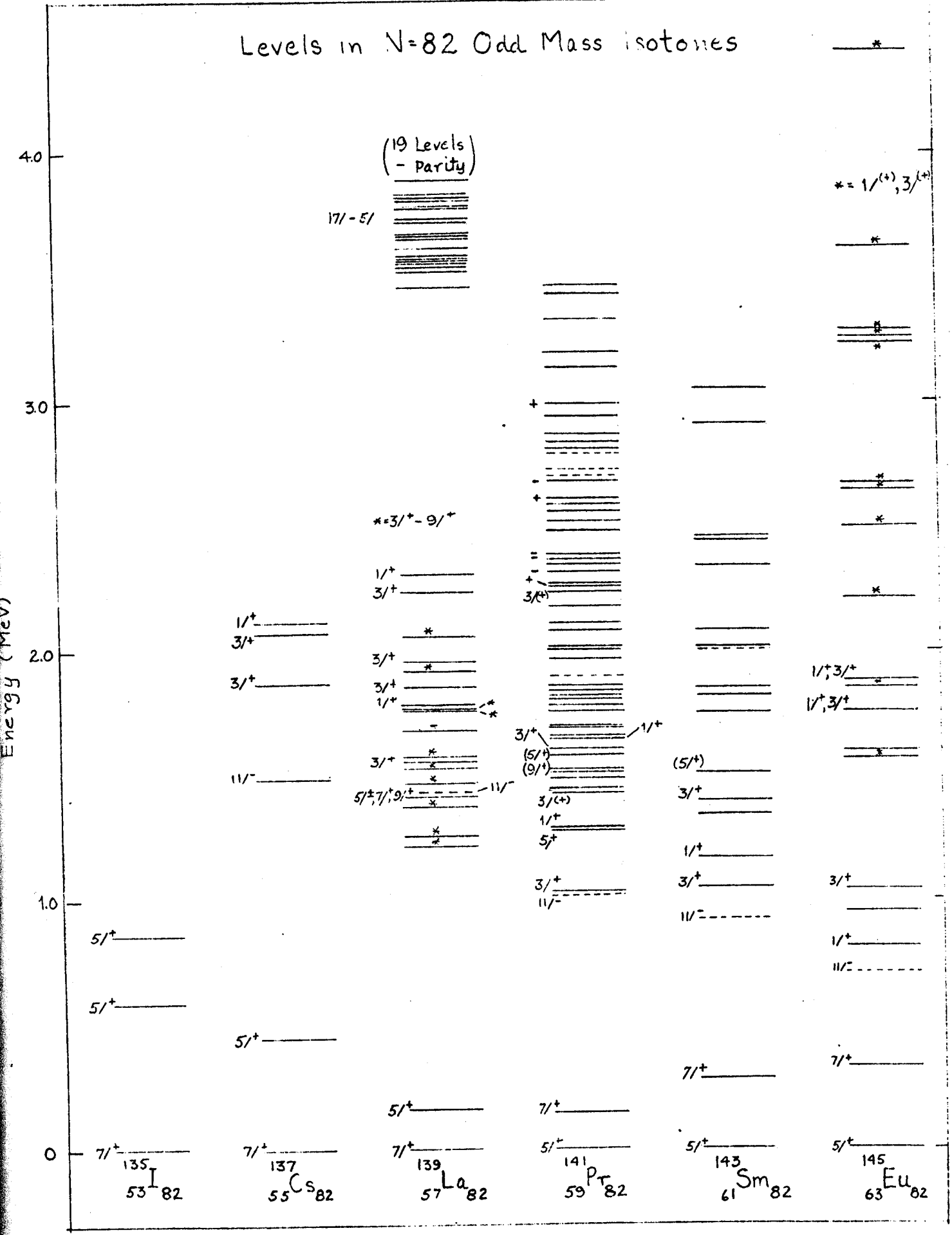

Figure 31. Experimental levels in the N=82 odd mass isotones.

A comparison of the two lowest levels in the N=80 and N=82 odd proton isotones, Figs. 17 and 31, shows that in both instances the spins of these levels are $5/2^+$ and $7/2^+$. For $Z \leq 57$ the ground state is $7/2^+$ and the first excited state is $5/2^+$, while the roles are reversed for $Z \leq 59$.

In the case of the odd proton N=82 isotones there is a decided gap between the first excited state and the next lowest level. The gap is observed to decrease with increasing Z. At ^{137}Cs the gap is $\sim$1 MeV and at ^{145}Eu it has decreased to $\sim$0.4 MeV. The gap probably arises because of the hard core formed by the closed neutron shell at N=82. The gradual decrease in the gap with increasing Z may be due to the increased proton occupation resulting in a somewhat softer nucleus.

In the case of the odd proton N=80 isotones the energy difference between the first excited state and the next lowest level is decidedly less. This is related to the presence of the two neutron holes in the N=82 shell which strongly influences all of the levels.

The effect of the relatively inert N=82 core is observable in Fig. 33. Here we show the relative energy spacing between the lowest $5/2^+$ and $7/2^+$ states in the odd proton N=80, 82, 84 nuclei. For the N=82 odd mass isotones the energy separation is greater and the curve rises more sharply. The relative spacings in N=80 and N=84 follow a similar trend. In the case

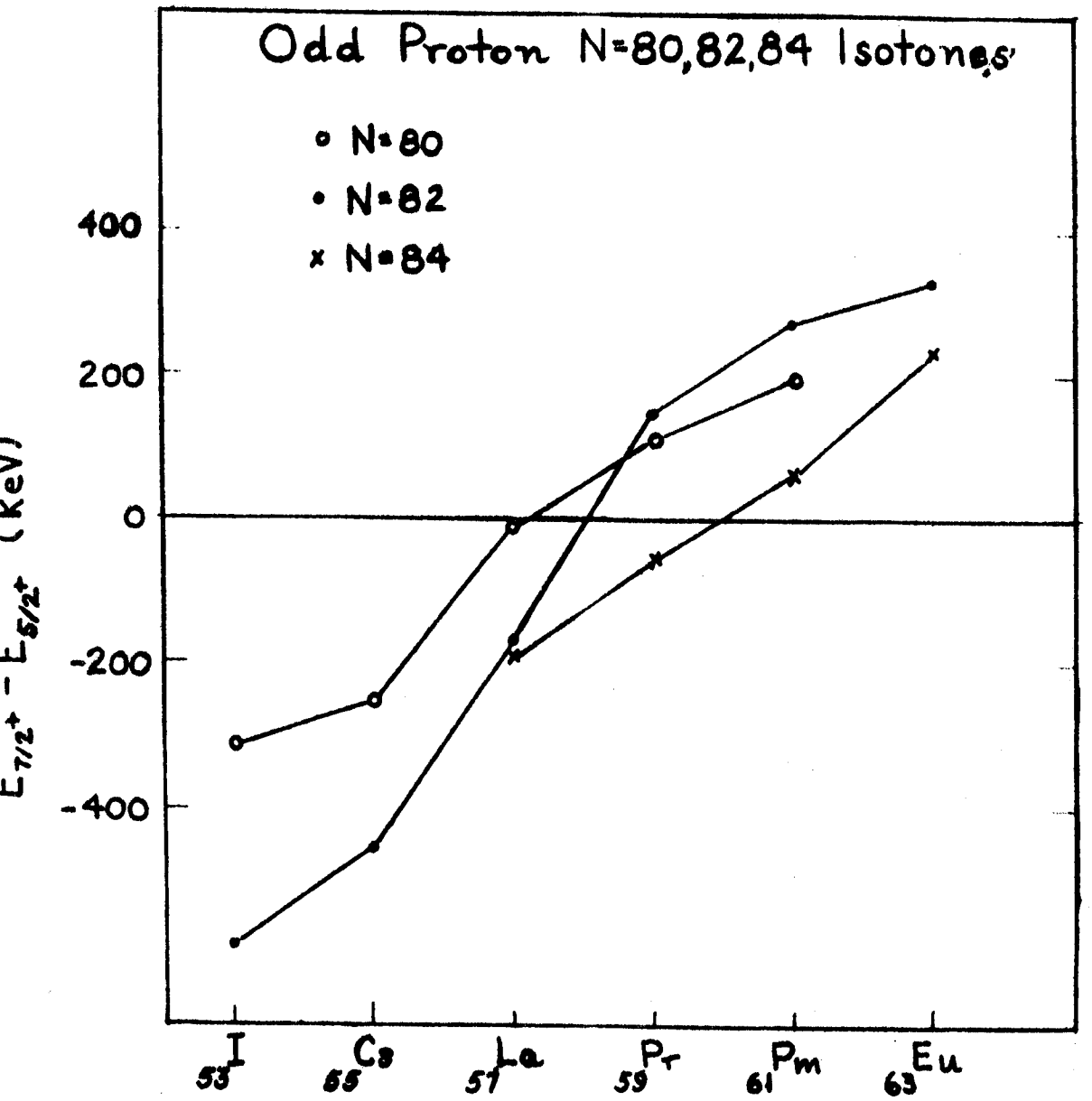

Figure 32. Systematics of the energy level spacings between the low lying $7/2^+$ and $5/2^+$ states in the N=80, 82 and 84 odd mass isotones.

of the N=80 the primary part of the ground state wave function is composed of a single proton in the $(g_{7/2})$ or $(d_{5/2})$ shell and two $(d_{3/2})$ neutron holes. In the N=84 odd proton isotones the ground state consists primarily of a single $(g_{7/2})$ or $(d_{5/2})$ proton and two neutrons in the $(f_{7/2})$ orbit. In either case the nucleus can be pictured as being softer because of the two neutron holes or particles. The result is that the relative spacing between the $5/2^+$ and $7/2^+$ levels is decreased and the variation of the curve is smoother and rises less sharply.

5.3 Levels in the Odd Neutron N=81 Nuclei

The level structure of the odd neutron, odd mass, N=81 isotones is shown in Fig. 32. The data are from the reaction studies of (Jol 71), (Cha 71), (Fos 71), (Ful 62), (Von Ehr 70), (Sch 66), (Yag 68) and the beta decay results of (Tre 69), (Mac 70), (Bee 69c), and (Fir 71) and Chapter 4 of this study.

From Fig. 32 it can be observed that below 1 MeV of excitation there are 3 identifiable levels in each isotope. These are the $3/2^+$ ground states, the $1/2^+$ first excited states and the $11/2^-$ states. These levels are generally referred to as neutron hole states and in shell model terms are characterized as $(\nu 3s_{1/2})^{-1}$, $(\nu 2d_{3/2})^{-1}$ and $(\nu h_{11/2})^{-1}$. The results of the reaction studies indicate these states

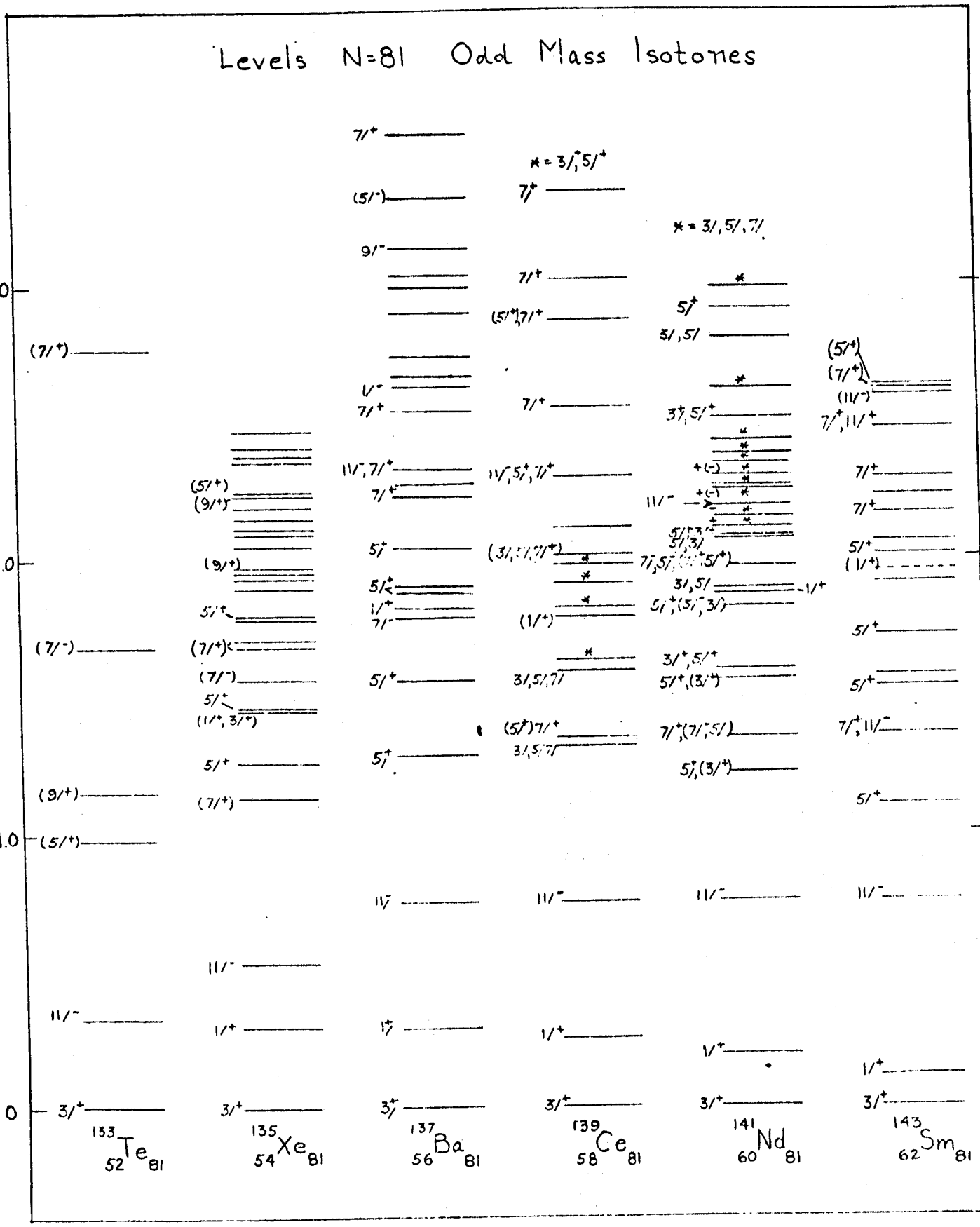

Figure 33. Experimental levels in the *N*=81 odd mass isotones.

are of a fairly pure single particle nature. The $(\nu h_{11/2})^{-1}$ states are isomeric levels which decay to the first excited state via M4 transitions and all exhibit half-lives ranging from 410m for ^{133}Te to 64s for ^{143}Sm. These states have been studied in detail by Jansen et al. (Jan 69).

Above 1 MeV in excitation the density of states increases rapidly and the large number of $5/2^+$ states suggests that the $(\nu d_{5/2})^{-1}$ strength may be considerably fragmented among several levels. These do not represent all the levels that exist in these nuclei. For instance the states observed in beta decay studies depend on the decay energy available and the beta decay selection rules.

The energy difference between the $s_{1/2}$ and the $d_{3/2}$ states is observed to decrease as a function of increasing Z. A plot of this separation energy versus Z can be seen in Fig. 34. This energy dependence as a function of Z is reproduced quite well by an equation of second order in Z. With the use of such a curve and by extrapolating the fit to Z=64 (i.e. ^{145}Gd), the results indicate the $1/2^+$ and $3/2^+$ cross one another between Z=62 and Z=64 (i.e., the ground state becomes $1/2^+$ and the first excited state $3/2^+$) and the relative spacing between them at Z=64 is ~8 keV.

These results seem to be in agreement with those of Eppley et al. (Epp 71) and Newman et al. (New 70) whose

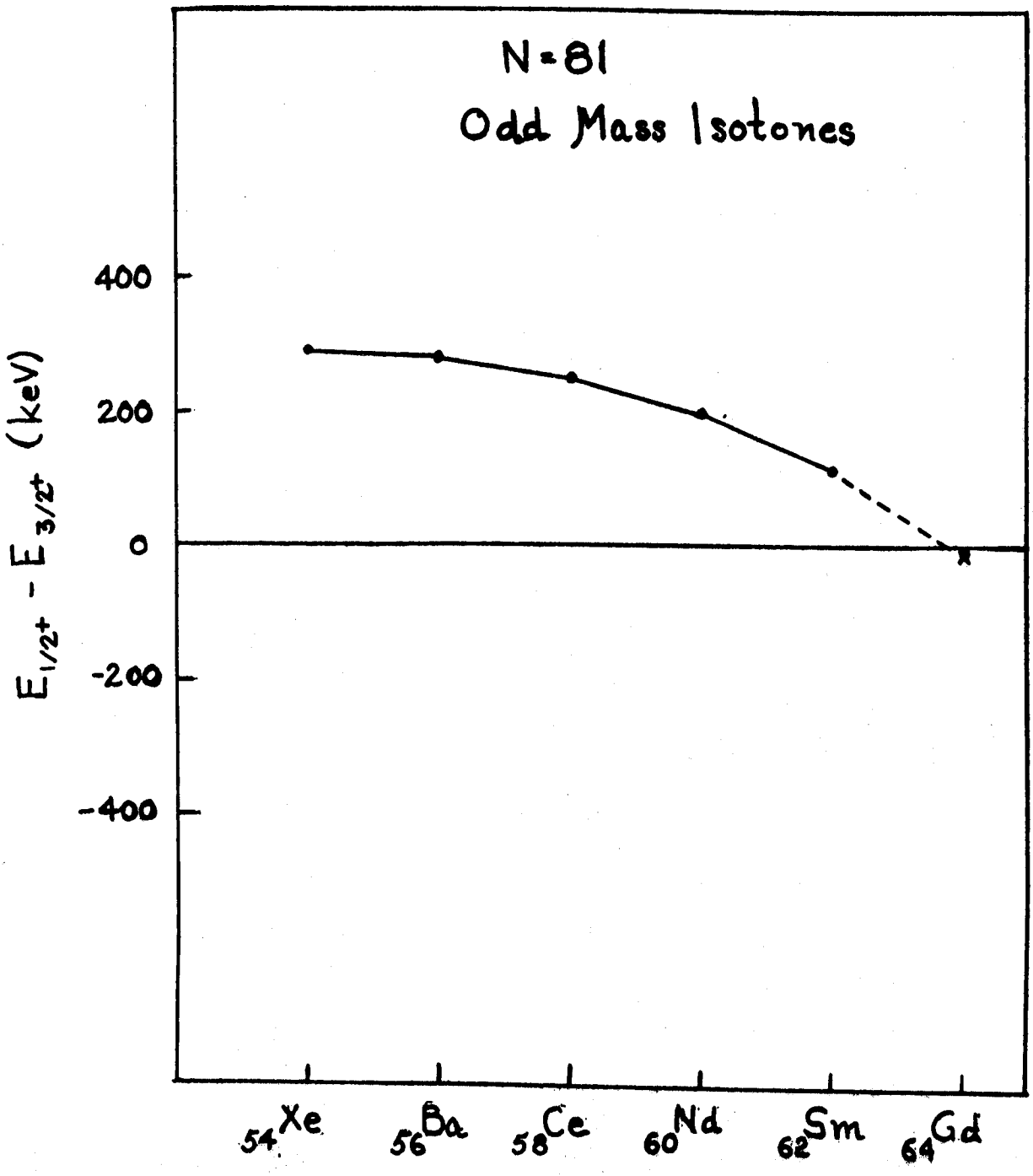

Figure 34. Systematics of the low lying $1/2^+$ and $3/2^+$ states in the N=81 nuclei demonstrating the apparent quadratic dependence of the energy spacing. The value for ^{145}Gd is a calculated (predicted) value.

beta decay studies of ^{145g}Gd indicated the ground state spin of ^{145}Gd is probably $1/2^+$. The energy of the $3/2^+$ state has not yet been determined.

It is interesting to note that the relative energy spacing of the holes in $d_{3/2}$ and $s_{1/2}$ neutron orbits exhibits a parabolic behavior similar to that observed in the antimony (Sb) isotopes and iodine (I) isotopes by Berzins (Ber 67) and Beyer (Bey 67).

5.4. Characteristics of Similar (Delayed) $11/2^-$ States in Odd Proton Odd Mass Nuclei in the Region of N=82

In the study of states of ^{141}Pm the 700 ns delayed state at 628.6 keV was of significant importance in the determination of the properties of the ^{141m}Sm decay scheme. This state is certainly an $11/2^-$ state and it deexcites to both the $7/2^+$ first excited state and the $5/2^+$ ground state of ^{141}Pm. These transitions are presumably of M2 and E3 multipolarity respectively (i.e. assuming the deexcitation to each level occurs with the lowest multipolarity possible). From the measurement of the half-life of the state (700 ns), the partial half-lives of each transition were determined and compared with theoretical estimates (Moskowski single-particle estimates). These results indicated the 431.8 keV M2 transition was retarded by a factor of 58 over the theoretical

Table XV Characteristics of Similar Odd Proton (Delayed) $11/2^-$ States Near N=82

tope (Ref.)	Transition Energy	State $t_{1/2}$ (ns)	Experimental Intensities	$\frac{I(E3)}{I(M2)}$	Theoretical $\frac{T_{s.p.}(E3)}{T_{s.p.}(M2)}$	E3 Enhancement
$^{147}Eu_{86}$(Ber161)	496.2 (E3) 346.5 (M2)	248	1.4 24	0.6	4.8×10^{-4}	1.4
$^{145}Eu_{84}$(Ber161)	625 (E3) 369 (M2)	740	4.7 36.6	0.12	1.75×10^{-3}	2.1
$^{143}Eu_{82}$(Epp70b)	716 386.6 (M2)					
$^{141}Pm_{82}$(Wi171)	962 (E3) 689 (M2)					
$^{141}Pm_{80}$(Chap.4)	628.6 (E3) 431.8 (M2)	700	3.1 43.6	0.07	0.78×10^{-3}	1.6
$^{139}Pr_{82}$(Dav70) (Sho71)	1117.6 (E3) 973 (M2)		10 90	0.11	0.76×10^{-3}	12.0
$^{137}Pr_{80}$(Bee69b)	821.9 (E3) 708.1 (M2)	40	1.4 27	0.05	0.42×10^{-3}	2.2
$^{137}La_{80}$(VanH67)	994 (E3) 1004 (M2+E3) 168 (E1)	$\geq$0.41	0.014 0.19 4.35	0.07		$\geq$7.8 $\geq1.12\times10^{-1}$ $\geq1.18\times10^{-4}$

estimate. However, this is not at all unusual; typical M2 retardations are on the order of 10 to 100. What is more interesting is that the 628.6 keV E3 transition is observed to be enhanced by a factor of 1.6 when compared to the theoretical value. This result is somewhat unusual since in general, all multipolarities except E2's are retarded.

In the region near N=82 several other odd proton, odd mass nuclei have been observed to exhibit similar ($11/2^- \rightarrow 5/2^+$) enhanced E3 transitions. In Table XV we compare the E3 enhancements and the E3/M2 gamma-ray intensity ratios (where available) with the theoretical single-particle estimates of similar $11/2^-$ states in nearby nuclei.

This somewhat unusual enhancement of E3 transitions ($11/2^-, 5/2^+$) could arise from the possible coupling of the $d_{5/2}$ single-particle state to the 3^- core octupole vibration. The amount of admixture necessary to account for this enhancement is small enough that the $11/2^-$ state retains its significant single-particle character. Some evidence of this possibility has been observed in inelastic scattering studies (Ell 69). In cases where the ground state is $5/2^+$ the $11/2^-$ state seems to be more easily excited via inelastic scattering than in cases where the ground state is $7/2^+$— possibly indicating the presence of a small $[d_{5/2} \otimes 3^-]_{11/2}$- admixture in the $11/2^-$ state (Wil 71a).

We have included in Table XV the $11/2^-$ states at 962 keV in ^{143}Pm and the 716.1 keV state in ^{145}Eu as possibly exhibiting decay via enhanced E3 transitions to the ground state. The lifetime of the 1117.6 keV state in ^{141}Pr has recently been determined to be 4.9±0.5 ns (Sho 71). The partial half-life of (~25 ns) for the E3 ground state transition indicates an enhancement of 12.4. This is the largest enhancement observed in this region and suggests that further such experiments on the odd proton N=82 isotones could prove interesting. Little is known currently about what appears to be the corresponding $11/2^-$ in ^{143}Pm. In fact, the 962 keV γ transition to the ground state has not been observed. In the case of ^{145}Eu the $11/2^-$ state at 716.1 keV is observed to be fed via the beta decay branch of the ^{145m}Gd decay, however the E3 transition to the ground state has not been observed in this case either.

The lifetimes of these $11/2^-$ levels in ^{143}Pm and ^{145}Eu may be measured relatively easily. A possible method of this would be via the in-beam reactions: $^{141}Pr(\alpha,2n\gamma)^{143}Pm$ and $^{144}Sm(p,\gamma)^{145}Eu$. We are planning to attempt these experiments in the near future.

BIBLIOGRAPHY

BIBLIOGRAPHY

(Alex 68) P. Alexander and J.P. Lau, Nucl. Phys. A121, 612(1968).

(Alp 62) S.S. Alpert, B. Budick, E. Lipworth, and R. Marrus, Bull. Am. Phys. Soc. 7, 239(1962).

(Arl 67) R. Arl't, B. Baier, G. Musiol, L.K. Peker, G. Pfrepper, Kh. Shtrusnyi, and D. Kristov, JINR, Dubna, Report 21 (1967).

(Arl 70a) R. Arl't, G. Baier, G. Musiol, L.K. Peker, G. Pfrepper, and H. Strusny, Bull. Acad. Sci. USSR-Phys. Serv. 34, No. 4, 667(1970).

(Arl 70b) R. Arl't, G. Beyer, G. Usiol, E.S. Rydina, S. Seidler, and H. Strusny, International Conference on the Properties of Nuclei Far from the Region of Beta-Stability, August 31-September 4, 1970, Leysin, Switzerland—Proceedings (CERN, Geneva, Report 70-30, 1970) p. 1141.

(Aub 67) R.L. Auble, D.B. Beery, G. Berzins, L.M. Beyer, R.C. Etherton, W.H. Kelly, and Wm.C. McHarris, Nucl. Instr. and Methods 51, 61(1967).

(Bae 71) H.W. Baer, H.C. Griffin, and W.S. Gray, Phys. Rev. C3, 1398(1971).

(Bee 71) D.B. Beery, W.H. Kelly, and Wm.C. McHarris, to be published.

(Bee 71a) D.B. Beery, W.H. Kelly, and Wm.C. McHarris, to be published.

(Bee 69a) D.B. Beery, Ph.D. Thesis, Michigan State University, (1969).

(Bee 69b) D.B. Beery, W.H. Kelly, and Wm.C. McHarris, Phys. Rev. 188, 1851(1969).

(Bee 69c) D.B. Beery, W.H. Kelly, and Wm.C. McHarris, Phys. Rev. 188, 1875(1969).

(Bee 68) D.B. Beery, W.H. Kelly, and Wm.C. McHarris, Phys. Rev. 171, 1283(1968).

(Berl 61) E. Yu Berlovich, V.N. Klementyev, L.V. Krasnov, M.K. Nikitin, and I. Yurski, Nucl. Phys. 23, 481(1961).

(Ber 67) G. Berzins, Ph.D. Thesis, Michigan State University, (1967).

(Ber 67) G. Berzins, W.H. Kelly, G. Graeffe, and W.B. Walters, Nucl. Phys. A104, 241(1967).

(Ber 69) G. Berzins, M.E. Bunker, and J.W. Starner, Nucl. Phys. A128, 294(1969).

(Bla 52) J.M. Blatt and V.F. Weisskopf, Theoretical Nuclear Physics (J. Wiley and Sons, New York, 1952) Chap. 12 and Appendix B.

(Bey 67) L.M. Beyer and W.H. Kelly, Nucl. Phys. A104, 274(1967).

(Ble 67) J. Bleyl, H. Münzel, and G. Pfinning, Radiochim. Acta 6, 200(1967).

(Bon 66) N. Bontsch-Osmolowskaja et al., JINR-P-2618(1966).

(Bro 59) A.R. Brosi, B.H. Ketelle, H.C. Thomas, and R.J. Kerr, Phys. Rev. 113, 239(1959).

(Cam 71) D.C. Camp and G.L. Meredith, Nucl. Phys. A166, 349(1971).

(Cha 71) A. Chaumeux, G. Bruge, H. Faraggi, and J. Picard, Nucl. Phys. A164, 176(1971).

(Char 70) A. Charvet, R. Duffait, A. Emsallem, et R. Chéry, Le Journal de Physique, 31, 737(1970).

(Dav 70) V.R. Dave, J.A. Nelson, and R.M. Wilenzick, Nucl. Phys. A142, 619(1970).

(DeF 70) D. DeFrenne, E. Jacobs, and J. Demuynck, Z. Phys. 237, 327(1970).

(DeF 68) D. DeFrenne, E. Jacobs, and J. Demuynck, Z. Phys. A110, 674(1968).

(Doe 69) R.E. Doebler, Michigan State University Nuclear Chemistry Annual Report for 1969. COO-1779-13, p. 159.

(DuB 71) J.L. DuBard, and Raymond K. Sheline, and James B. Ball, Phys. Rev. C3, 1391(1971).

(Ell 69) C. Ellegaard, G. Samosvat, P. Vedelsby, and K. Jorgensen, Bull. Am. Phys. Soc. 14, 492(1969).

(Epp 71) R.E. Eppley, Wm.C. McHarris, and W.H. Kelly, Phys. Rev. C3, 282(1971), and references therein.

(Epp 70a) R.E. Eppley, Ph.D. Thesis, Michigan State University, (1970).

(Epp 70b) R.E. Eppley, Wm.C. McHarris, and W.H. Kelly, Phys. Rev. C2, 1929(1970).

(Epp 70c) R.E. Eppley, Wm.C. McHarris, and W.H. Kelly, Phys. Rev. C2, 1077(1970).

(Epp 71) R.E. Eppley, Wm.C. McHarris, and W.H. Kelly, Phys. Rev. C3, 282(1971).

(EVE) EVENT: A two parameter data acquisition program written for the MSU Cyclotron Laboratory Sigma-7 computer by D. Bayer, D.B. Beery, and G.C. Giesler.

(Fel 70) J. Felsteiner and B. Rosner, Phys. Letters 31B, 12(1970).

(Fir 71) R.B. Firestone and Wm.C. McHarris, in progress.

(Fir 71a) R.B. Firestone, private communication.

(Fir 71b) R.B. Firestone, private communication.

(Fis 52) V. Kistiakowsky Fischer, Phys. Rev. 87, 259(1952).

(Fos 71) J.L. Foster, Jr., O. Dietzsch, and D. Spalding, Nucl. Phys. A169, 187(1971).

(Fra 64) R.B. Frankel, Ph.D. Thesis, University of California, Berkeley, Lawrence Radiation Report No. UCRL-11871 (1964).

(Ful 62) R.H. Fulner, A.L. McCarthy, and B.L. Cohen, Phys. Rev. 128, 1302(1962).

(Gei 65) J.S. Geiger, R.L. Graham, I. Bergström, and F. Brown, Nucl. Phys. 68, 352(1965).

(GEORGE) GEORGE, a data taking code with live oscilloscope display developed by P. Plauger for use on the MSU Cyclotron Laboratory Sigma-7 computer.

(Gies 71) G.C. Giesler, Wm.C. McHarris, R.A. Warner, and W.H. Kelly, Nucl. Instr. and Methods 91, 313(1971).

(Gol 70) R.W. Goles, Wm.C. McHarris, W.H. Kelly, and R.A. Warner, Bull. Am. Phys. Soc. 15, 1670(1970); also to be published.

(Gou 65) Fred S. Goulding, University of California Lawrence Radiation Laboratory, Report No. UCRL-16231.

(Hag 68) R.S. Hager and E.C. Seltzer, Nucl. Data 4A, 1(1968).

(Hes 69) K. Hesse, Z. Phys. 220, 328(1969).

(Heyd 71) K. Heyde and M. Waroquier, Nucl. Phys. A167, 545(1971).

(Hil 67) J.C. Hill and M.L. Wiedenbeck, Nucl. Phys. A98, 599(1967).

(Heyd 69) K. Heyde and G. Vanden Berghe, Nucl. Phys. A126, 381(1969).

(HYD) HYDRA: A JANUS task which allows for independent control of 4 13-bit ADC's with 8 way fanout capability.

(Ish 69) Toshiyuki Ishimatsu, Haruko Ohmura, Takashi Awaya, Takemi Nakagawa, Hikonojo Orihara, and Kohsuke Yagi, Jour. of Phys. Soc. of Japan, 28, 291(1970).

(Jac 67) E. Jacobs, K. Heyde, M. Dorkens, J. Demuynck, and L. Dorikens-Vanpraet, Nucl. Phys. A99, 411(1967).

(Jan 69) G. Jansen, H. Morinaga, and C. Signorini, Nucl. Phys. A128, 247(1969).

(Jon 71) W.P. Jones, L.W. Borgman, K.T. Hecht, John Bardwick, and W.C. Parkinson, Phys. Rev. C4, 580(1971).

(Jol 71) R.K. Jolly and E. Kashy, Phys. Rev. C4, 887(1971).

(Kis 60) L.S. Kisslinger and R.A. Sorensen, Dan. Mat.-Fys. Medd. 32, No. 9(1960).

(Kis 63) L.S. Kisslinger and R.A. Sorensen, Rev. Mod. Phys. 35, 853(1963).

(Kos 69) K. Kosanke and J. Black, Michigan State University Nuclear Chemistry Annual Report for 1969, COO-1779-13, p. 153.

(Lad 66) I.M. Ladenbauer-Bellis, Radiochim, Acta 6, 215(1966).

(Mac 70) E.S. Macias, J.P. op de Beeck, and W.B. Walters, Nucl. Phys. A147, 513(1970).

(Mal 66) H.P. Malan, H. Münzel, and G. Pfinning, Radiochim. Acta. 5, 24(1966).

(McH 70) Wm.C. McHarris, R.E. Eppley, R.A. Warner, R.R. Todd, and W.H. Kelly, International Conference on the Properties of Nuclei Far from the Region of Beta-Stability, August 31-September 4, 1970, Leysin, Switzerland—Proceedings (CERN, Geneva, Report 70-30, 1970) p. 435.

(McH 69) Wm.C. McHarris, D.B. Beery, and W.H. Kelly, Phys. Rev. Letters 22, 1191(1969).

(Mos 65) S.A. Moszkowski, in Alpha-, Beta-, and Gamma-Ray Spectroscopy, ed. by K. Siegbahn (North-Holland Publ. Co., Amsterdam, 1965); S.A. Moszkowski, Phys. Rev. 89, 474(1953).

(Muth 71) R. Muthukrishnan and A. Kromminga, Phys. Rev. C3, 229(1971).

(Myr 65) W.D. Myers and W.J. Swiatecki, Lawrence Radiation Laboratory, Berkeley, Report No. UCRL-11980(1965).

(NDS) Nuclear Data Sheets (The National Academy of Sciences—National Research Council): reissued by Academic Press.

(New 70) E. Newman, K.S. Toth, R.L. Auble, R.M. Gaedke, M.F. Roche, and B.H. Wildenthal, Phys. Rev. C1, 1118(1970).

(NSA) Nuclear Science Abstracts (U.S.A.E.C., Division of Technical Information).

(Par 68) B. Parsa, G.E. Gordon, and W.B. Walters, Nucl. Phys. A110, 674(1968).

(Pav 57) F.I. Pavlotskaya and A.K. Lavrukhina, Sov. J. Nucl. Ener. 5, 149(1957).

(POL) POLYPHEMUS: A JANUS task which handles four 13-bit ADC's independently.

(Ree 71) B. Reehal, private communication.

(Rem 63) V.V. Remaev, Yu. S. Korda, and A.P. Klyucharev, Izv. Akad. Nauk. SSSR, Ser. Fiz. 27, 125(1963).

(Rou 69) J. T. Routti and S.G. Prussin, Nucl. Instr. and Methods, 72, 125(1969).

(Sch 66) E.J. Schneid and Baruch Rosner, Phys. Rev. 148, 1241(1966).

(Sho 71) R.L. Shoup and H.C. Griffin, Bull. Am. Phys. Soc. 16, 538(1971).

(TI 67) C.M. Lederer, J.M. Hollander, and I. Perlman, Table of Isotopes, 6th Ed., Wiley, (1967).

(TOO) D. Bayer, Ph.D. Thesis, Michigan State University, (1970).

(Tre 69) W.J. Treytl, Phys. Rev. 188, 1831(1969).

(Von Ehr 70) D. von Ehrenstein, G.C. Morrison, J.A. Nolen, Jr. and N. Williams, Phys. Rev. C1, 2066(1970).

(Van H 67) J.R. Van Hise, G. Chilosi, and N.J. Stone, Phys. Rev. 161, 1254(1967).

(War 70) M. Waroquier and K. Heyde, Nucl. Phys. A144, 481(1970).

(War 71) M. Waroquier and K. Heyde, Nucl. Phys. A164, 113(1971).

(Wil 69) B.H. Wildenthal, Phys. Letters 29B, 274(1969).

(Wil 69a) B.H. Wildenthal, Phys. Rev. Letters 22, 1118(1969).

(Wil 71) B.H. Wildenthal, E. Newman, and R.L. Auble, Phys. Rev. C3, 1199(1971).

(Wil 71a) B.H. Wildenthal, MSU, private communication (1971).

(Yag 68) K. Yagi, T. Ishimatsu, Y. Ishizaki, and Y. Saji, Nucl. Phys. A121, 161(1968).

(Zwe 57) Phys. Rev. 107, 329(1957).